NBSIR 80-1642

DEVELOPMENT OF STANDARDS FOR SUPERCONDUCTORS

Annual Report
FY 80

F.R. Fickett, L.F. Goodrich, and A.F. Clark
Electromagnetic Technology Division
National Engineering Laboratory
National Bureau of Standards
Boulder, Colorado 80303

DECEMBER 1980

Work performed under Department of Energy contract EA-77-A-01-6010 and Massachusetts Institute of Technology contract POML-162265

NBSIR 80-1642

DEVELOPMENT OF STANDARDS FOR SUPERCONDUCTORS

Annual Report
FY 80

F.R. Fickett, L.F. Goodrich, and A.F. Clark
Electromagnetic Technology Division
National Engineering Laboratory
National Bureau of Standards
Boulder, Colorado 80303

DECEMBER 1980

Work performed under Department of Energy contract EA-77-A-01-6010 and Massachusetts Institute of Technology contract POML-162265

U.S. DEPARTMENT OF COMMERCE, Philip M. Klutznick, Secretary
Jordan J. Baruch, Assistant Secretary for Productivity, Technology, and Innovation
NATIONAL BUREAU OF STANDARDS, Ernest Ambler, Director

CONTENTS

	Page
Abstract	v
I. INTRODUCTION	1
II. EVALUATION OF PRESENT STATUS	4
A. Test Specification Survey	5
B. Round Robin Test	6
C. A Discussion of Current Transfer	9
III. PREPARATION AND DISSEMINATION OF STANDARDS	13
A. Standard for Terminology	13
B. Standard for Critical Current Measurement	14
C. Standard Reference Materials	15
IV. EXPERIMENTAL PROGRAM: CRITICAL CURRENT	17
A. Sample Mounting	17
B. I_c Criterion	30
C. Sample Current, Resistance Ratio, and Self Field	33
D. Field Orientation and Uniformity	40
E. Conductor Parameters	42
V. CONTRACTOR REPORTS	49
A. Airco Superconductors	51
B. Intermagnetics General Corporation	91
C. Magnetic Corporation of America	141
D. Supercon, Inc.	185
VI. REFERENCES	203
APPENDICES	
A. Publications and Presentations	
B. Staff and Contacts	
C. Minutes of ASTM Subcommittee B01.08 on Superconductors	

DEVELOPMENT OF STANDARDS FOR SUPERCONDUCTORS

F. R. Fickett, L. F. Goodrich, and A. F. Clark
Electromagnetic Technology Division
National Bureau of Standards
Boulder, Colorado 80303

Modern practical superconductors are complex materials and the determination of their critical parameters is a difficult task. Many approaches are possible for determining a given parameter and the results often depend on which one is chosen. The goal of this program, a cooperative venture involving DoE, NBS, and private industry, is to arrive at a set of useful voluntary standards for measurements on modern practical superconductors that will be acceptable to both manufacturers and users. Agreement on a set of standard definitions for the commonly used terms is also necessary. This report describes the status of the program at the end of the second year. The work in FY 80 has concentrated nearly exclusively on the critical current standard. Experimental determinations of the effect of various parameters on the measurement have been made by NBS and by the wire manufacturers. Significant progress has been made in the preparation of the actual critical current measurement standard and the definition standard. Draft copies of both are now ready for comment.

Key words: Critical current; electrical property; magnetic property; stability; standards; superconductor.

I. INTRODUCTION

The goal of the superconductor standards program is the development of standards of definition and measurement for the various critical parameters of practical superconducting materials, usually in the form of wires or cables. The production of superconducting materials is a growing industry in this country and elsewhere. Because of the complexity of a superconducting composite, it is imperative that everyone be agreed as to how its properties are to be measured. Two perfectly reasonable and justifiable measurements of critical current, for example, may give values that differ by 30-40%. It was in an attempt to avoid such problems that this program was conceived. The superconductor standards program is a cooperative program between NBS and three divisions of DoE (Fusion Energy, High Energy Physics, and Magnetohydrodynamics through the Francis Bitter National Magnet Laboratory).

As used here, the term "standard" may indicate: standardization of terminology; a detailed description of a measurement technique; an experimental apparatus; or a reference material. All of these aspects of standardization are being considered by this program. The specific parameters to be treated by the overall program are: critical current, transient losses, matrix properties, critical temperature and critical field.

This report describes the work during the second year of the program. The first year's work is described in detail in an earlier report [1]. During the first year: a great deal of work was done on standardization of terminology; a preliminary assessment of the current status of superconductor measurements around the country was made; an ASTM subcommittee on superconductors was formed; preliminary transient loss measurements were made; critical

temperature measurements on practical materials were made and, after evaluation, it was decided that specific standards for this parameter were not appropriate yet; extensive research on factors that influence the determination of critical current was done by NBS and the four wire manufacturers.

The second year's work described in this report has concentrated heavily on the critical current measurement standard. Figure 1 lists the various aspects of this experimental program. Each of them is treated in detail here. In addition, the present state of measurement capability was evaluated by means of a survey that also determined presently used criteria and precision and accuracy values for critical current measurements. Also, a round robin test of several superconducting materials was made among the wire manufacturers and NBS. The last of four papers on definitions of terms for practical superconductors was published [2] and ASTM draft standards for definitions and critical current measurement were prepared and an initial presentation made to the committee. A number of publications and presentations have resulted from this work. They are listed in Appendix A.

Much of the experimental work was performed by the superconducting wire manufacturers under contract to NBS. Their reports are included here in Section V and selected data have been used throughout this report. We are grateful for their help and for their enthusiastic support of the standards effort in general. A complete list of those involved in this program is given in Appendix B along with addresses and telephone numbers. The reader with questions should feel free to contact anyone on the list.

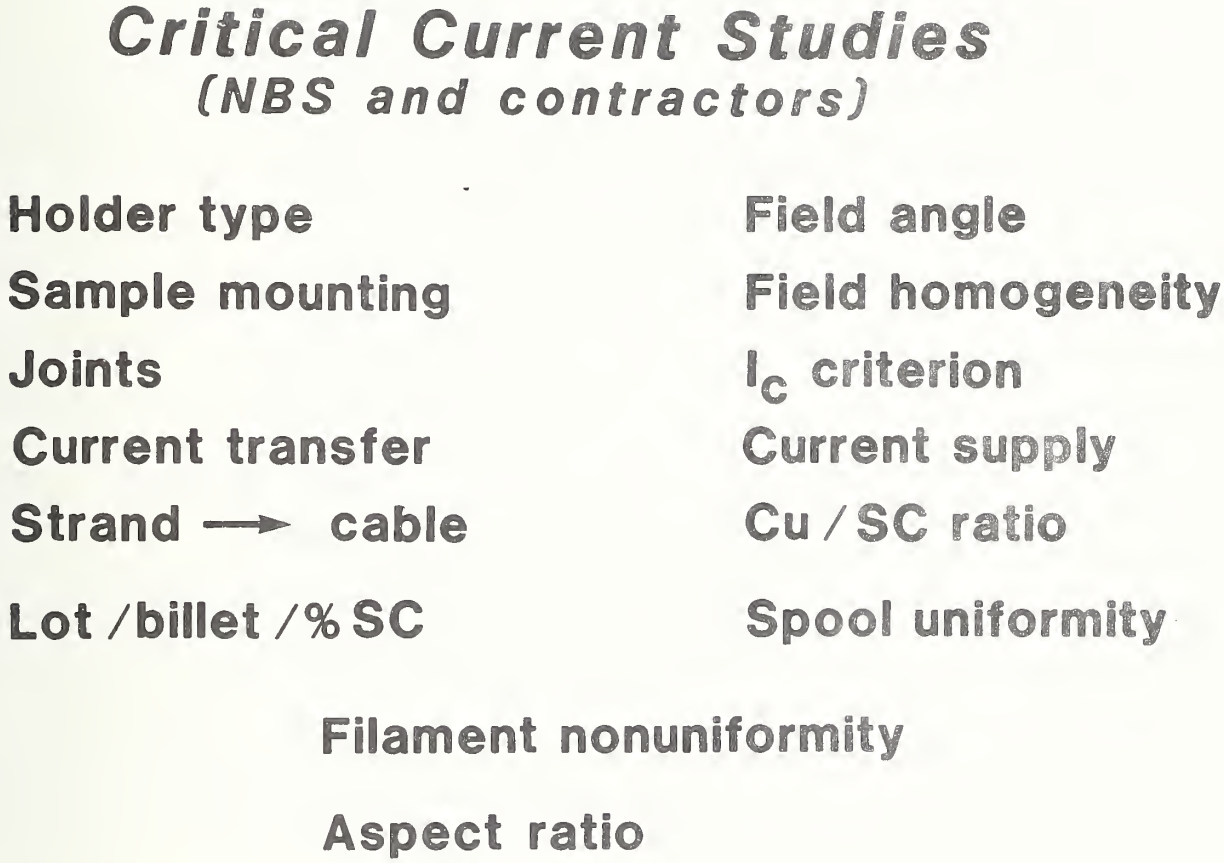

Figure 1. Aspects of critical current measurement treated in this report.

II. EVALUATION OF PRESENT STATUS

An important component of a successful standards effort is the assessment of present practices in the field. A good understanding of these is essential to the creation of a standard that will be both understandable and useful. Furthermore, the technique used to assess the present practices allows many people to have input to the formative stages of the standard - a step that is very helpful in developing the required concensus. Last year we made a preliminary survey of methods of measurement. This year we performed the more detailed survey described below. Another excellent technique for determining the state of the art for measurement is to send similar materials to various laboratories and ask them to make the measurement - a round robin test. Our test for critical current is described in the second subsection here. Finally, there was some indication throughout our interactions that the concept of current transfer in multifilamentary superconductors is not generally well understood. We have attempted to rectify that situation in the final subsection with a brief discussion of the effect, its various sources and manifestations.

A general assessment of the present overall situation regarding the measurement and reporting of critical current data for practical conductors is as follows: measurements are usually made with 10-15% accuracy, but often this number is exceeded; improper measurement of I_c nearly always results in a lower value than the correct one; few laboratories have setups for the routine determination of I_c; seemingly innocuous practices can have a dramatic effect on the measurement, such as heavily greasing a sample in place or making a holder from a material with a total thermal contraction that differs significantly

from that of the wire to be measured. The need for standard techniques, devices, and definitions seems clear and imperative to us.

A. Test Specification Survey

A detailed evaluation of presently used critical current test specifications was made by means of a survey of some forty people in industry, government, and university laboratories. Specific values for precision, accuracy and other properties of pertinent test variables were solicited. The parameters considered were:

Critical current

Applied magnetic field

Electrical field criterion

Angle between current and field

Test temperature

Sample identification

Strain

In addition, comments were requested on the use of operational checks for determining the effect on the measurement of:

Quench-protect circuitry

Contact heating

Lorentz force

The response was excellent with many replies providing great detail on the reason for a particular choice. The results were tabulated and evaluated at NBS and, finally, presented to the ASTM subcommittee. Briefly, we found:

- Little agreement on any specific values for accuracy and precision.
- Sample mounting is a serious problem and should either be specified in a standard or appropriate operational checks should be required.

• The transfer voltage is not a well-understood concept and a method of correcting for it should be specified in the standard.

• The effect of transient spikes and ripple from the sample current supply is unknown.

• Accurate magnetic field measurement techniques are needed.

• Stress effects on I_c are becoming understood and appreciated, leading to the use of more conservative bend radii and allowed differential thermal contraction in test fixture design.

• The use of an electric field criterion for determination of I_c is not universally accepted, many favor a resistivity criterion.

B. Round Robin Tests

The round robin tests were performed with the help of the wire manufacturers. Three different superconductors were sent to each of them for critical current measurement. These materials were chosen to represent a range of sizes and types. They were:

Multifilamentary NbTi, I_c ∿100 A at 8 T

Multifilamentary Nb_3Sn, I_c ∿100 A at 8 T

Tape Nb_3Sn, I_c ∿170 A at 8 T

The details of the materials are shown in the metallographic photos of Fig. 2. Measurements of I_c were requested at fields of 6 and 8T for NbTi, and at 8 and 10 T for the Nb_3Sn conductors. No other instructions were given. The samples were also measured at NBS.

The test results are summarized in Fig. 3. There is obviously a very large spread in the measured values, even for the NbTi wire. There are many valid reasons why this happened and there is no real point to be served by discussing

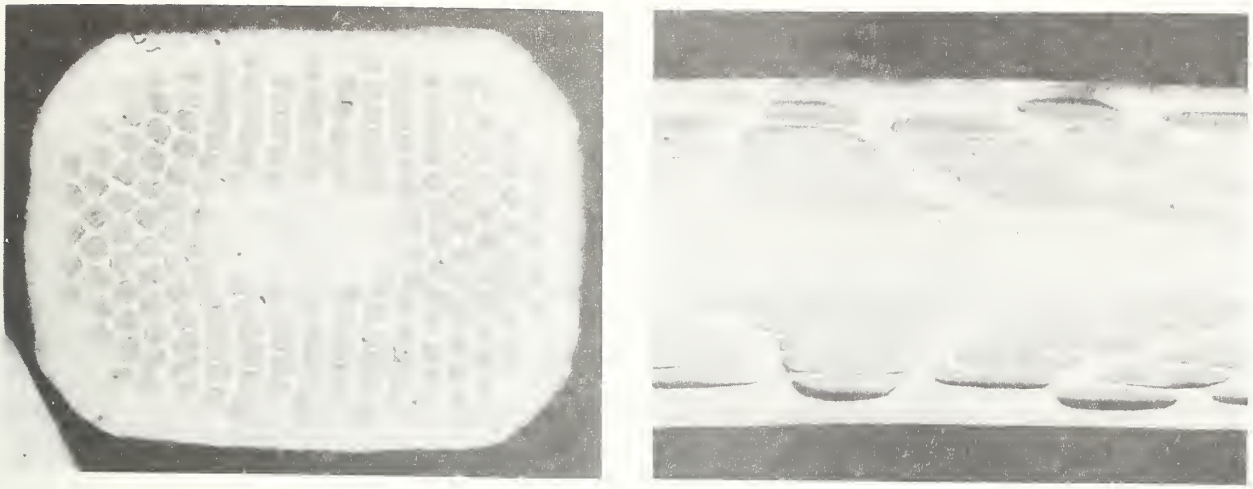

Multifilamentary NbTi, 0.53 x 0.68 mm

Round Robin Samples

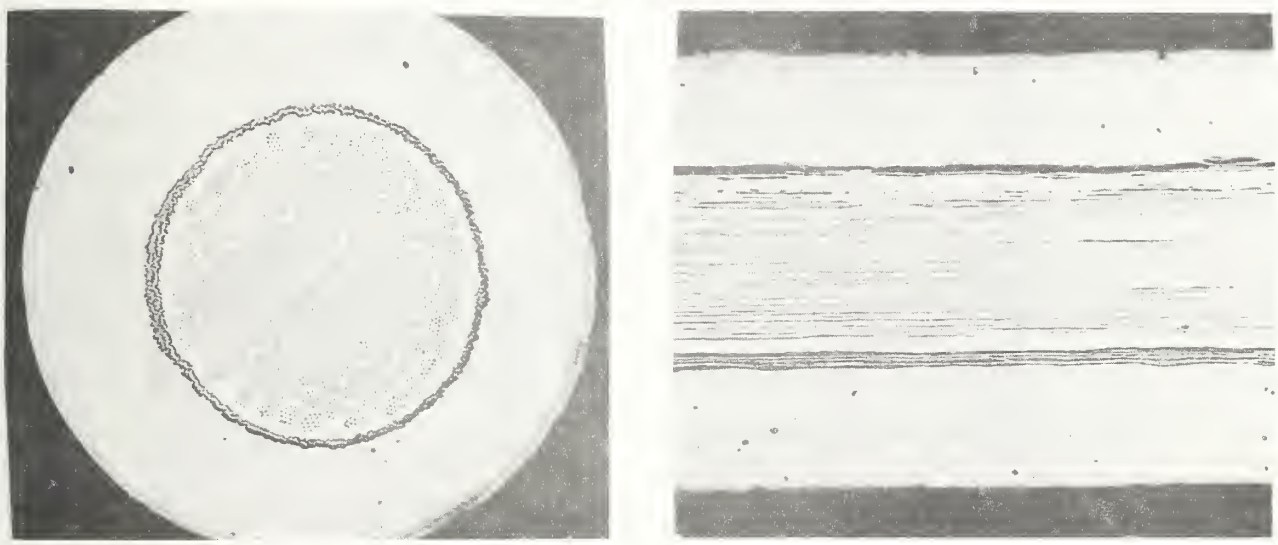

Multifilamentary Nb_3Sn, 0.7 mm diameter

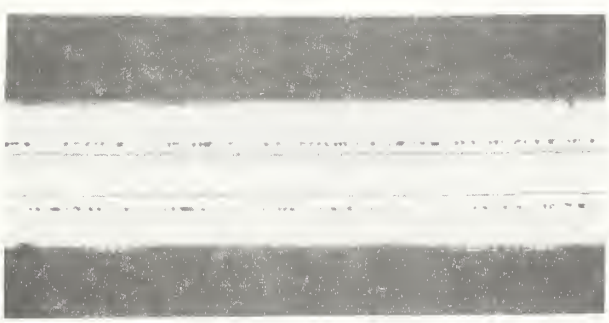

Tape Nb_3Sn, 2.3 x 0.2 mm

Figure 2. Samples used for the round robin critical current tests.

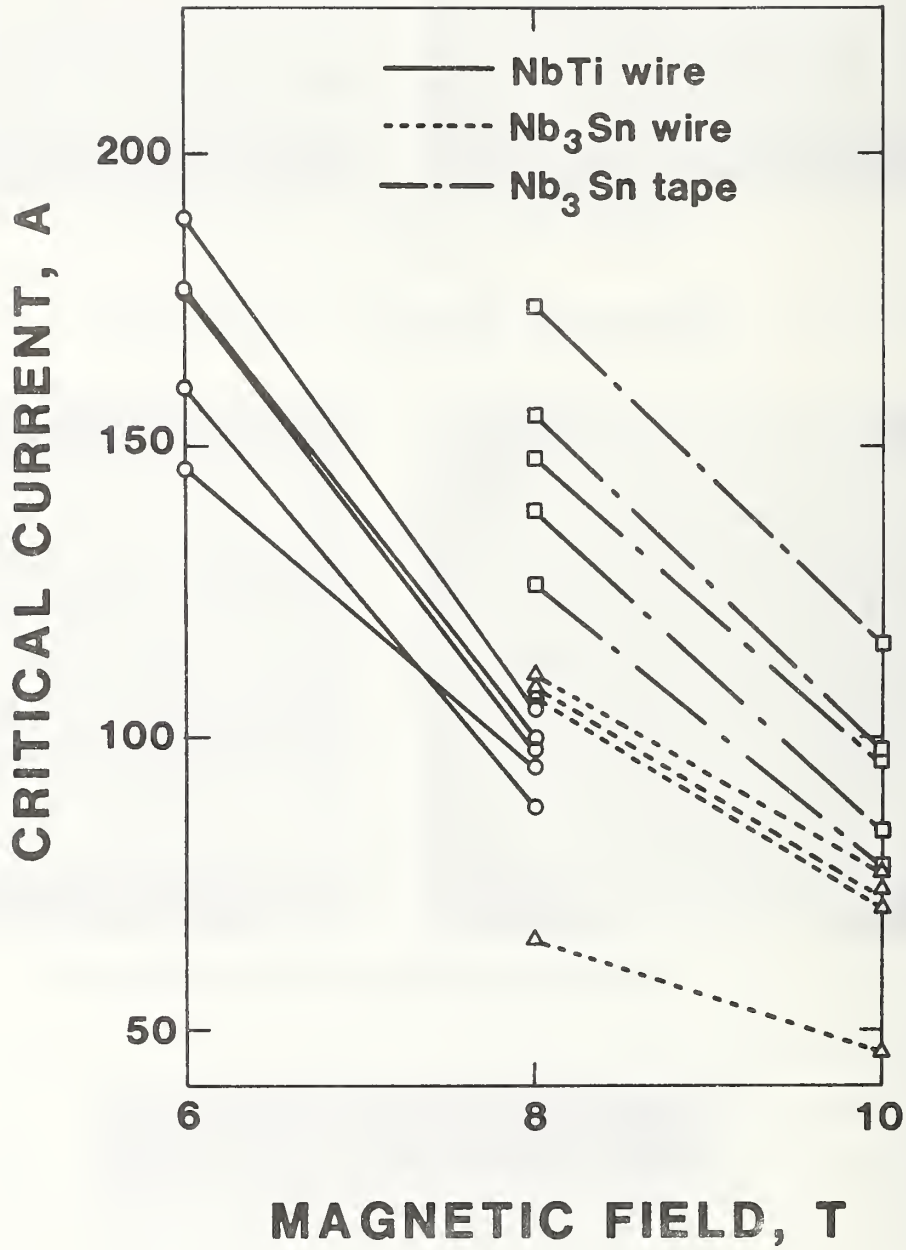

Figure 3. Results of the round robin tests. Open symbols show actual data points for each material type. Each of the five sets of measurements for each material were made by different organizations.

them all; suffice it to say that the plot shows dramatically the need for everyone to agree on a standard measurement technique and standard values for the critical parameters in the measurement of I_c.

Our plan is to redo the round robin test after the standard is in general use. This will provide an excellent measure of its success. Also, it is our intention to include more laboratories in the next round robin.

C. A Discussion of Current Transfer

Current transfer is the redistribution of current among the filaments of a multifilamentary superconductor. This change in distribution of the current requires that some of the current flow through the normal metal matrix, giving a voltage drop referred to as the current-transfer voltage. The current distribution is a function of both current and position along the wire near any of the following: a joint, a change in the local superconducting properties of the filaments (due to a defect, breakage, or local strain), or a change in the magnitude or relative angle of the external magnetic field. The resulting current-transfer voltage will be added onto the usual intrinsic voltage-current relationship and can complicate determination of the intrinsic critical current.

The theory [3,4,5] and measurement [6] of current transfer in multifilamentary superconductors has been the subject of several papers. It is a rather complex problem involving current transfer adjacent to an input lead. This is where the effect is largest and a very useful first order approximation to this effect is given in [4]. That theory starts with all of the current on the outer of two concentric rings of superconducting filaments at one position along the wire, say $x = 0$. Then the theory follows the current

redistribution and current-transfer voltage along the wire as a function of total current. It is assumed that the whole wire can be made up of such concentric rings and thus the results follow for a whole wire of any size.

Two important results of the theory (within its approximations) are that the current transfer voltage is linear with total current and that the magnitude of this effective current-transfer resistivity is a simple function of position, x. The linear relationship between the current-transfer voltage and the current allows the easy subtraction of the current transfer effect from the voltage-current characteristic of the superconductor as illustrated by Fig. 4. This figure is a schematic representation of the voltage-current characteristic in the intrinsic region and the current-transfer region. The measurement of the electric field is made relative to the current-transfer component of the sample voltage. The second result, that the magnitude of the current-transfer resistivity is a function of position, can be turned around to calculate a so called current-transfer length, relative to an acceptable value of the current-transfer resistivity. This can be used to determine the required spacing between the current and voltage contacts in order that the current-transfer resistivity be less than a chosen value. Typical current-transfer lengths for an acceptable value of current-transfer resistivity equal to 10^{-12} Ωcm would be approximately 7 wire diameters for a NbTi superconducting wire and about 60 wire diameters for a Nb_3Sn superconducting wire. These theoretical results have been verified experimentally [6].

The above correction for the current transfer effect is adequate for most practical applications and is fairly well accepted by the scientific community. However, when the electric field critical-current criterion is less than the

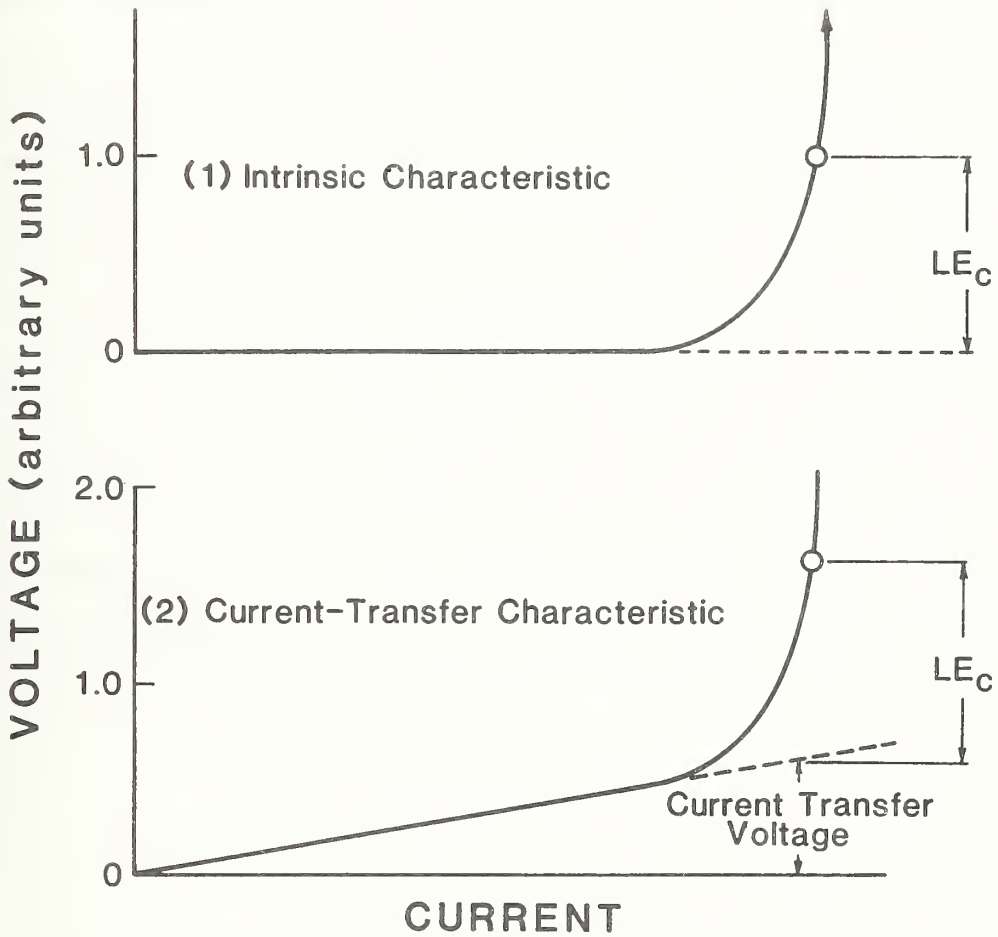

Figure 4. Schematic representation of the composite superconductor's V-I characteristic in two regions: 1) Intrinsic characteristic showing the usual resistive transition as I approaches I_c and 2) current-transfer characteristic exhibiting a linear region at low current.

current-transfer electric field, the assumptions and approximations have to be reconsidered. It was for this reason that the standard test method for measurement of the critical-current (§III B) includes a requirement that the electric field critical-current criterion be greater than the current-transfer electric field. Nonlinearity of the current-transfer voltage with current could be caused by non-symmetric current injection or by nonuniformities in any of the other current transfer mechanisms. This would result in an incomplete accounting for the current-transfer voltage and, perhaps, an erroneous critical current value. Another concern is whether the full-cross-section is being tested if the electric field criterion is less than the current-transfer electric field. An obvious solution to this problem is to change the geometry of the sample such that the current-transfer voltage is lower; this is not always practical, however. Some new experimental data on this matter are discussed in the sample mounting section of this report (§II A). They illustrate the concerns that arise when the current-transfer electric field is comparable with the electric field criterion.

III. PREPARATION AND DISSEMINATION OF STANDARDS

The first product of this program and the culmination of all the research efforts will be acceptable voluntary standards which have been adopted by a recognized standards organization. Early in the program it was concluded that the most appropriate first steps should be through ASTM and thus a Subcommittee on Superconductors (B01.08) was formed within the committee on Conductors (B1). An organizational meeting was held in June 1979 outlining the tasks to be done, and several informal sessions have occured since at various scientific meetings. The second formal meeting of the subcommittee was held September 4-5, 1980 in Santa Fe, New Mexico at the conclusion of the Applied Superconductivity Conference. The preparations for and actions taken by the subcommittee are described below by task and summarized in the minutes of the meeting which are included as Appendix C. Briefly, the meeting consisted of reports of research, presentation of draft standards for definitions and small conductor critical current, working task group sessions to modify the drafts, and a concluding session to point to future needed work. Two specific needs were expressed: a) a strong recommendation that NBS generate a standard reference material for critical current, and b) work begin immediately on the problems of ac loss measurements in superconductors.

A. Standard for Terminology

As mentioned earlier, the fourth and final paper prepared by the NBS staff proposing definitions of terms related to superconductivity has now been published [2]. This set of four papers plus comments by many others was used as the basis for a set of definitions of terms to be used in critical current

standards for ASTM. Only those terms that were expected to occur in the standard for critical current were included and in many cases were shortened and changed to a simpler language appropriate for everyday use. This draft set of terms was presented by task group chairman S. J. St. Lorant to the subcommittee for discussion, and the next day the task group on definitions modified, deleted, and added to it. The task group then approved the set for presentation to the subcommittee by mail for a vote of approval. This process is in progress at the present time.

B. Standard for Critical Current Measurement

In preparation for the ASTM Subcommittee on Superconductors meeting, three draft measurement standards for critical current were prepared. One for a straight geometry specimen was prepared by R. Schwall of IGC and R. Scanlan of LLL, another for a coil geometry by W. Fietz of ORNL and P. Sanger of AIRCO, and a third "generic" standard by NBS. After discussion, the subcommittee decided that there were enough common elements to warrant only one standard for all geometries. As long as all the various criteria were met then any geometry could be used with suggested ones being preferred. The following day the task group adroitly chaired by R. Schwall went through the NBS "generic" standard item by item, incorporating parts of the others, modifying or deleting as necessary. When consensus was not achieved it was left to the NBS staff to determine the alternatives and recommend a choice while still ennumerating the dissent. In brief outline form the draft standard covered:

1. Scope of the standard
2. Critical current definition
3. Precision and accuracy of the apparatus

4. Test specimens

5. Procedure

6. Significance and use

7. Reporting

The results of the meeting and subsequent efforts to resolve some of the still open questions were combined in a draft standard which was distributed to all of the attendees accompanied by a discussion of all objections and open questions. Responses from these will be combined into a draft standard which will be submitted to the subcommittee for approval by mail.

The succession of steps through the ASTM process are approval by the subcommittee, approval by the whole committee on conductors, and finally approval by the society as a whole. At each step all conflicts must be resolved so there is necessarily a great deal of work required to obtain this approval, but the final product should be acceptable to everyone.

The next problem to be addressed for critical current measurements is a draft standard for larger current conductors, more than 600 amperes.

C. Standard Reference Materials

The ASTM subcommittee strongly recommended at the September meeting that NBS initiate the development of a standard reference material for critical current. Exploratory discussions were held with the NBS Office of Standard Reference Materials and it appears that additional support from NBS may be made available for this effort. The criteria will be established based on some of the contractual research and the requirements of the critical current standard. It appears questionable now whether a standard production run can produce the homogeneity necessary and further development or pre-production criteria may have to be set on the fabrication of materials. The present

thinking is that NBS should procure several kilometers of a common NbTi multifilamentary conductor and provide it in several meter increments. The major question at the moment is whether it is more cost efficient to over-characterize a standard production run or carefully control a special production. Prominent problems are those of maintaining constant copper-to-superconductor ratio, residual resistivity characterization, assuring filament continuity, and the uniformity of the final cold-working. A great deal has yet to be done.

IV EXPERIMENTAL PROGRAM: CRITICAL CURRENT

Nearly all of the experimental work performed this year has been directed toward understanding the various phenomena that affect the measurement of critical current. As we showed in Fig. 1, there are many of these. Some, such as sample mounting, field orientation effects, and the choice of criterion are of prime importance and have been investigated in considerable detail. Others, such as self field, current supply ripple, and field uniformity have turned out to have a relatively minor influence on the determination of I_c and, thus, they have not been treated as intensively.

In general, the first two subsections here report NBS experimental work and the last three the work of the contractors. There are exceptions, however, and we have attempted to give proper credit in each case. In any event, the reader should look at the complete reports of the next section to get the whole story on the various contractor results reported here.

A. Sample Mounting

The critical current of a sample can be measured in a number of different mounting geometries. The most common geometries, illustrated in Fig. 5, are: short straight, hairpin, coil, and long straight. In all of the geometries the applied magnetic field is essentially perpendicular to the sample axis (between the voltage taps), which is the orientation that has the lowest critical current and is the limiting situation for most applications. Also, in each geometry a test fixture can be designed such that the Lorentz force on the sample is into the fixture thus minimizing the resulting strain on the sample.

There are a number of considerations that determin which mounting geometry to use. They are: extent of the contact heating, size of the current-transfer

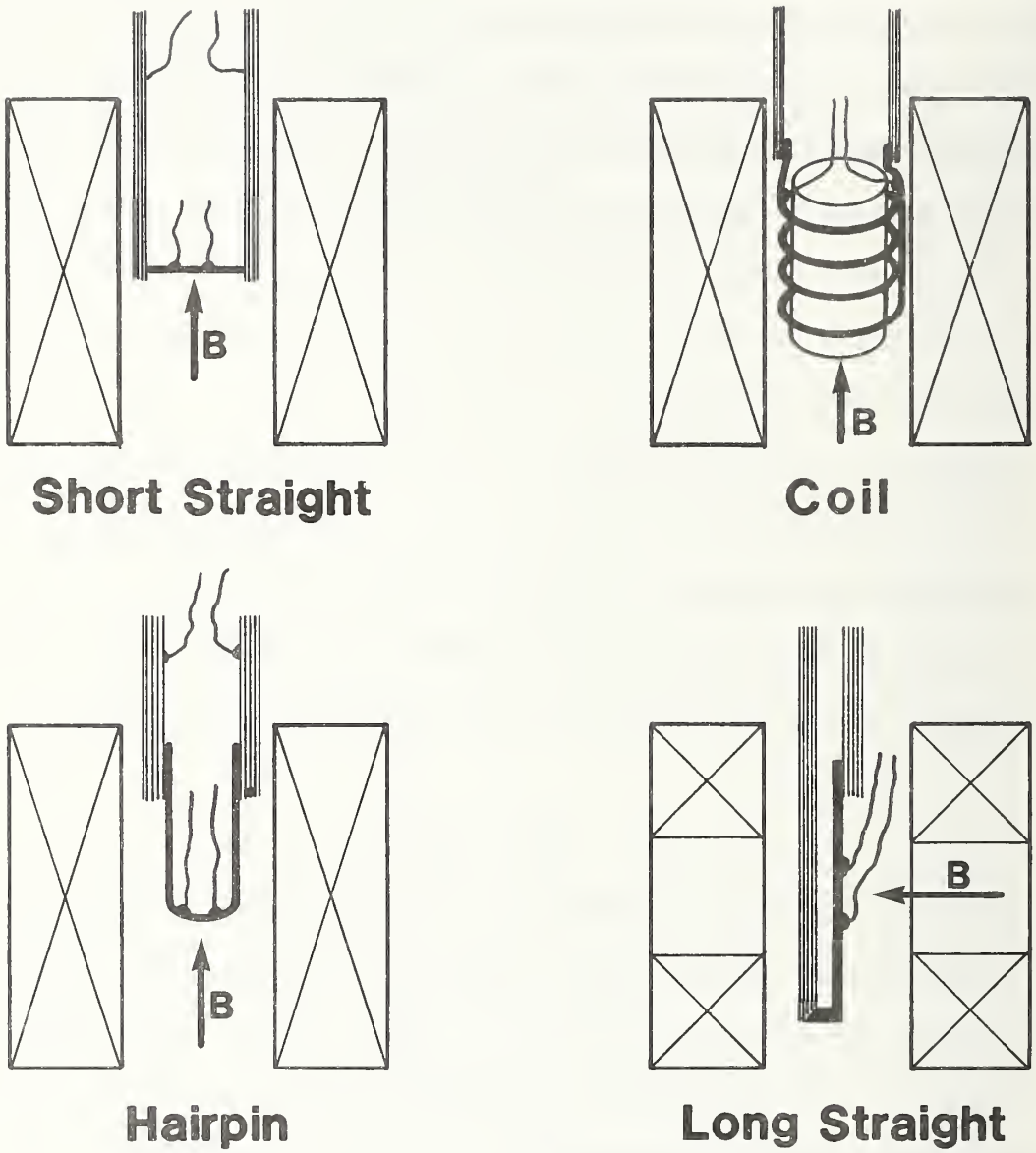

Figure 5. Common sample mounting geometries illustrated with magnet, bus bar, sample and voltage leads.

voltage, detectable level of the electric field, simplicity of the geometry, and magnetic field geometry. Each of these considerations has been addressed and Table 1 lists advantages and disadvantages of each geometry.

Table 1. Sample geometry comparison

Sample geometry	Advantage	Disadvantage
Short straight	simple geometry solenoidal magnet	high contact heating high current transfer high electric field criteria
Long straight	low contact heating medium electric field criteria simple geometry	some current transfer split-pair magnet
Hairpin	low contact heating medium electric field criteria solenoidal magnet	some current transfer moderate geometry
Coil	low contact heating low current transfer low electric field criteria solenoidal magnet	complicated geometry

The extent of the contact heating will determine if the intrinsic critical current of a sample can be measured. If the contact heating is too large the sample will be at an elevated temperature and an incorrect critical current measurement will result. It is also possible that the sample will be driven into the normal state by the propagation of a normal zone from the contact through the entire sample at a current well below the intrinsic critical current. The contact heating depends on the contact resistance and the critical current. This problem was the subject of some recent experimental measurements [7] of the lap-joint resistance of a multifilamentary NbTi superconducting wire and the critical current of this wire adjacent to the joint.

The lap joint gives a symmetric model of contact resistance and allows for the separation of the total resistance into (1) interface and (2) current-transfer components. The results of this work indicated that the interface contribution to the joint resistance can be calculated for any other rectangular conductor. The current-transfer contribution is conductor dependent, but the results can be generalized to give an upper limit to this contribution for any conductor. However, this generalization needs to be tested for the extreme case of large current-transfer effects in a multifilamentary Nb_3Sn wire. Critical-current measurements made adjacent to the lap joint indicated that, when the voltage-current characteristic was reversible, the measurement was within 2% of the intrinsic-critical current of the wire. The intrinsic-critical current was determined by measuring a control sample without a joint. The critical-current measurements also indicated that when the voltage-current characteristic was irreversible, the measured current was systematically (as a function of magnetic field) low indicating that joint heating is affecting the measurement. The onset of irreversibility was correlated with a power per unit surface area of the joint perimeter larger than 1 W/cm^2. This suggests that there is a limit to the power per unit area than can be dissipated into the helium bath. The thermal conductivity of the matrix may affect this result. It should also be tested for the case of multifilamentary Nb_3Sn wire.

These results [7] allow the designer to estimate the joint resistance and determine if contact heating will affect the critical current measurement. Contact heating is of the most concern in the short straight geometry since this is the only geometry were the length of the current contact is severely

limited. In other geometries the designer can estimate the joint resistance and, in most cases, easily keep joint heating from affecting the critical current measurement.

As mentioned in the discussion of current transfer, when the electric field meeting the critical-current criterion is less than the current-transfer electric field, the accuracy of the critical current measurement is questionable because of the assumptions and approximations of the current transfer correction. When the electric field meeting the criterion is much larger than the current-transfer electric field the correction works very well. But, a closer look at the experimentally observed current-transfer voltage indicates that it is not linear with current, especially at low currents (where the slope is smaller) and at high currents (where the slope is larger). There is a fairly linear section in the middle of the voltage-current characteristic, but the resulting correction is slightly arbitrary and incomplete. This is illustrated in Fig. 6, which is a plot of the percent difference between the critical current (at electric fields of 1, 2, and 10 μV/cm) for multifilamentary Nb_3Sn measured in the short-straight geometry and in the long-straight geometry as a function of magnetic field. It should be noted that the baseline of this plot is the critical current appropriate to the particular electric field as measured in the long-straight geometry. (The differences in the critical current between the baseline electric field criteria was about 4% between 1 and 2 μV/cm and about 9% between 2 and 10 μV/cm.) The current-transfer electric field in the short-straight geometry was approximately 3.5 μV/cm at 4T (I_c ∿248A at 1 μV/cm) and 2.0 μV/cm at 7T (I_c ∿136A at 1 μV/cm). The first observation is that with a criterion of 10 μV/cm, which is much larger than the current-transfer electric field, the critical current data agree to about

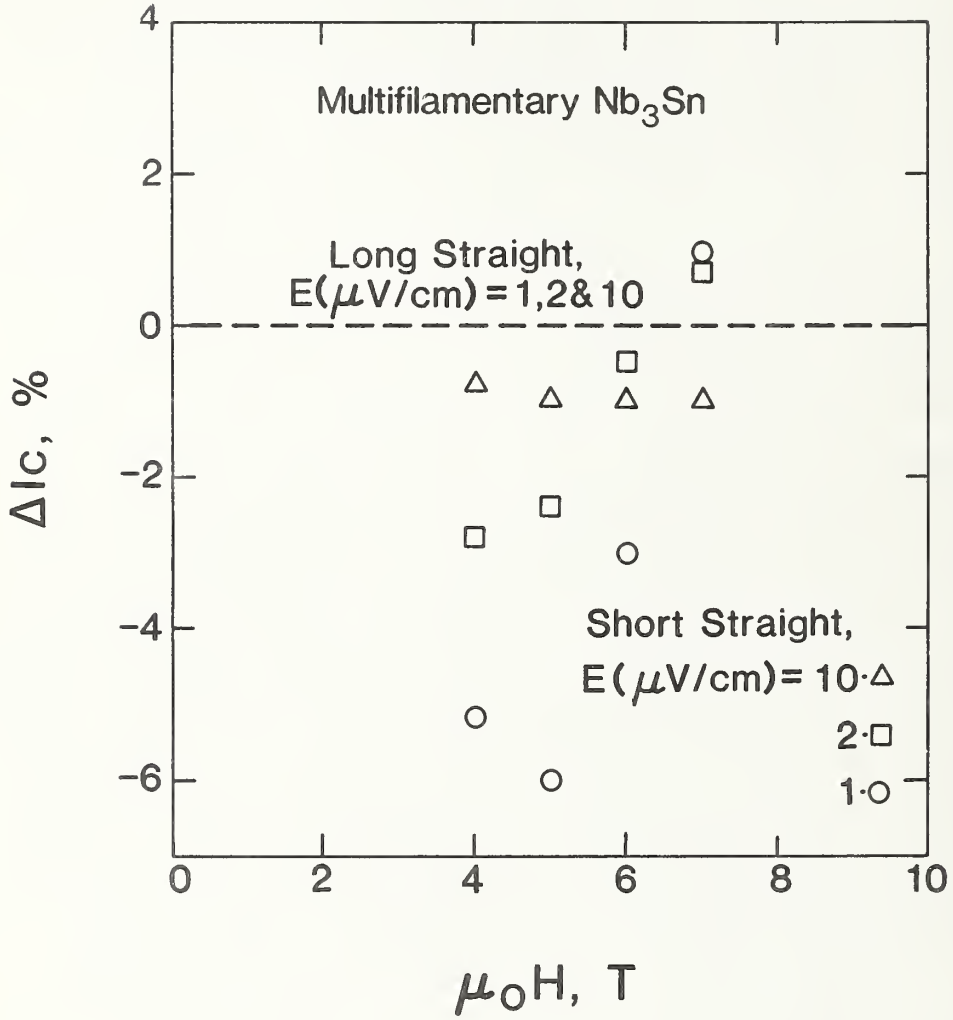

Figure 6. Comparison of short straight and long straight critical current measurements at various electric fields as a function of magnetic field.

1% for the entire range of overlap in magnetic field. The 2 μV/cm criterion data deviate from each other systematically and do not agree to 1% until the current-transfer electric field is about 2 μV/cm also. There is more scatter in the 1 μV/cm data, but they indicate a similar, only larger, systematic deviation. These data indicate that the current-transfer effect correction tends to underestimate the effect and the resulting critical current may be in error by about 5% if the current-transfer electric field is three times the field defining the critical current. It is in agreement to about 1% if the criterion is equal to or greater than the current-transfer electric field.

The current-transfer effect is largest next to a current contact, so its worst case is the short straight geometry. The current-transfer effect in the long straight geometry is, for the most part, due to the change in magnitude of the external magnetic field and is relatively small. The same is true of the current-transfer effect in the hairpin geometry, where the main cause is the change in angle of the external magnetic field. For the coil geometry the current-transfer effect is easily minimized by placing the voltage taps well away from the current contacts and avoiding regions of high magnetic field gradients. As mentioned in the discussion of current transfer, the current-transfer length is approximately ten times longer in Nb_3Sn wires than it is in NbTi wires. Therefore, it is easy to compare some of the different sample geometry measurement methods using a NbTi wire. The critical current measured in the hairpin and long straight geometries are compared to the short straight geometry in Fig. 7. The agreement is within 1.5% of short straight values for the entire range of overlap. The electric field criterion used was 2 μV/cm. Very similar plots would have resulted for other electric field criteria in the range of overlap.

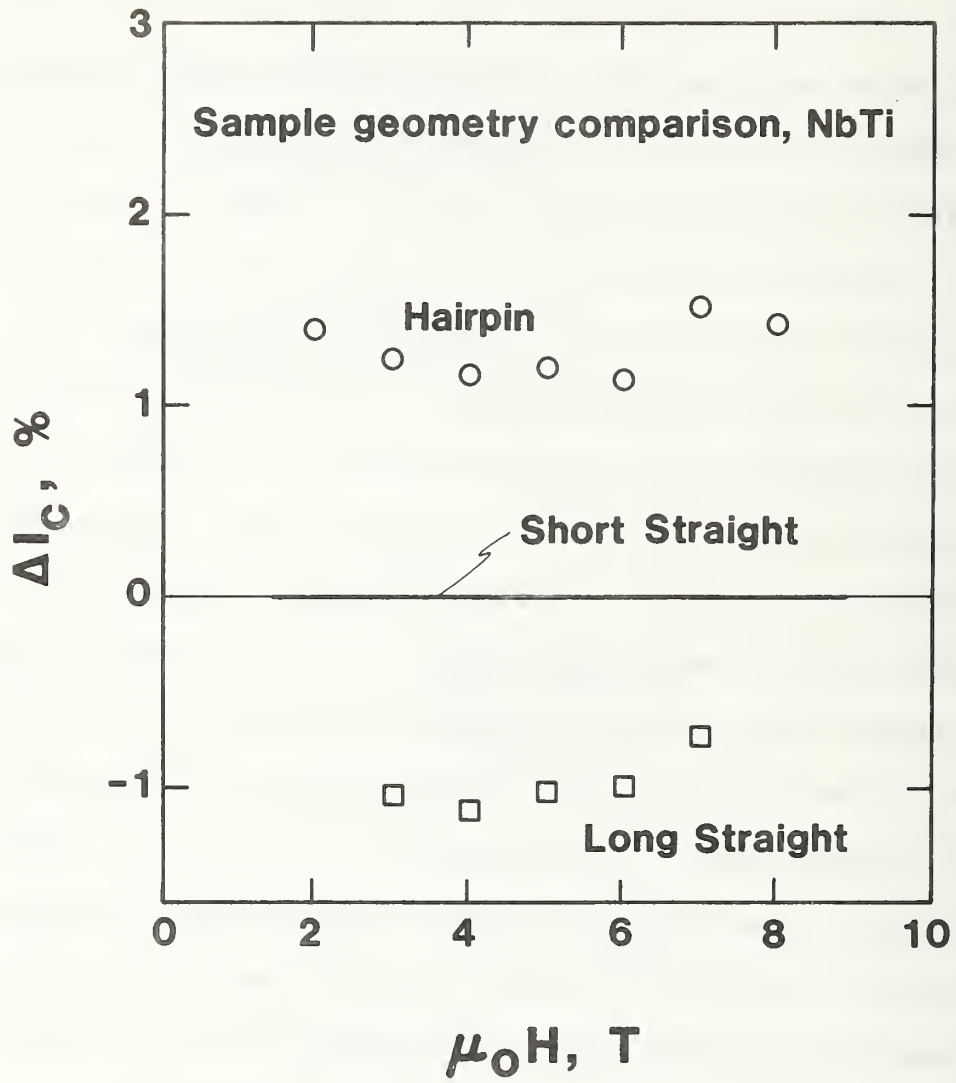

Figure 7. Sample geometry comparison relative to short straight sample data.

The detectable level of the electric field is a function of the following: voltmeter sensitivity, electronic noise level, changes in thermoelectric voltage, changes in the voltage induced by the ramping of the sample current, voltage tap separation, and level of the current-transfer electric field. The round robin samples (§IV B) were measured with two types of voltmeters, an analog nanovoltmeter and a digital multimeter with an analog output. This allowed comparisons between data taken with the highly processed signal of the digital multimeter and with an analog device. This comparison was made using both a 600 ampere SCR regulated power supply and a 600 ampere battery power supply. In both cases the agreement between the two types of voltmeters was within 0.5%. A comparison of the two power supplies will be given in a later section (§IV C). One source of electronic noise is the SCR switching in SCR regulated power supplies. A digital voltmeter will average out this noise but an analog device is very sensitive to it. This noise reduced the sensitivity of the analog device to about 100 nV, the same as the sensitivity of the digital-voltmeter. However, when the battery power supply was used for the sample current, the residual noise level was about 2 nV for the analog device.

Another source of electronic noise is from the magnet used to generate the external magnetic field at the sample. If the field is provided by a superconducting maget this noise contribution is minimal. However, conventional magnets such as those at the Francis Bitter National Magnet Laboratory can add significant electronic noise to the sample voltage.

Electronic noise can also arise due to sample motion under the influence of the Lorentz force. Under most circumstances this motion can be restricted by the design of the sample fixture, keeping the Lorentz force into the fixture.

However, when the magnet is very noisy, or if the fixture cannot be designed to balance the Lorentz force in all cases, an adhesive, such as silicone grease or varnish, can be used to restrict the motion of the sample. Adhesives tend to impede the heat flow, so their use should be conservative.

Changes in thermoelectric voltages can be minimized by using continuous copper wires from sample to the connection with the voltmeter input and keeping this connection at a fairly constant temperature. This can keep the changes in the thermoelectric voltage at the nanovolt level over the time of a voltage-current trace.

Changes in the the voltage induced by the ramping of the sample current can be minimized by using a constant ramp rate or by minimizing the area enclosed by the voltage taps and sample. This is especially important in the inductive coil geometry, where the voltage leads should be co-wound with the sample to minimize this pick-up. Voltage tap separation can limit the detectable level of the electric field. This is most severe in the case of the short-straight and hairpin geometries where the voltage tap separation may be a centimeter or less. In the long straight geometry, the voltage tap separation can be a few centimeters. The coil geometry allows the most freedom in separation of the voltage taps, with separations of several meters possible. The current-transfer voltage can also limit the detectable level of the electric field, as discussed in the previous paragraph. This is most pronounced in the short-straight geometry and is of secondary concern in the hairpin and long straight geometries and only of minor concern in the coil geometry.

Simplicity is another consideration in deciding what mounting geometry to use. An important concern is the amount the sample will be strained during mounting, cool-down, and by the Lorentz force. Limits on the bending strain, to keep the critical current measurement accurate to 2%, are 0.1% for Nb_3Sn

and 2% for NbTi based superconductors. Most NbTi wires are delivered on large diameter spools and, from this slight curvature, they can be mounted on short-straight or long-straight test fixtures without exceeding the strain limits. They can also be bent onto hairpin and coil test fixtures if the diameter of the fixture is large enough. Since the Nb_3Sn superconductors require a heat treatment at the end of their processing to form the brittle Nb_3Sn, they can be formed to fit the test fixture before the heat treatment. The straight geometries are obviously the easiest. The hairpin is a little more difficult and the coil geometry is quite complicated. Earlier work at NBS addressed the problem of strain in the sample introduced by the differential thermal contraction of the sample and sample holder [8]. This work indicated that suitable materials for the test fixture were NEMA G-10 or G-11 epoxy-fiberglass. The strain caused by the Lorentz force can generally be adequately balanced by the test fixture, if the sample is reasonably well fitted to the fixture.

The common magnet geometries are either solenoidal or split-pair. The short-straight, hairpin, and coil sample geometries are particularly suited to solenoidal magnets. The bore diameter of the magnet determines the overall length of the short-straight sample and the diameter of the curvature of the hairpin and coil geometries. The split-pair magnet is required for the long-straight sample geometry. This magnet is not as common and generally has a lower maximum field.

Two of the round robin samples were rectangular in cross-section. This introduces the possibility of the critical current variation due to the orientation of the conductor with respect to the perpendicular magnetic field.

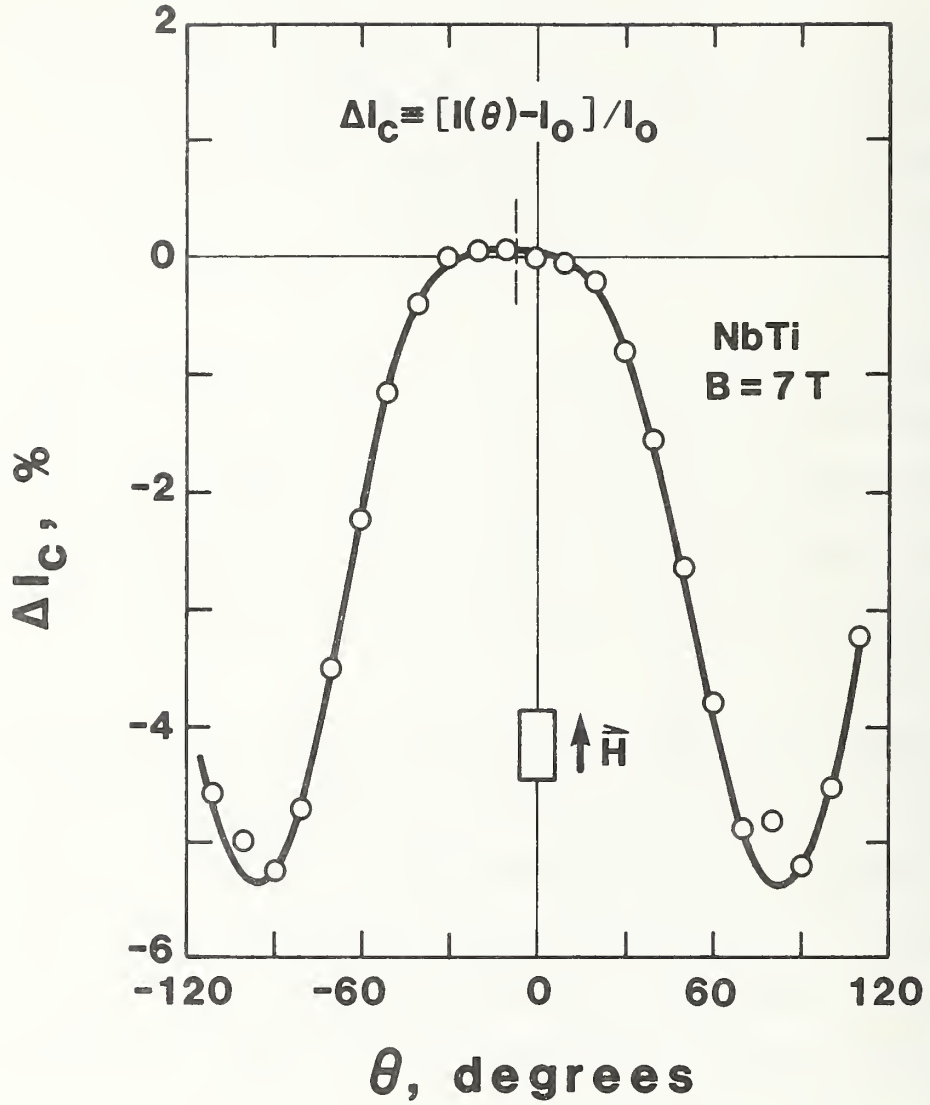

Figure 8. Angular-dependence of the critical current for a rectangular NbTi conductor. At 0°, H is parallel to the wide face.

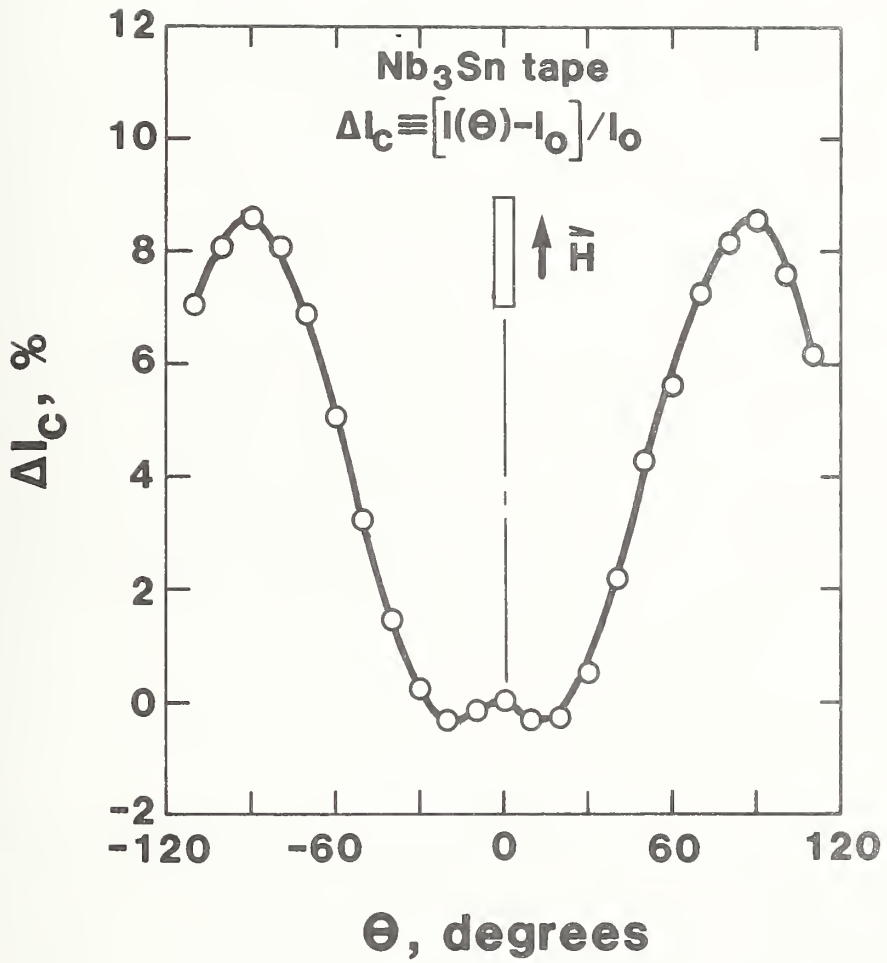

Figure 9. Angular-dependence of the critical current of a Nb_3Sn tape conductor at 7T. At 0°, H is parallel to the wide face of the tape.

Checking this dependence was easily done in the long-straight geometry since the sample could be rotated in the split-pair magnet. The usual orientation for measurement would be the one that is expected to limit the performance of the conductor in its application, that is, the magnetic field parallel to the wide face of the conductor. The rectangular NbTi conductor (0.53 x 0.68 mm) was measured with the magnetic field parallel to both the wide face, and the narrow face of the conductor on the short-straight, hairpin, and long-straight sample fixtures. The data on Fig. 7 was taken with the magnetic field parallel to the wide face of the conductor. The data from the other orientation showed similar agreement among the sample geometries. Critical currents for both the NbTi wire and the Nb_3Sn tape (0.2 x 2.3 mm) were measured as a function of angle between the wide face and the magnetic field in a split-pair magnet. The data at 7T are presented in Figs. 8 and 9. It was observed that this angular-dependence effect was opposite for the two materials. This is believed to be caused by differences in the flux-pinning mechanisms. The relative size of the anisotropy was not a strong function of magnetic field in the range of 3 to 7 Tesla.

B. I_c Criterion

The term "critical-current criterion" defines the specific value of a property that is reached at the critical current. The most commonly used criteria are electric field and resistivity. The criterion is applied to the voltage-current characteristic of the superconductor. A typical voltage-current characteristic is shown in Fig. 4. The low current portion of the characteristic shows virtually zero voltage, or perhaps a small current-transfer voltage. The high current portion shows an onset of flux-flow voltage

which increases sharply with current. The voltage in the flux-flow region is reversible and constant in time. It can be measured in some superconductors over many orders of magnitude in voltage. If the sample could be held at a constant temperature, this flux-flow voltage would increase with current until the normal state voltage-current characteristic was reached. However, the power dissipation in the flux-flow region will generally cause an irreversible transition (thermal runaway) from the flux-flow region into the normal state.

The electric field criterion indicates the voltage drop per unit length of the superconductor in the flux-flow state at the critical current. Typical values range from 0.1 to 10 μV/cm for conductors with critical currents of less than 600 amperes. The resistivity criterion refers to the effective resistivity of the superconductor in the flux-flow state, that is, the voltage drop per unit length divided by the current per unit area ($\rho = VA/LI$). Typical values for the resistivity criterion range from 10^{-12} to 10^{-10} Ωcm using the total cross-sectional area of the conductor. One problem with the resistivity criterion is deciding what area is to be used to calculate the resistivity. In the case of a NbTi conductor one of two cross-sectional areas is commonly used, the total area of the conductor, or just the area of the NbTi. For a Nb_3Sn conductor the cross-sectional area used may be: the total area of the conductor, the non-copper area (which may include the area of the diffusion barrier, bronze, Nb, and Nb_3Sn), the area of the Nb and Nb_3Sn, or the area of the Nb_3Sn alone. The determination of some of these areas involves extensive metallography and statistical techniques, which means they are difficult and very time consuming for another investigator to verify. For the round robin multifilamentary Nb_3Sn superconductor, the total cross-sectional area was about 14 times the cross-sectional area of the Nb and Nb_3Sn. The resulting

critical current measurement using a resistivity criterion of 10^{-11} Ωcm and these two areas gave critical-current values different by about 19% at 7 tesla.

The choice of the area involves the particular interpretation or use of the resulting data. For a designer, the resistivity criterion using the total cross-sectional area of the conductor is most appropriate considering the helium refrigeration requirements. The manufacturer, however, considers the use of the other areas appropriate as a figure of merit for a particular process and considers the use of the total area as a competitive penalty for highly stabilized conductors. This natural polarity in the choice of the area seemed to be unresolvable, so the electric field criterion was adopted for the standard test method for measurement of critical current.

The electric field criterion does not penalize the highly stabilized conductor and can easily be converted into an equivalent resistivity criterion using the total cross-sectional area of the conductor. One should note that a given electric field criterion does not correspond to the same resistivity criterion at all values of magnetic field. At high fields a given E_c corresponds to a larger value of resistivity than it does at low fields. This could be a problem very near to the upper critical field, H_{c2}, but our standards effort is specifically restricted to fields less than 0.8 H_{c2}. Furthermore, if desired, the effect can be circumvented by calculating the specified electric field criterion on the basis of any other criterion, which may depend on magnetic field and/or current. Under this framework the electric field criterion is considered to be expedient and verifiable.

The criterion dependence of the critical current was measured on each of the round robin samples. The percentage change in critical current relative

to the critical current at 1 μV/cm is given as a function of magnetic field in Figs. 10, 11, and 12. The critical current (as measured by NBS) of each of the round robin samples at 4 K and an electric field of 1 μV/cm was: 281A at 4T and 111A at 8T for the NbTi; 248A at 4T and 114A at 8T for the MF Nb_3Sn; 308A at 4T and 177A at 8T for the Nb_3Sn tape. At a given magnetic field, the flux-flow electric field (E), and thus the criterion dependence, can best be described by the following expression:

$$E \alpha I^n \qquad (1)$$

where I is the sample current and n is a real number. In general, n is a weak function of E and magnetic field. The multifilamentary NbTi (n ∿40) and the multifilamentary Nb_3Sn (n ∿20) samples had values of n which were very weak functions of E and magnetic field for the range tested. The value of n for the Nb_3Sn tape was ∿200 at 4T and ∿100 at 8T.

C. Sample Current, Resistance Ratio, and Self Field

There is presently no detailed study indicating the effect of current variations on the critical current measurement process. These variations occur both as current ripple and, for higher current supplies, SCR spikes. Two, very preliminary, attempts to look at this problem were made. The first, illustrated in Fig. 13, compares the values of I_c obtained (by NBS) at various magnetic fields using a battery to those found using an SCR-regulated supply. Sample currents were in excess of 400 A at the lower fields. Two different wires were compared. The results clearly indicate no significant effect. Measurements were also made on a high-current (∿7000 A at 6T) conductor by Airco using varying degrees of filtering of a 12 kA dc power supply. The critical current was measured in the presence of ripple (120-360 Hz)

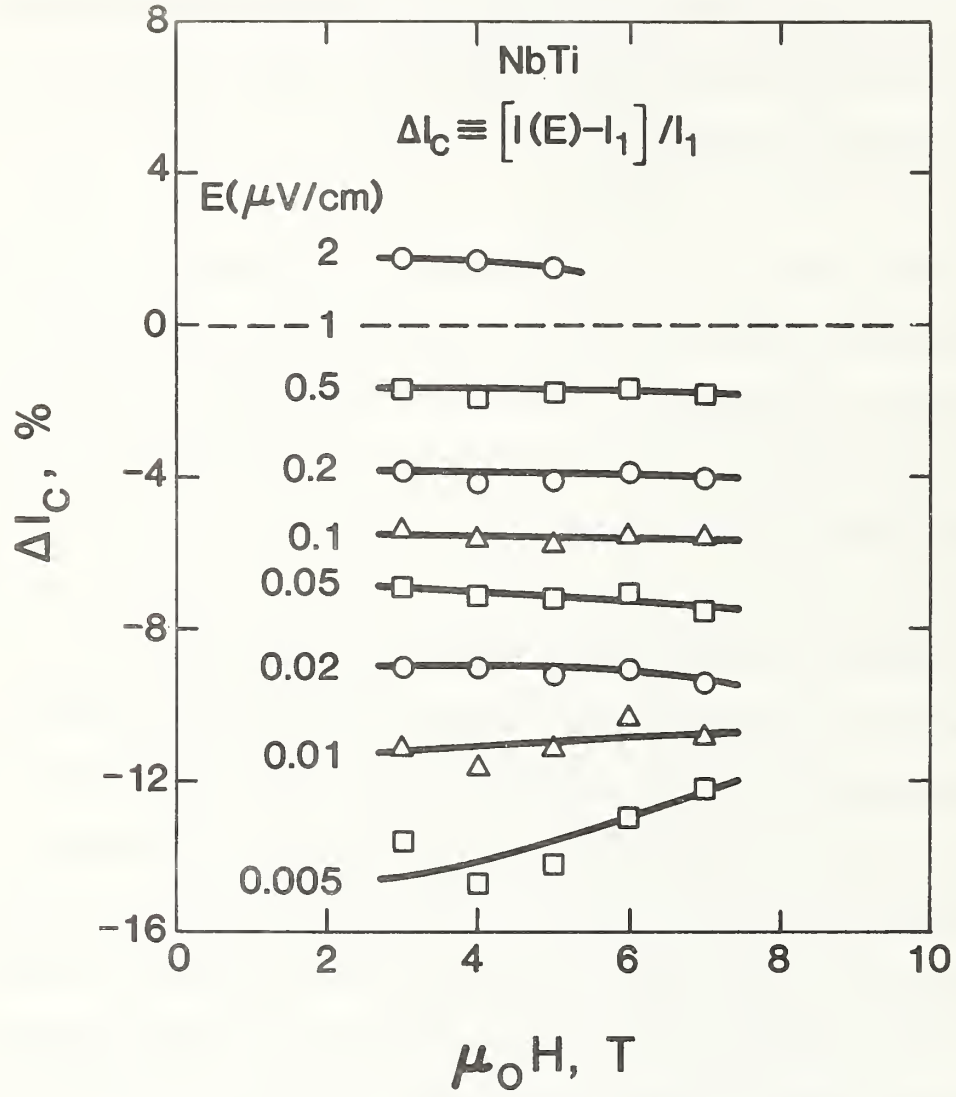

Figure 10. Relative criterion dependence of the critical current of a NbTi conductor. The base value used is 1 μV/cm.

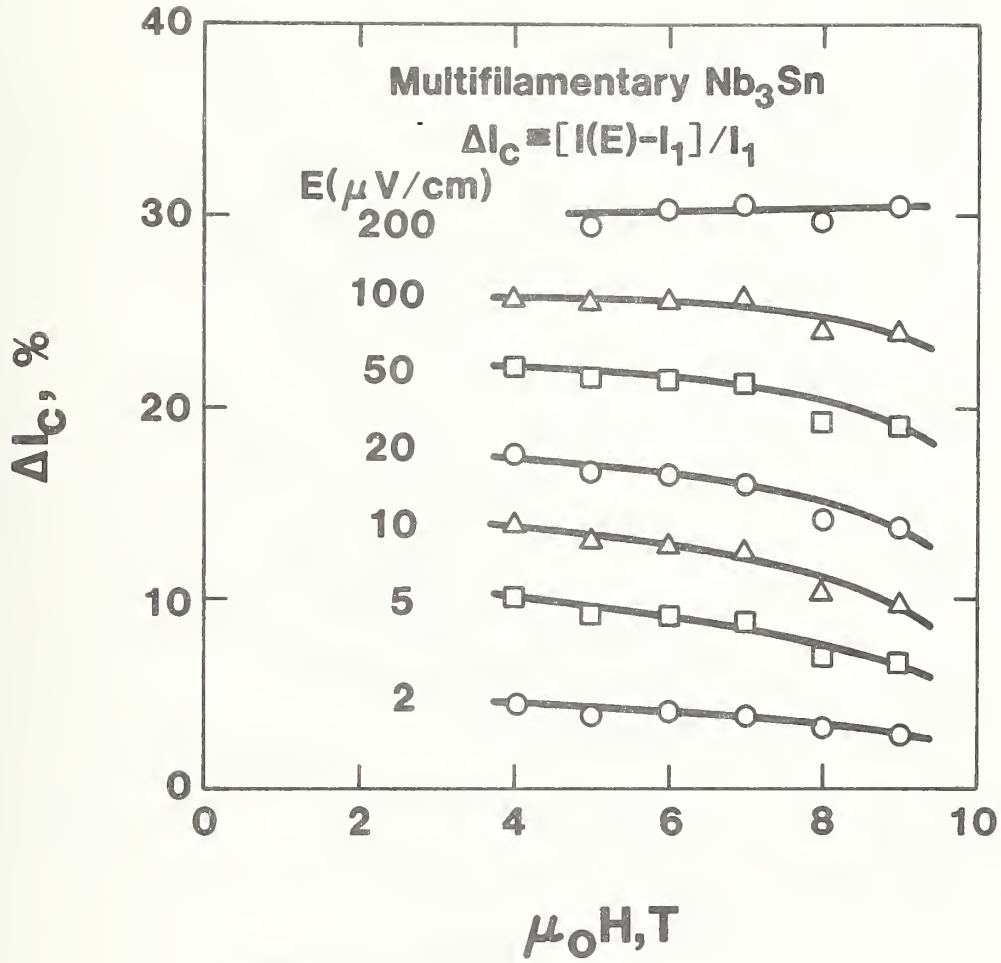

Figure 11. Relative criterion dependence of the critical current of a multifilamentary Nb_3Sn conductor. The base value used is 1 μV/cm.

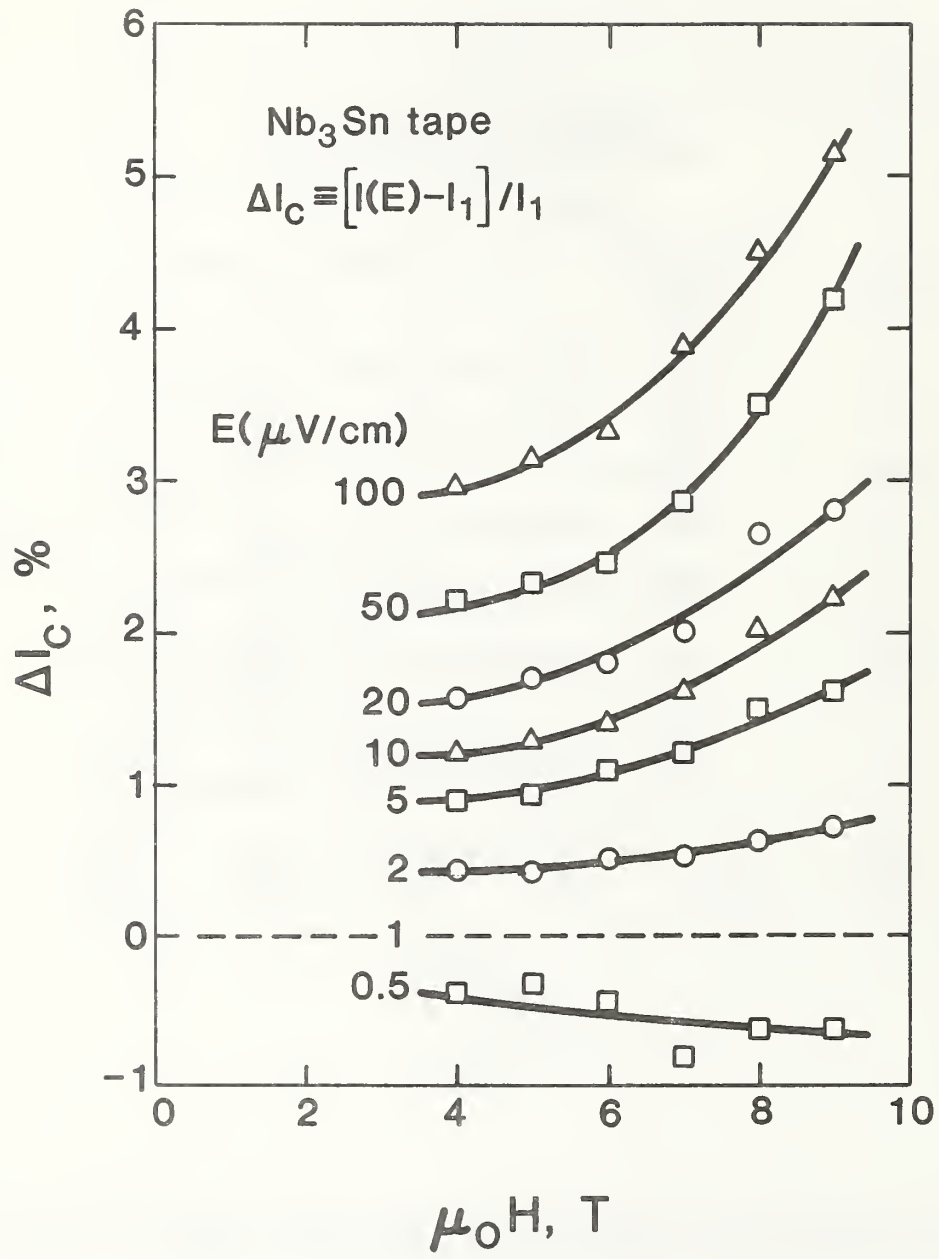

Figure 12. Relative criterion dependence of the critical current of a Nb_3Sn tape conductor. The base value used is 1 μV/cm.

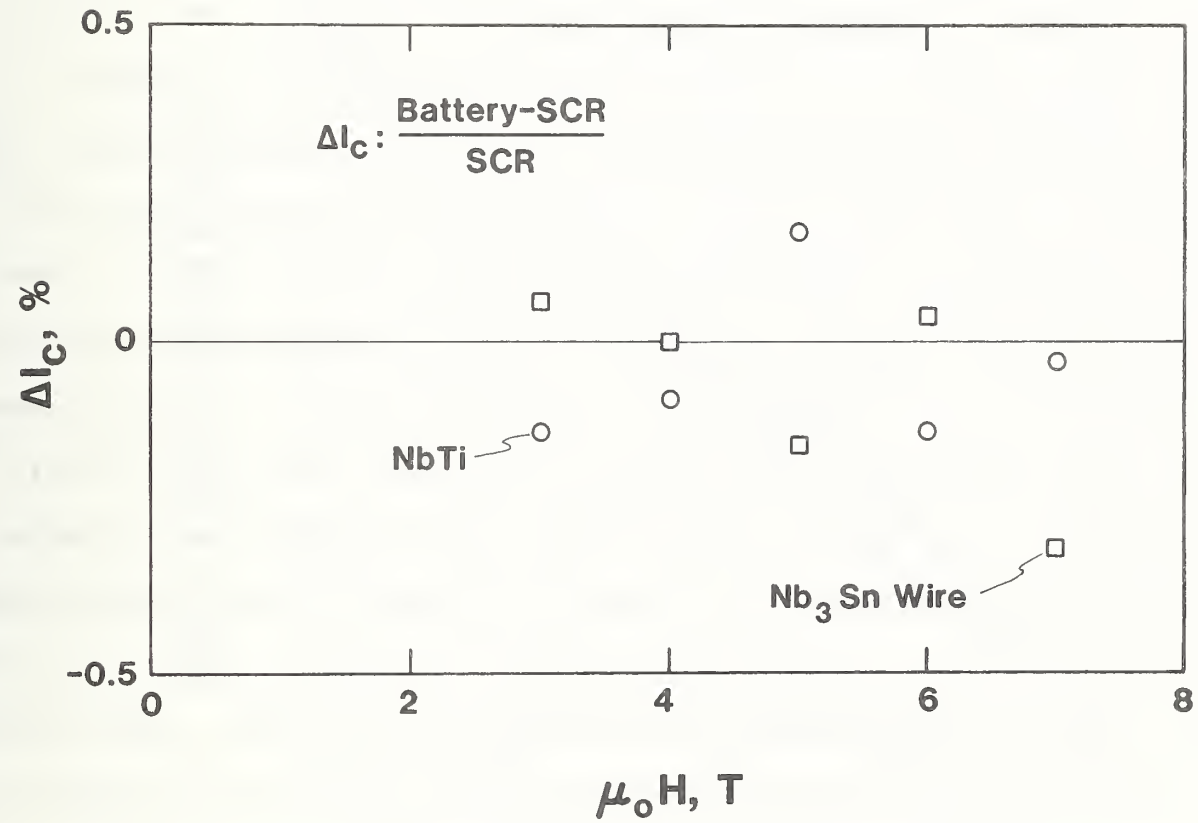

Figure 13. Comparison of critical current measurements made using different sources of sample current. Data for two types of wire are shown.

comprising 14, 22 and 110% of the dc current. The quench currents were essentially the same, but they were quenches and not the smooth, reversible behavior required for a true I_c determination. In summary, it appears that sample current variations are probably not a serious source of error in critical current measurement. However, the question is by no means settled and work is continuing.

The resistivity of the matrix of a practical superconductor is an important parameter in the determination of conductor stability. The effect of matrix resistivity on the measured critical current is not well known. Again, some preliminary results related to this question were obtained. The effect of adding matrix material to a wire was studied by MCA. Results of their experiment, in which strands of pure copper were cabled with a superconducting wire to effect an increase in copper-to-superconductor ratio, are shown in Fig. 14. It appears that, as expected, there is a "threshold" amount of copper required, but that beyond that, additional copper does little to increase I_c. The (tougher) question that remains to be answered is whether varying the resistivity of a fixed amount of copper will have a similar effect. Techniques for the reproducible measurement of resistance ratio of the stabilizer of a practical superconductor were investigated by IGC. Their report describes a device for making these measurements and gives resistance ratio data for a number of their conductors. It is worth noting that the measured resistance ratio for the composite superconductor is not that of the copper alone unless the superconductor resistivity is quite high and its normal state resistance ratio is small.

It has been more or less accepted that the self field due to currents in conductors of the size treated in this program (I_c < 600 A) has a negligible effect on the critical current measurement. On the other hand, it could be a

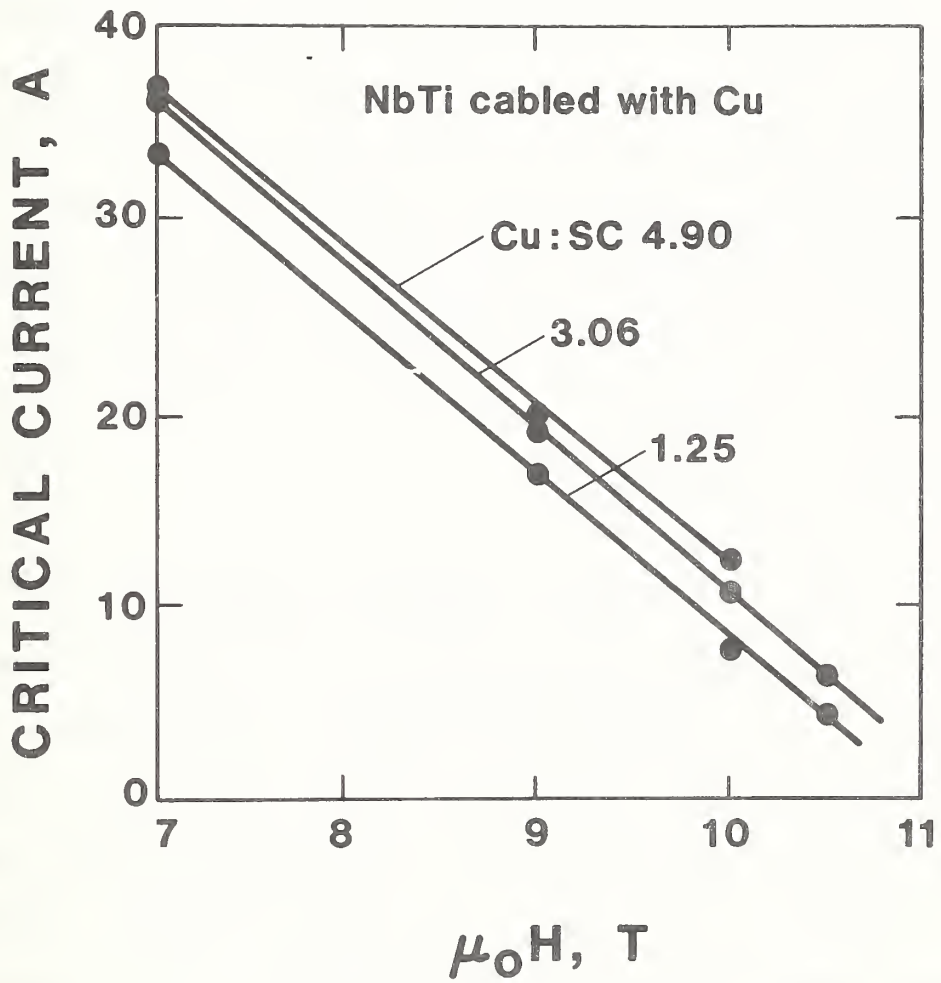

Figure 14. The effect of added copper on the critical current of a practical superconductor. Copper strands were added by cabling. Contractor data (see page 149).

significant effect in large conductors with high current densities. Both of these contentions were treated by IGC in their theoretical and experimental work on self field effects. Their theory indicates that one should expect a very small effect in practical wires that most likely would be masked by other conductor variables. However, as expected, the effect will be largest in the larger conductors. An attempt to see the effect in large conductors was made using a 10 kA conductor with twist pitches varying from infinity to 2.5 cm, the latter representing five wire diameters. Various experimental difficulties were encountered, but the tentative conclusion was that no effect of twist pitch could be detected. Measurements on smaller conductors gave somewhat ambiguous results perhaps indicating a decrease in I_c with twisting. It seems reasonable to make the general conclusion that if twist pitch has little or not effect then the self field is not a large contributor to uncertainty in critical current determination.

D. Field Orientation and Uniformity

The effect on the critical current of field orientation relative to the dimensions of a rectangular conductor has been described above (see Figs. 8 and 9). Large variations are found and their sense depends on the specifics of the conductor. Those measurements were made with the field always normal to the conductor axis and, thus, to the current direction. Figure 15 shows a different aspect of the field-orientation problem. In this experiment by Airco a round NbTi conductor was used to wind several coils with different twist pitches so that the effect of field angle with respect to the current direction could be determined. The important conclusion from the data is that the critical current measured in a coil sample wound in any reasonably normal fashion will not be significantly different from the intrinsic value.

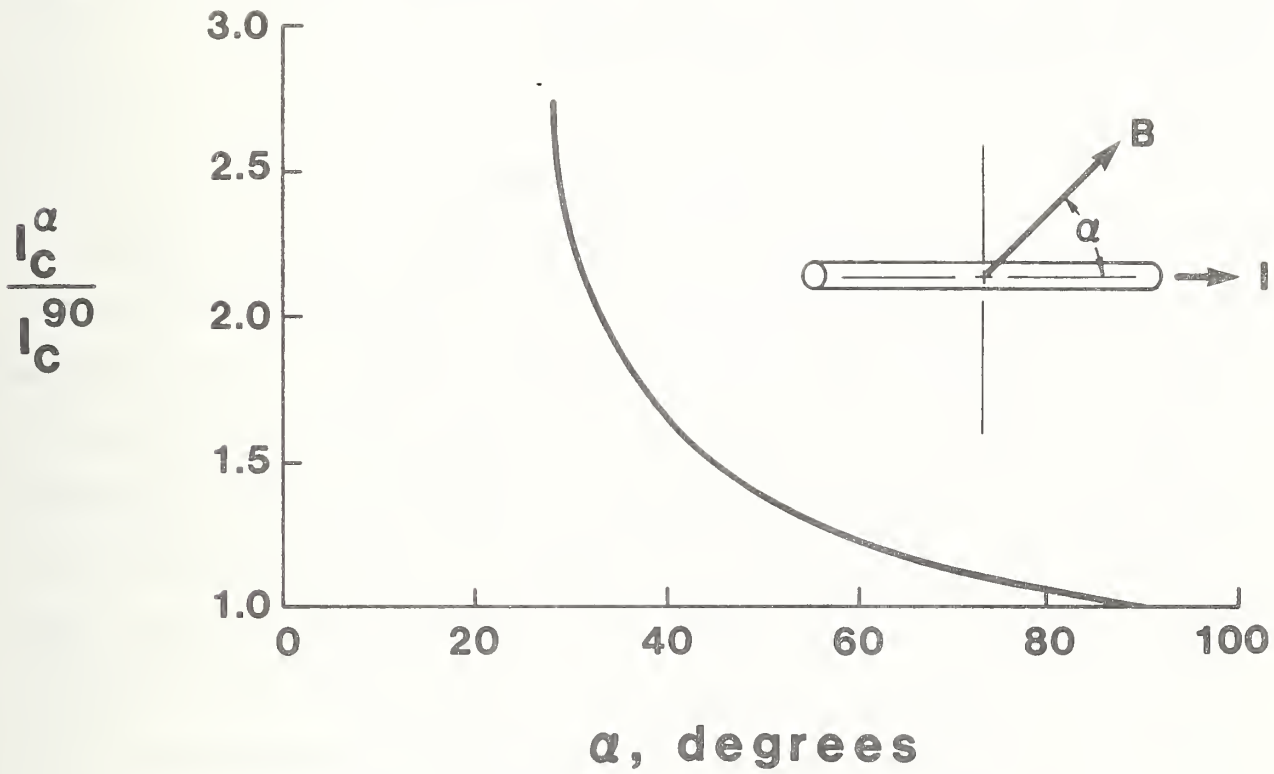

Figure 15. Relative critical current values as a function of angle between the magnetic field and the current direction in a circular NbTi conductor. The data represent values averaged over magnetic fields to 9T. Contractor data (see page 83).

Another component of the Airco study dealt with the effect of magnetic field inhomogeneity on critical current test results. Noninductively-wound coil samples were placed in various field gradients with a fixed value of maximum field and their critical currents measured. The results are shown in Fig. 16 taken directly form their report. Again, the conclusion is that, with reasonable care in positioning a sample, no significant critical current error should be introduced by field gradient effects.

E. Conductor Parameters

Much of the work reported here implies that modern practical superconductors are of very uniform composition. In fact, significant variations may exist even in the relatively easily produced NbTi conductor. Several experiments were done to investigate the effect of such variations on the critical current determination. Also, many large conductors are made up of smaller strands and we wished to see if this cabling had an effect on the resulting value of I_c. This last question is easily disposed of by considering Table 2, made up from Airco data. The cables are made up of sets of triple strand multifilamentary Nb_3Sn wires. The cable labeled 3^4 is fully transposed and compacted in a copper tube. Clearly, the final I_c of a multi-strand cable is just the product of the I_c value for the basic strand and the number of strands. It is suggested that this satisfying result may not occur in highly deformed cables such as the common flat braid.

The remainder of the studies described here were done by Supercon and involved the measurement of critical current values for nominally similar NbTi wires from many billets representing several different lots of NbTi. Nearly all measurements were made in a 6T field. Figure 17 shows the overall

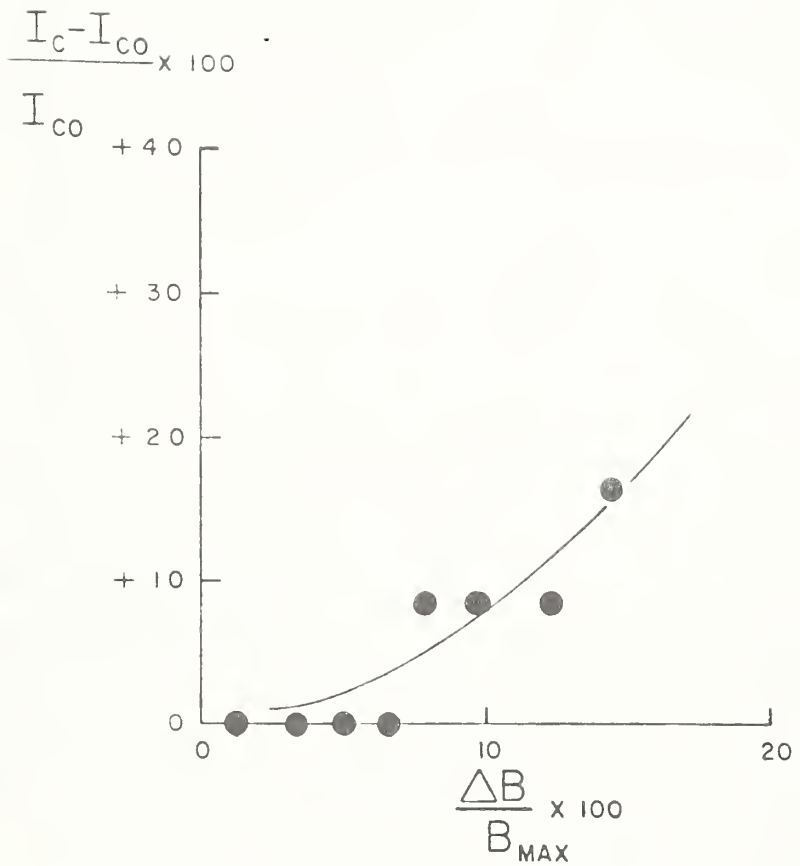

Figure 16. Critical current variation due to nonuniform applied magnetic fields. Contractor data (see page 77).

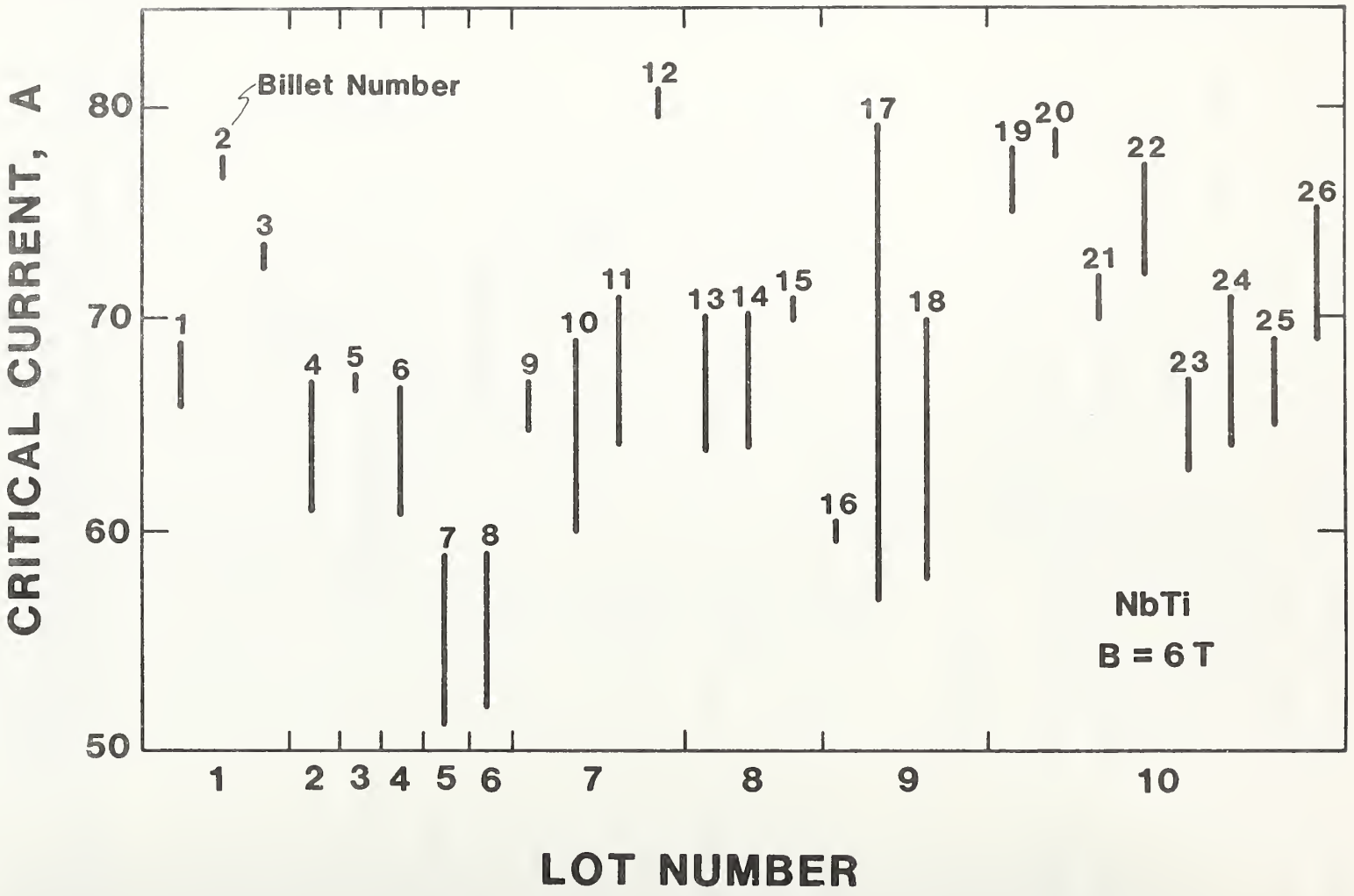

Figure 17. Variation observed in critical current of similar NbTi wires processed from different billets. Each lot number indicates a different lot of NbTi alloy. Contractor data (see page 199).

Table 2. Critical current of cables from a basic strand

Type	No. of strands	I_c @ 8T, A	I_c (cable)/I_c (strand)
Single strand	1	125	-
3 strand triplet	3	374	3
3^2 cable	9	1125	9
3^4 cable	81	9500	79*

*I_c = 120 A for the single strand used to make this cable.

variation observed among the samples. Note that in some cases, more than one billet was prepared from NbTi of a given lot. Within a lot, a correlation was observed between the percentage of superconductor in the final wire and the critical current as shown in Fig. 18. This is not especially surprising, but note that the lines for different lots are not parallel, probably reflecting compositional differences in the NbTi. The variation in critical current observed along the wire from a single billet is shown in Fig. 19 again correlated with the variation in percent of superconductor measured along the same wire. Finally, the effect of severe deformation of the filaments on the critical current was investigated by measuring purposely deformed lengths of conductor. Their cross sections and critical currents are shown in Fig. 20. When the variation in I_c due to percent superconductor is accounted for, only the most severly deformed conductor shows any significant variation in critical current due to the deformation.

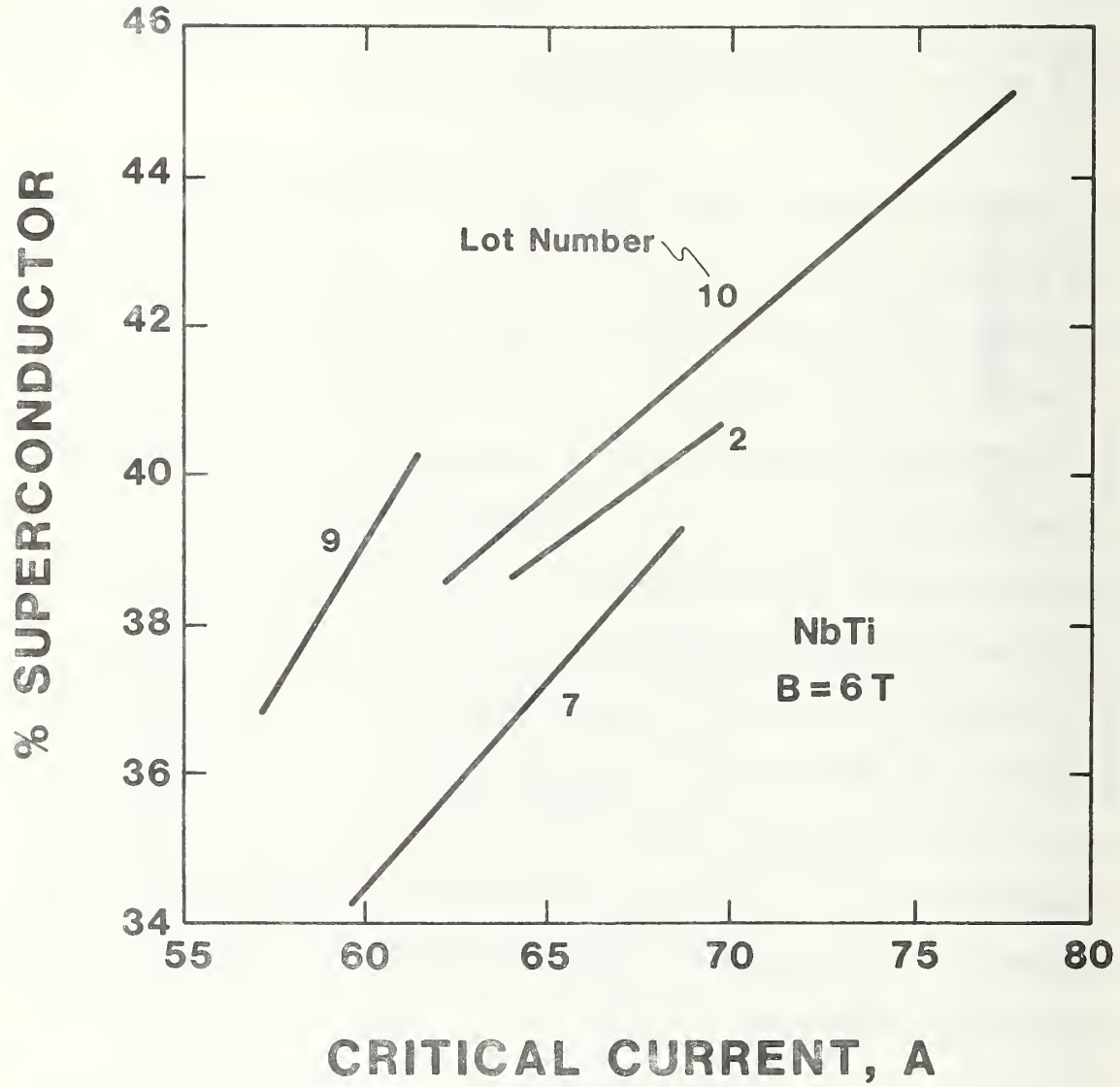

Figure 18. Correlation of critical current with percent superconductor in the final wire for several lots of NbTi alloy. Contractor data (see page 198).

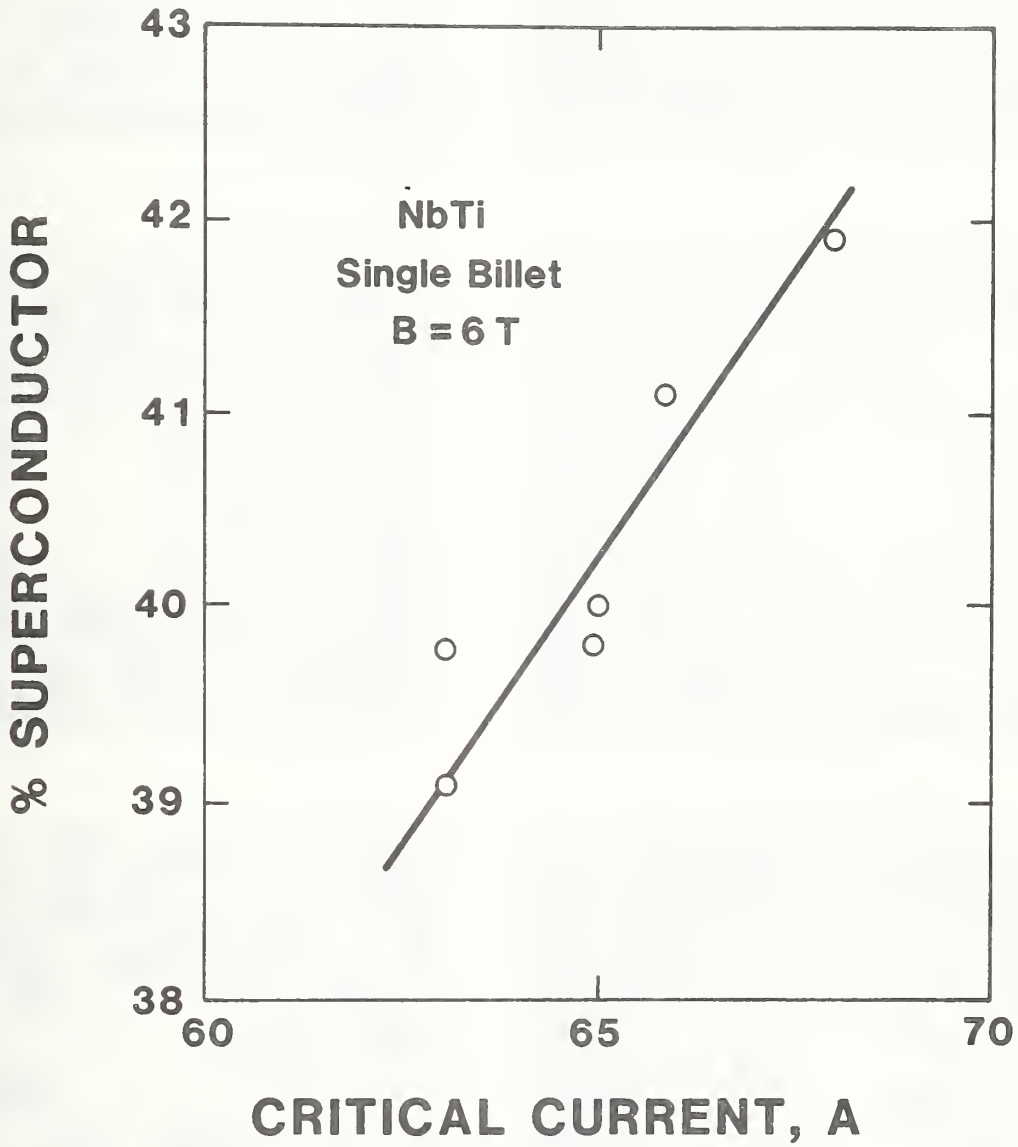

Figure 19. Variation in critical current observed along a wire from a single billet correlated with the measured percent superconductor. Contractor data (see page 200).

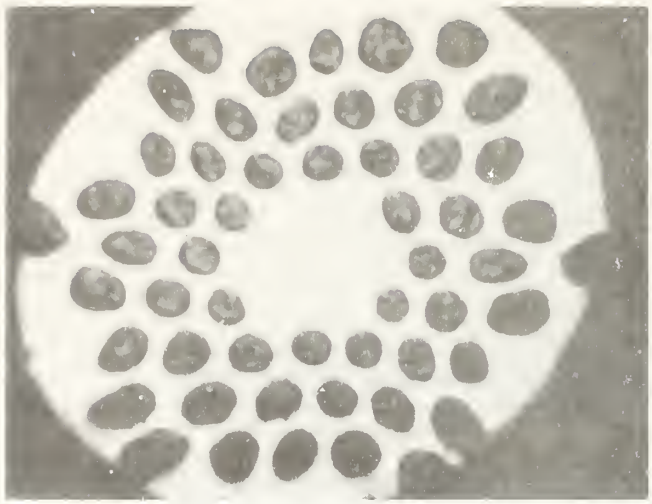

I_c = 856 A @ 8 T

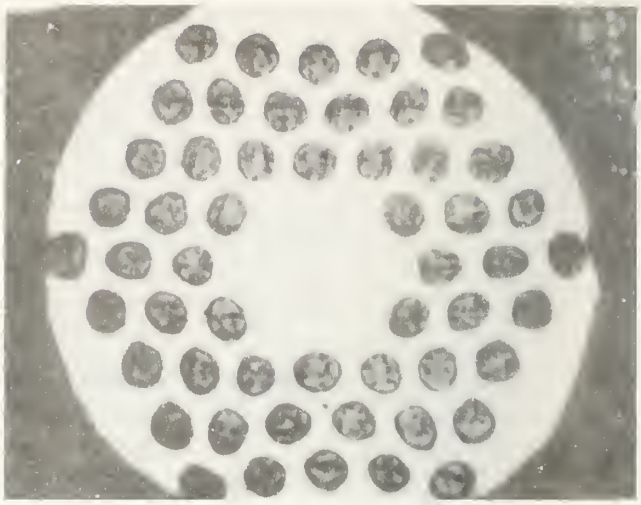

I_c = 911 A @ 8 T

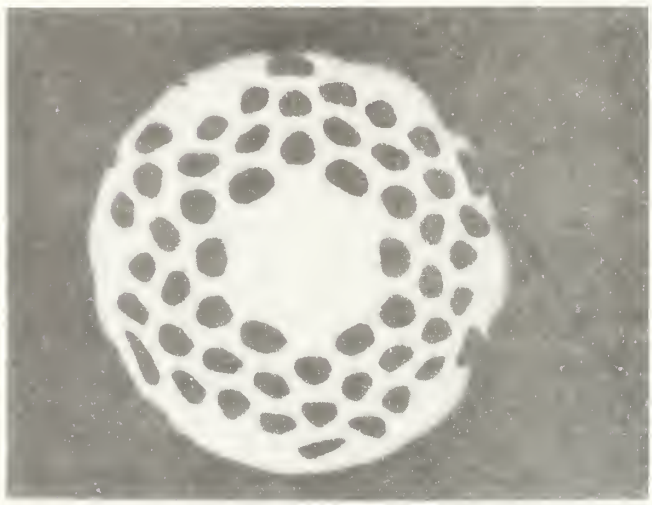

I_c = 788 A @ 8 T

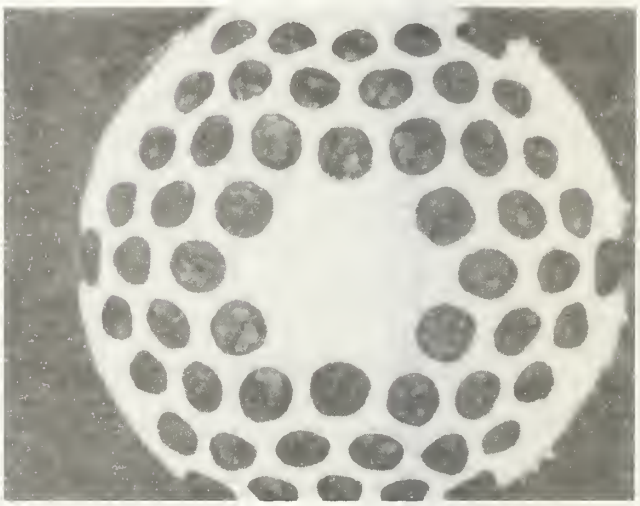

I_c = 786 A @ 8 T

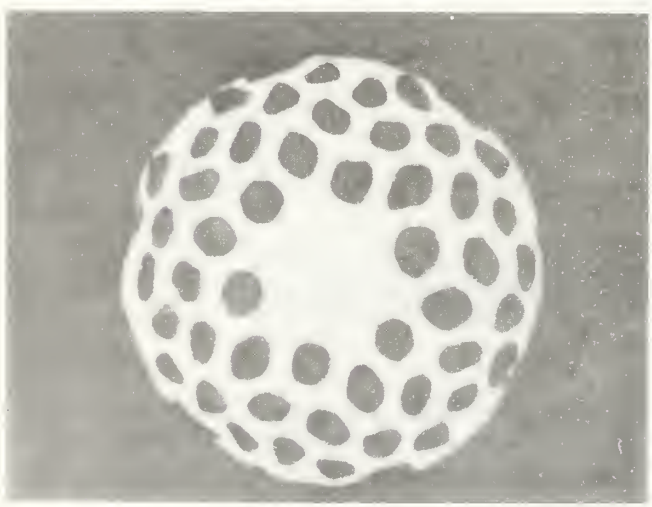

I_c = 856 A @ 8 T

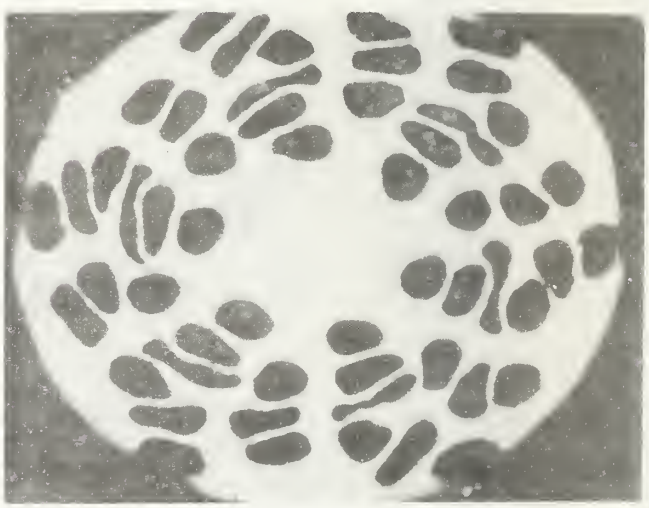

I_c = 759 A @ 8 T

Figure 20. Cross sections of deformed NbTi conductors and their measured critical currents. Contractor data (see page 202).

V. CONTRACTOR REPORTS

Many results from the research carried out by the U.S. wire manufacturers under this program have been presented and discussed above. The complete contractor program is described in last year's report [1]. The contract reports as provided to NBS are reproduced here. There has been only minor editing for format. The content of each report is the responsibility of the originating company. A list of contacts for each organization is given in Appendix B.

A. Airco Superconductors

DEVELOPMENT OF TESTING STANDARDS FOR SUPERCONDUCTORS

FINAL REPORT FOR WORK DONE UNDER
NATIONAL BUREAU OF STANDARDS

CONTRACT NO.: NB79RAC90029

Submitted by:
AIRCO SUPERCONDUCTORS
600 Milik Street
Carteret, New Jersey 07008

TABLE OF CONTENTS

SECTION

1.0 INTRODUCTION

2.0 EXPERIMENTAL STUDIES
2.1 Description of the Test Facility and Testing Geometries
2.2 Round Robin Test Series
2.3 Effect of Magnetic Field Inhomogeneity on Critical Current Measurements
2.4 Effect of Conductor Orientation with Respect to the Magnetic Field on Critical Current Meaurement
2.5 Effects of Imperfect Rectification and Filtering of an SCR Controlled Current Source
2.6 Support for the Validity of Determining I_c (Cable) from I_c (Strand)

3.0 CONCLUSIONS AND RECOMMENDATIONS

1.0 INTRODUCTION

This report is an account of the work carried out at Airco Superconductors during the period from September 10, 1979 to April, 1980. The purpose of this effort is to assist the National Bureau of Standards in the development of standards fulfilling the needs of the superconducting industry. In the present contract, this assistance has been directed first, at participating in all the various group activities being pursued to generate these standards, and second, at investigating and measuring several parameters required as a data base for the establishment of tolerances in the standards.

In the former catergory Airco Superconductors is participating in the workings of ASTM Subcommittee B-1.08 on Superconductors, prepared samples for and completed the round robin critical current measurements (these results are presented in this report), responded to the critical current measurement questionnaire, and is cooperating with other superconducting technologists on formulating a draft of testing standards.

The experimental portion of this effort has included preliminary studies of the variation of critical current due to:

1) the effect of magnetic field inhomogeneity;
2) the effect of orientation of sample conductor with respect to the magnetic field;
3) the effect of imperfect rectification and filtering of an SCR controlled current source.

Furthermore, experimental test data is being contributed to the program so that it may be used in the formation of a reliable standards data base. In particular, measurements on both cabled conductors and the individual strand of the cable have been made and are included in this report.

2.0 EXPERIMENTAL STUDIES

2.1 DESCRIPTION OF THE TEST FACILITY AND TESTING GEOMETRIES

The first task of the experimental program was directed at recalibrating and verifying the accuracy of the superconducting solenoid test magnet as well as the current shunts and voltmeters.

2.1.1 Test Facility

The test solenoid is dimensionally specified in Figure 1 and can be used to generate magnetic fields of up to 9.5 T. Both its transfer constant and field profile were confirmed using a Rawson-Lush rotating coil probe. The radial and the axial magnetic field components were measured for three radial positions (0.0, 1.6, and 2.2 cm) and 18 axial locations. These measurements are presented in Table 1 and were used to determine the absolute magnitude of the magnetic field at the locations where the sample test fixtures were to be placed. For example, /H/ is given for r = 2.2 cm as a function of z in Figure 2. This profile will be used later in evaluating the test data taken for the non-inductively wound long sample test fixture. In general, the field profiles obtained in this manner correspond well to the expected behavior of a solenoid.

2.1.2 Test Geometries

It has generally been the rule that the test methods adopted by a particular organization are governed not only by the size and shape of the conductor, but also by the available facilities. For this reason, Airco Superconductors has developed three

TABLE 1: Axial (H_z) and Radial (H_r) Components of Magnetic Field as a Function of Distance Above Center (z) at Three Radial Positions (r)

	r=0.0cm		=1.6		=2.2	
	H_r	H_z	H_r	H_z	H_r	H_z
z=0.00cm	---	[49989]	---	50249	----	50269
1.03	100	49630	566	49960	----	50100
1.67	63	49230	---	49590	1422	49600
2.30	110	48550	773	48990	1506	48820
2.94	114	47600	927	48200	1907	47900
3.57	190	46400	1088	47150	2150	46700
4.21	212	45000	1303	45730	2803	45250
4.84	271	43420	1507	44000	3165	43550
5.48	327	41750	1786	42050	3606	41500
6.11	349	39750	2007	39800	4494	38900
6.75	399	37600	2211	37400	5311	36320
7.38	252	34800	2390	34500	6040	33600
8.02	204	31600	2538	31400	6383	31020
8.65	204	27950	2568	28350	6345	28300
9.29	242	23700	2572	24200	----	25700
9.92	248	-----	2436	-----	6053	23020
10.56	2740	-----	----	-----	5336	20050
11.19	----	-----	----	-----	3849	17800

ALL FIELD UNITS IN 10^{-4} TESLA

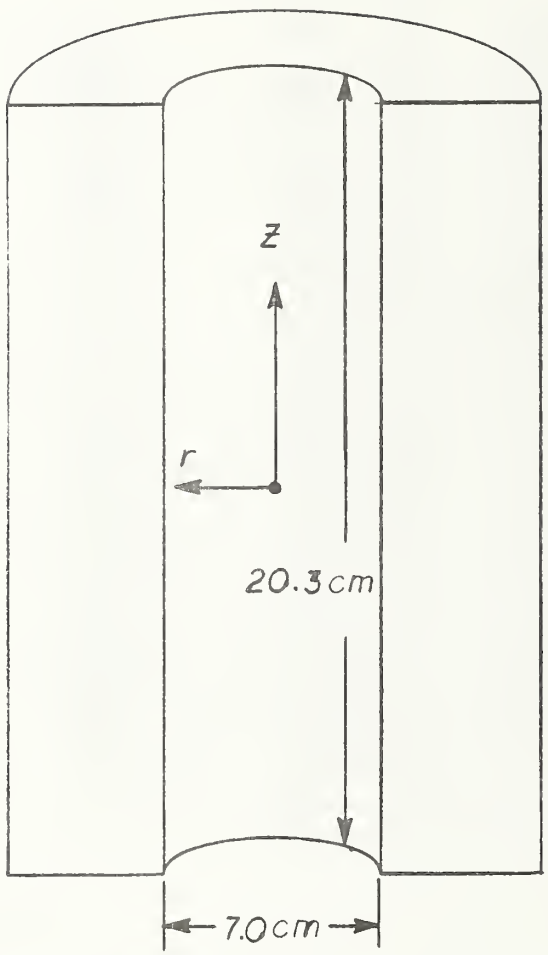

Figure 1. Coordinate System and Dimension of the Test Magnet Utilized in this Program.

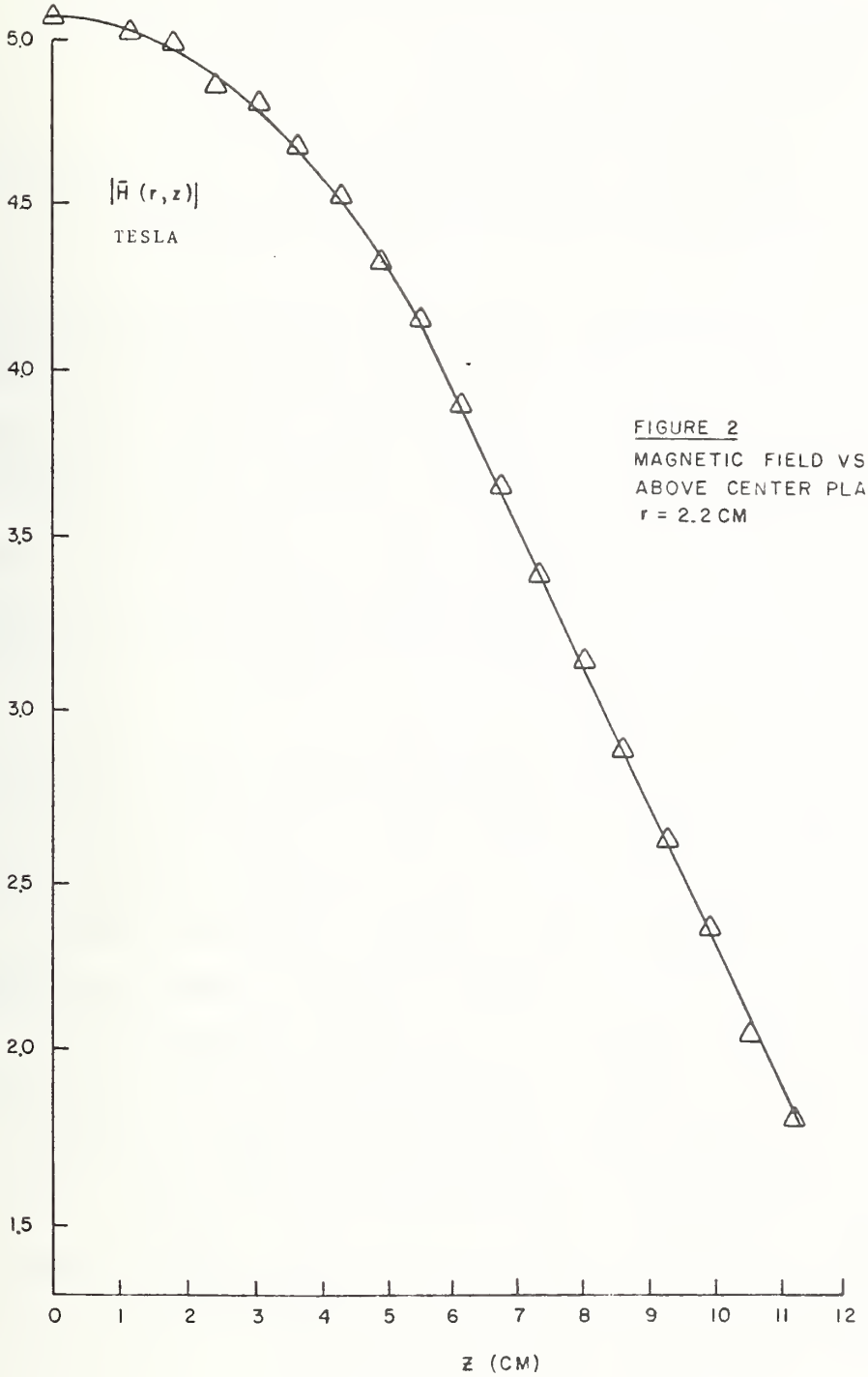

FIGURE 2
MAGNETIC FIELD VS DISTANCE
ABOVE CENTER PLANE FOR
r = 2.2 CM

types of test fixtures which meet 95% of its testing needs and are compatible with its facilities. The three types of samples which can be tested are:

1) noninductively wound long samples;
2) inductively wound short samples and;
3) a hairpin shaped sample.

Specific test fixture parameters are delineated in Table 2.

The noninductively wound long sample test fixture, shown in Figure 3, is particularly suitable for testing small diameter NbTi wire and permits accurate critical current measurement at very low voltage sensitivities. However, Nb_3Sn superconductor can not be easily tested on this fixture. This fixture was used in the round robin measurement of the NbTi wire and selected as the configuration most suitable for the study of field inhomogeneity effects (Section 2.3).

Two variations of the inductively wound cylindrical test fixture are being used and differ only in the placement of the voltage taps. In the first variation (designated 2a), the voltage taps measure one full turn of sample. One voltage lead is co-wound parallel to the turn of sample conductor being measured to reduce noise pick-up. The second configuration (2b), shown in Figure 4, samples only a 2 cm length of conductor in the central most portion of the sample coil. Either configuration can be readily used for both NbTi and Nb_3Sn. Both of the Nb_3Sn samples included in the round robin tests were testd on these test fixtures. The orientation studies (Section 2.4) were also performed on these fixtures.

TABLE 2: TEST FIXTURE GEOMETRIES

Winding Configuration	Characteristic Dimensions	Distance Between Voltage Taps	Suitability for Wire Types
1. Noninductively wound, cylindrical	5 cm dia. x 2.1 cm long	40 cm	Small NbTi
2a. Inductively wound, cylindrical	4.16 cm dia x 2.1 cm long	13.7 cm	NbTi and Nb_3Sn
2b. Inductively wound, cylindrical	3.59 cm dia. x 2.1 cm long	2.0 cm	NbTi and Nb_3Sn
3. Hairpin	6.9 cm wide with 3 cm corners	1.9 cm	NbTi and Nb_3Sn

FIGURE 3: Noninductive wound long sample test fixture used for small diameter NbTi wire.

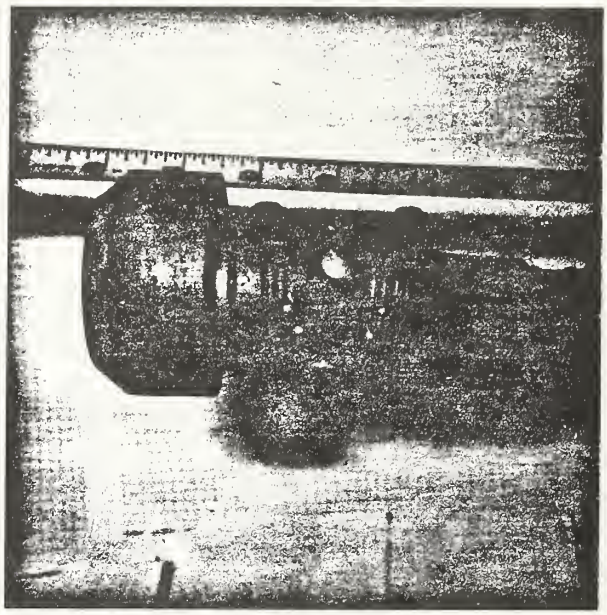

FIGURE 4: Inductive wound cylindrical test fixture.

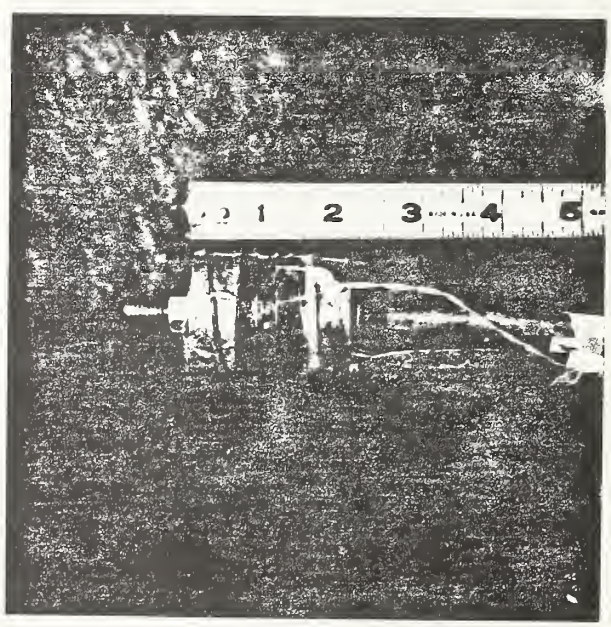

The third and final type of test fixture (shown in Figure 5) is the simple hairpin shape which is suitable for both Nb_3Sn and NbTi but is sensitive to field nonuniformities. This fixture is particularly useful when aspected conductors, such as tapes have to be measured with the applied magnetic field perpendicular to the broad face of the conductor. In both of the cylindrical fixtures, the field is applied parallel to the broad face of the conductor. For this reason, the Nb_3Sn tape in the round robin series was also measured on the hairpin test fixture.

FIGURE 5: Hairpin critical current test fixture.

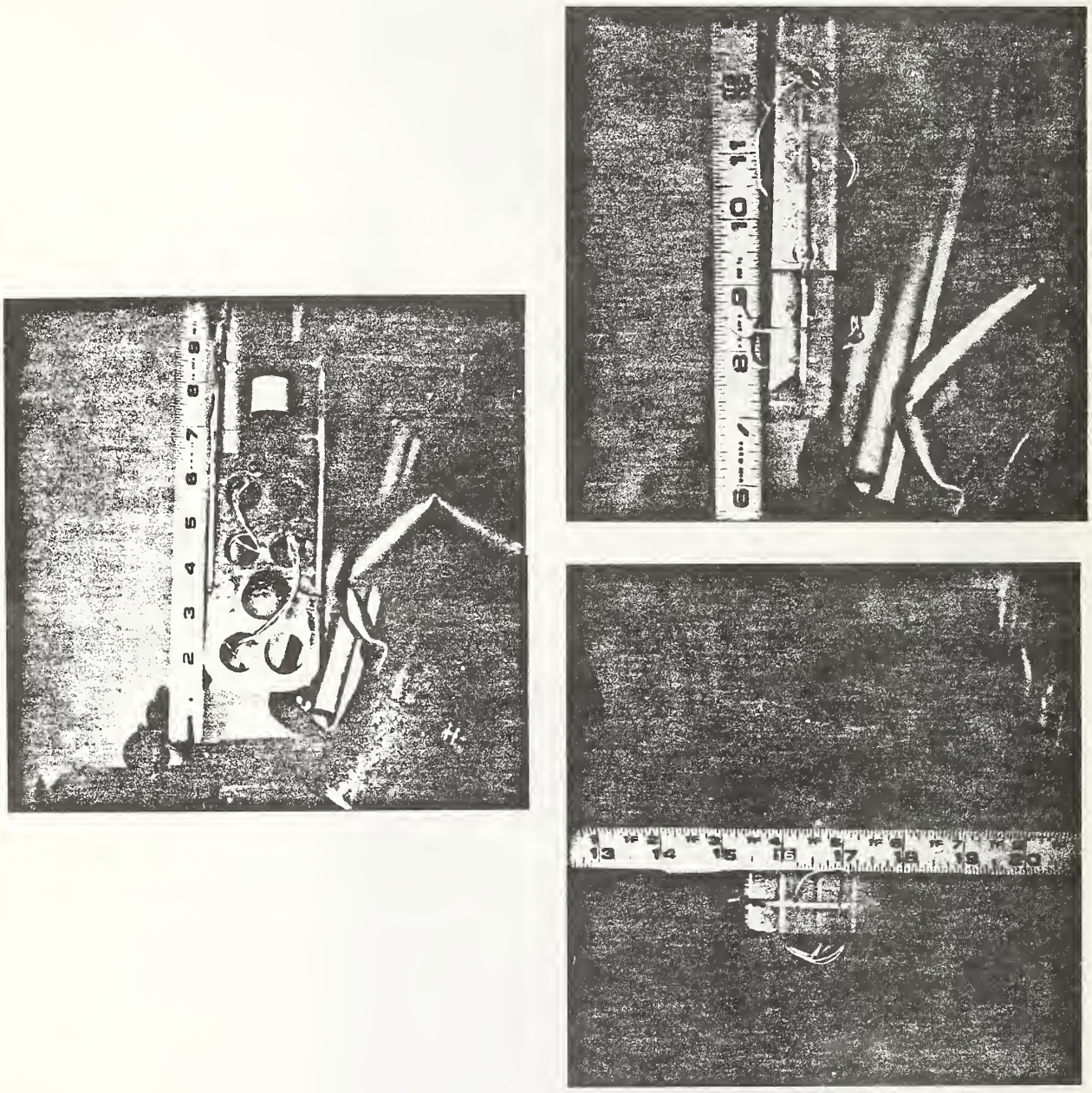

2.2 ROUND ROBIN TEST SERIES

Three different conductors were supplied to all the superconductor suppliers with the request that they be measured in the normal manner for each organization. It was recognized that differences between measurements of the various participants will be attributed not only to the test fixtures but also to the choice of voltage criteria. It is our experience that one single criterion can not adequately fulfill the requirements of the various types of wire produced by Airco Superconductors. Our organization therefore opted to avoid a debate on the merits of a particular criterion but rather to reduce the data using as many of the criteria as possible and reasonable including both of the two most widely used criteria, resistivity and electric field, in the hopes that comparisons can be more easily accomplished. The critical current obtained using these options has been tabulated in Table 4-7. Finally, for the specific wire type being measured, the criterion consistent with Airco Superconductors standard practice was used and the resulting values reported in Table 8.

2.2.1 Critical Current Criterion

The resistivity criterion requires not only a choice of the acceptable resistivity value but also of the cross-sectional area to be used in determining the resistance and subsequently the voltage. In the case of NbTi superconductor, this choice is straight forward and nominal resistivity levels of $1x10^{-12}$ and $1x10^{-11}$ ohm·cm were used in the round robin test series. The choices for Nb_3Sn conductors are more complicated since a simple division between superconducting components and low normal resistivity components is impractical to measure without subscribing to

extraordinary means. In this case, choices of several possible and appropriate cross-sectional areas have been made. They include the area of Nb_3Sn, the area of Nb + Nb_3Sn, and the area of Ta + Bronze + Nb + Nb_3Sn (sometimes referred to as the non-copper area). Once again nominal resistivity levels of 10^{-11} and 10^{-12} ohm·cm were used.

Applying the electric field criterion, to these tests is much simpler and clearer but its utility to a magnet designer can be debated. Sensitivities of 0.25 μ V/cm and 1.0 μV/cm were chosen for the round robin test series.

The test fixture, test conditions and these various criteria options are presented in detail in Table 3 for the three conductors measured.

2.2.2 Round Robin Test Results

For the purpose of this report, each conductor was described by a photomicrograph, a typical V-I curve at 6 T (Figures 6-8) and the critical current determinations for the various criteria feasible (Figures 6-8 and Tables 4-7). The critical currents, as would normally be defined by Airco Superconductors, are given for each wire in Table 8 and shown in graph form in Figure 9. A word of caution against drawing too many conclusions from Figure 9 is appropriate. The three different conductors range so widely in design that an absolute comparison based on current is not valid. General characteristics of NbTi and Nb_3Sn superconductors are illustrated particularly at high fields where NbTi is approaching its critical field.

Most of the values appear to be slightly less than the expected values. This apparent discrepancy may turn out to be associated with the critical current criteria. The difference between the two measurements of the Nb_3Sn tape can be attributed to the aspected

TABLE 3: CRITICAL CURRENT CRITERIA USED IN THE ROUND ROBIN SERIES

MATERIAL	CROSS-SECTIONAL AREA (cm^2)	TEST FIXTURE	RESISTIVITY CRITERION[+] (μV @ 50 A)	ELECTRIC FIELD[++] (μV)
Sample 1: NbTi composite	$A^{*}_{NbTi} = 1.33 \times 10^{-3}$	(1) Noninductively wound long sample	1.5 @ 1×10^{-12} Ω·cm 15 @ 1×10^{-11} Ω·cm	10 @ 0.25 μV/cm 40 @ 1.0 μV/cm
Sample 2: Nb_3Sn tape	$A^{**}_{Nb+Nb_3Sn} = 1.8 \times 10^{-3}$ $A_{Nb_3Sn} = 0.5 \times 10^{-3}$	(2a) Inductively wound sample	Using A_{Nb+Nb_3Sn} 0.6 @ 1.5×10^{-12} Ω·cm Using A_{Nb_3Sn} 2.03 @ 1.5×10^{-12} Ω·cm	3.4 @ 0.25 μV/cm
		(3) Hairpin sample	Using A_{Nb+Nb_3Sn} 0.1 @ 1.5×10^{-12} Ω·cm 1.0 @ 1.5×10^{-11} Ω·cm Using A_{Nb_3Sn} 0.28 @ 1.5×10^{-12} Ω·cm 2.8 @ 1.5×10^{-11} Ω·cm	0.5 @ 0.25 μV/cm 1.9 @ 1.0 μV/cm
Sample 3: Multifilamentary Nb_3Sn	$A^{***}_{Ta+Bronze+Nb+Nb_3Sn} = 1.41 \times 10^{-3}$ $A^{**}_{Nb+Nb_3Sn} = 0.28 \times 10^{-3}$	(2b) Inductively wound sample	Using $A_{Ta+Bronze+Nb+Nb_3Sn}$ 0.35 @ 1×10^{-11} Ω·cm Using A_{Nb+Nb_3Sn} 0.18 @ 1×10^{-12} Ω·cm 1.8 @ 1×10^{-11} Ω·cm	2 @ 1.0 μV/cm

* Measure by weight difference assuming Nb 46.5 w/o Ti.

** Using dimensions taken from photomicrographs.

*** Using actual wire dimensions after etching copper away.

\+ Total voltage in μV at 50A transport current for each conductor area and sample length. This point is used to define a constant resistance line whose insertion with the sample V-I curve determines the critical current.

++ Total voltage in μV for each conductor and the sample length of the fixture from Table 2.

FIGURE 6: a) Photomicrocgraph of NbTi aspected conductor measured in the Round robin Tests, and

(125x)

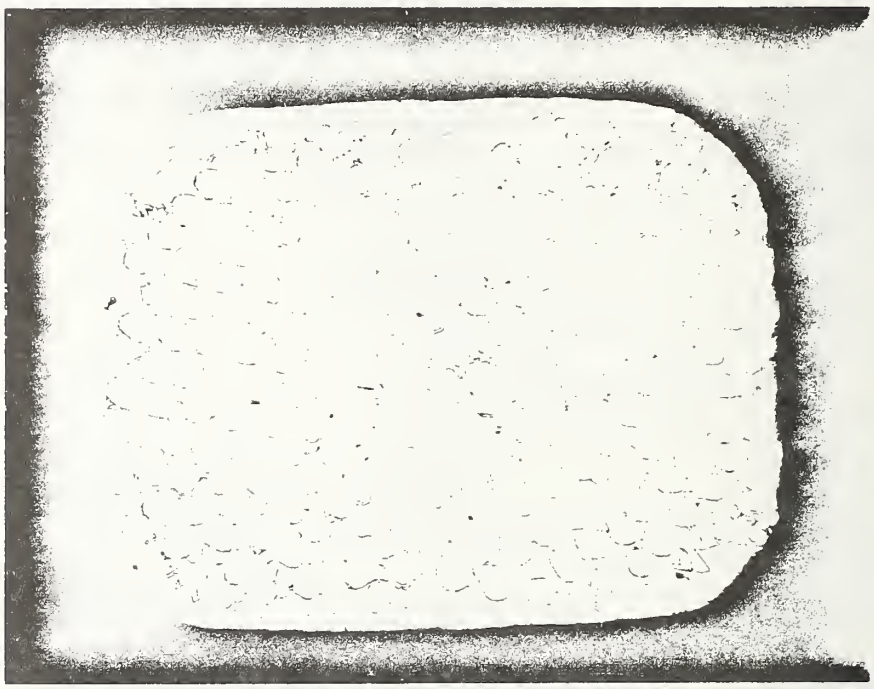

FIGURE 6: b) Typical V-I curve for this conductor

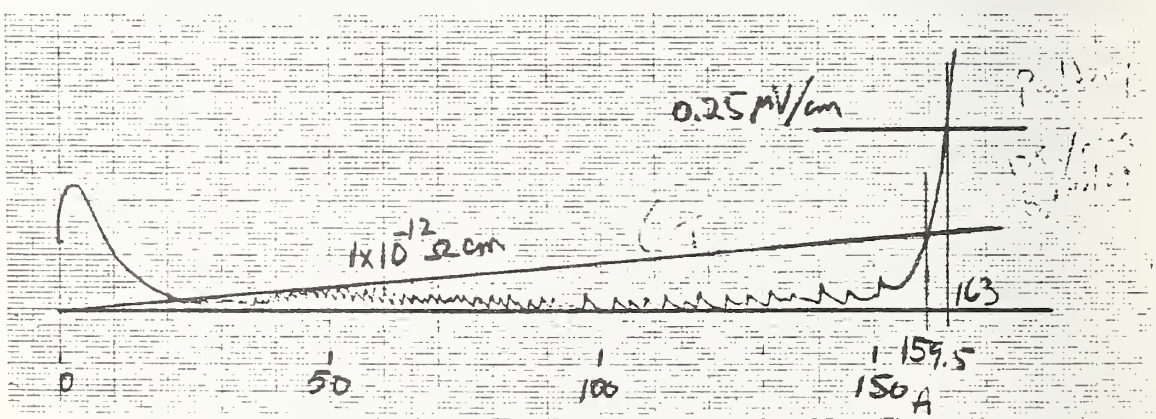

TABLE 4 TEST RESULTS for the NbTi CONDUCTOR PROVIDED in the ROUND ROBIN TEST

H Tesla	$I_c^{(1)}$ Amperes	$I_c^{(2)}$ Amperes	$I_c^{(2)}$ Amperes	$I_c^{(3)}$ Amperes
9.5	32.25	36	36	39
9.0	51.25	54	51.5	56
8.0	88.1	-	99	98
7.0	122.8	125.5	130	130
6.0	159.5	163		
5.0	200	203		
4.0	246	249		
3.0	306	306		
2.0	399	401		
1.0	590	590		
E_c [μV/cm]	--	0.25	--	1.0
ρ [ohm-cm]	1.0×10^{-12}	--	1.0×10^{-11}	--
	A_{NbTi}	--	A_{NbTi}	

FIGURE 7: a) Nb_3Sn tape provided for the Round Robin test program.

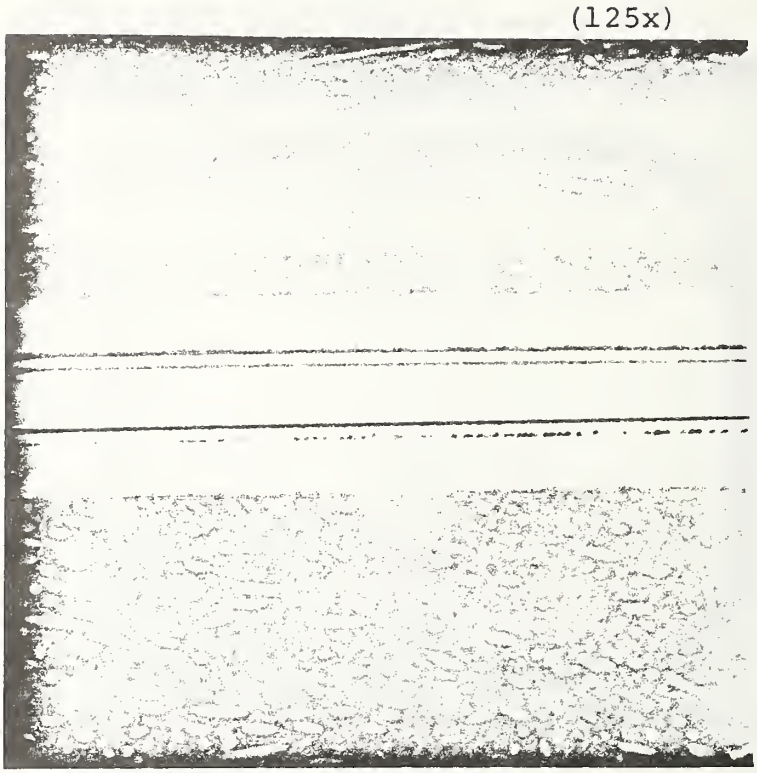

FIGURE 7: b) Typical V-I curve.

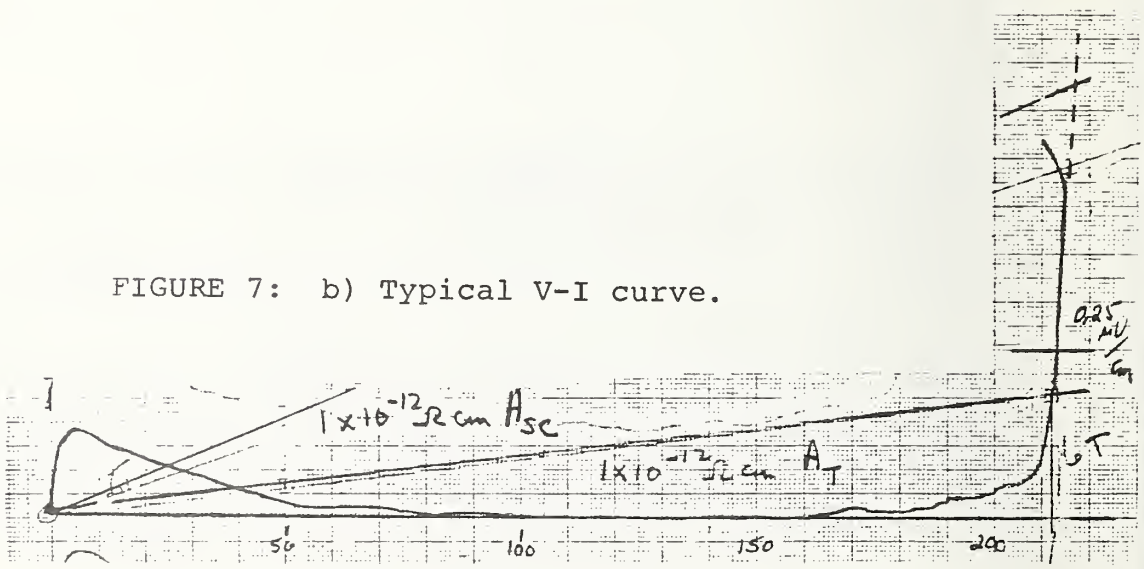

TABLE 5: TEST RESULTS FOR THE Nb_3Sn TAPE PROVIDED IN THE ROUND ROBIN SERIES MEASURED ON THE INDUCTIVELY WOUND CYLINDRICAL FIXTURE

H	I_c (1)	I_c (2)	I_c (3)
Tesla	Amperes	Amperes	Amperes
9.5	108	(111)	-
9	122	125	124
8	149	155	152
7	183	(186)	184
6	212	217	213
5	245	-	245.5
4	274	-	274
3	306	-	306
2	342	-	342
1.5	370	-	369
1.0	416	-	415
E_c [μV/cm]	--	--	0.25
ρ [ohm-cm]	1.5×10^{-12} Using A_{Nb+Nb_3Sn}	1.5×10^{-12} Using A_{Nb_3Sn} only	--

TABLE 6: TEST RESULTS FOR THE Nb_3Sn TAPE PROVIDED IN THE ROUND ROBIN SERIES MEASURED ON THE HAIRPIN FIXTURE

H	$I_c^{(1)}$	$I_c^{(2)}$	$I_c^{(3)}$	$I_c^{(4)}$	$I_c^{(5)}$
Tesla	Amperes	Amperes	Amperes	Amperes	Amperes
9.5	-	-	-	-	-
9	116	-	114	116	113
8.5	132	-	130	131	128
8	147	142	144	146	144
7.5	163	158	162	162	160
7	180	162	177	179	175
6.5	202	192	195	197	194
6	214	-	212	213	-
5	243	240	242	243	240
4	278	270	273	274	270
3	307	301	304	303	301
2	344	334	337	337	334

E_c [μV/cm]	--	--	--	1.0	0.25
ρ [ohm-cm]	1.5×10^{-11}	1.5×10^{-12}	1.5×10^{-12}	--	--
	---using $^{A}Nb + Nb_3Sn$-		-using $^{A}Nb_3Sn$ only-		

FIGURE 8: a) Photomicrograph of the multifilamentary Nb_3Sn wire measured in the Round Robin Test.

(160 x)

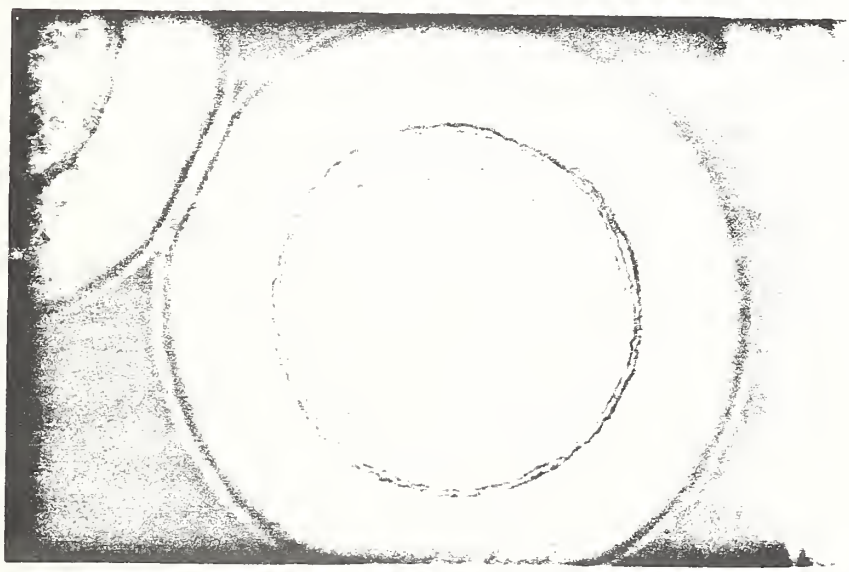

FIGURE 8: b) Typical V-I curve.

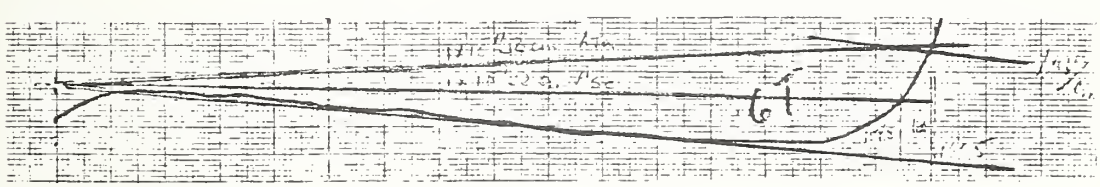

TABLE 7 TEST RESULTS for the Nb_3Sn MULTIFILAMENTARY WIRE PROVIDED in the ROUND ROBIN SERIES

H	I_c(1)Ta	I_c(1)SC	I_c(2)SC	I_c(3)
Tesla	Amperes	Amperes	Amperes	Amperes
9.5	79	83	75	79
9.0	87	93	84	88
8.0	105	110	102	103
7.0	127	137	122	128
6.0	160.5	170	154.5	160
5.0	196	210	185	191
4.0	254	264	249	235
3.0	317	343	302	304
2.0	433	464	408	395
1.5	521	558	511	505
E_c [μV/cm]	--	--	--	1.0
ρ [ohm-cm]	1.0×10^{-11} using $A_{Ta+Bronze+Nb+Nb_3Sn}$	1.0×10^{-11}	1.0×10^{-12} Using A_{Nb_3Sn} only	--

TABLE 8 RESULTS of the ROUND ROBIN CRITICAL CURRENT MEASUREMENTS (currents in Amperes)

Magnetic Field(T)	NbTi Wire(1)	Nb_3Sn Tape(2)		Nb_3Sn Multifilamentary Wire(3)
		Hairpin	Cylindrical	
2	399	337	____	433
4	246	273	____	254
6	159.5	212	217	160.5
8	88.1	144	155	105

CRITERIA

1.) NbTi wire: 1.0×10^{-12} Ω.cm and A_{NbTi}

2.) Nb_3Sn tape: 1.5×10^{-12} Ω.cm and A_{Nb_3Sn}

3.) Nb_3Sn MF wire: 1×10^{-11} Ω.cm and $A_{Ta + Bronze + Nb + Nb_3Sn}$

FIGURE 9

CRITICAL CURRENT VS APPLIED MAGNETIC FIELD FOR ROUND ROBIN TEST

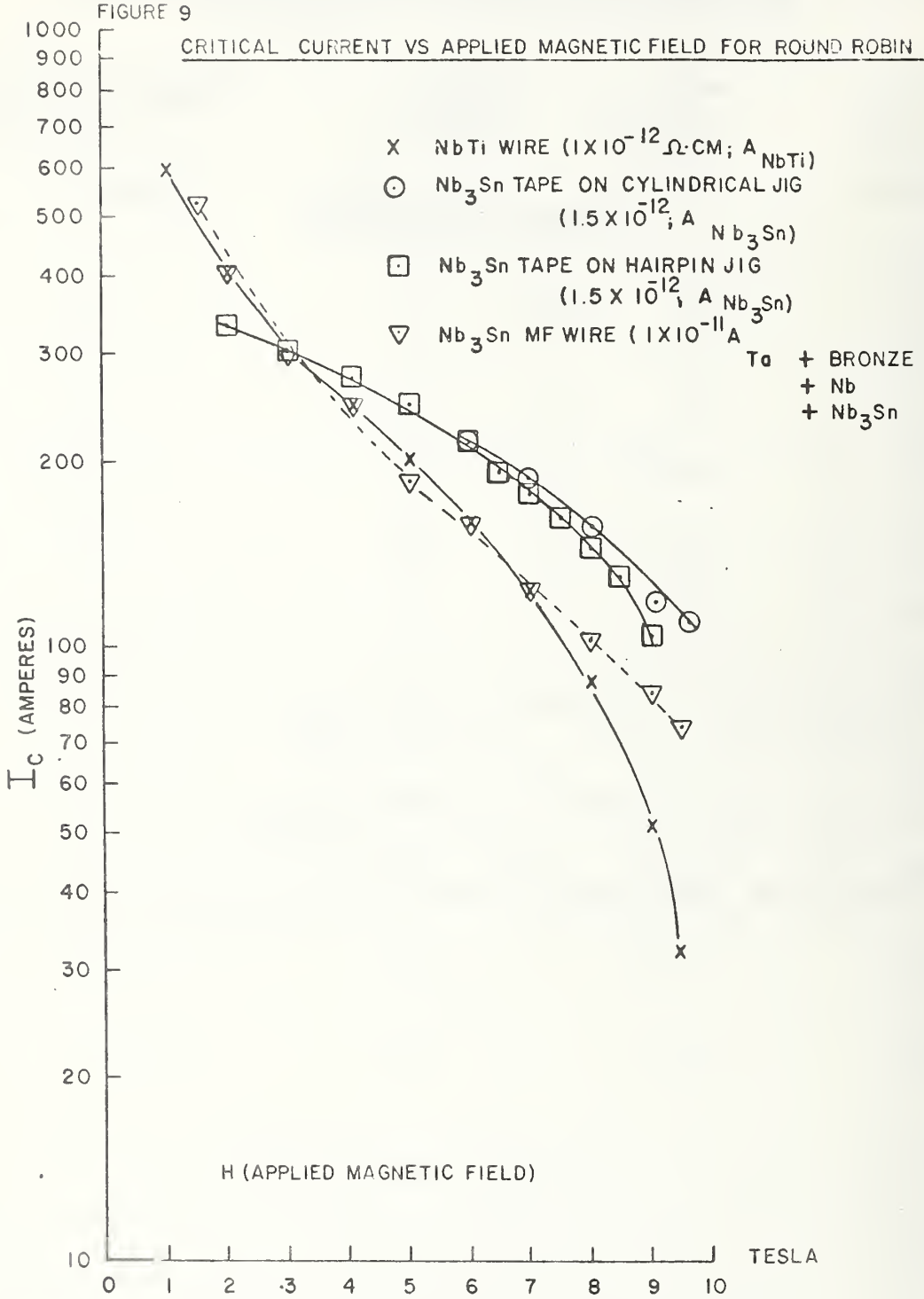

configuration. It is well known that the critical current of highly aspected conductors varies with the magnetic field orientation with respect to the broad side of the conductor. The lower critical current when the field is perpendicular to the broad face is consistent with this effect.

2.3 THE EFFECT OF MAGNETIC FIELD INHOMOGENEITY ON CRITICAL CURRENT MEASUREMENTS

The question of field homogeneity is a recurring dilemma to the superconductor tester. The problem arises in defining how good the field uniformity must be. The series of measurements described in this section attempts to clarify this situation using the noninductively wound long sample test fixture.

2.3.1 Test Procedure

The noninductively wound test fixture measures a 40 cm long sample in an axial length of 1.9 cm on a coil radius of 2.5 cm. The measurements begin with the bottom of the coil at z=0 and the magnet at 5 T. After the critical current is measured, the test fixture is raised about 5 mm, the magnet current increased such that the magnetic field at the bottom of the coil (in its new position) is once again at 5 T and the critical current measured. It is clear from Fig. 2 that this procedure will keep the maximum magnetic field (B_{max}) on the sample the same, but it lowers the minimum magnetic field that the sample experiences (ΔB increases). This procedure was repeated at seven positions along the axis.

2.3.2 Test Results

The result of these critical current measurements for a resistivity of 1×10^{-12} ohm·cm are shown in Fig. 10. As one can see the effect is very small, less than 2%, for a ΔB of slightly greater than 15%. It is important to note that the 15% change is spread out over 20 cm of sample for an effective 0.75%/cm. This effect on this type of fixture can be partly attributed to the nonuniformity in resistivity along the sample.

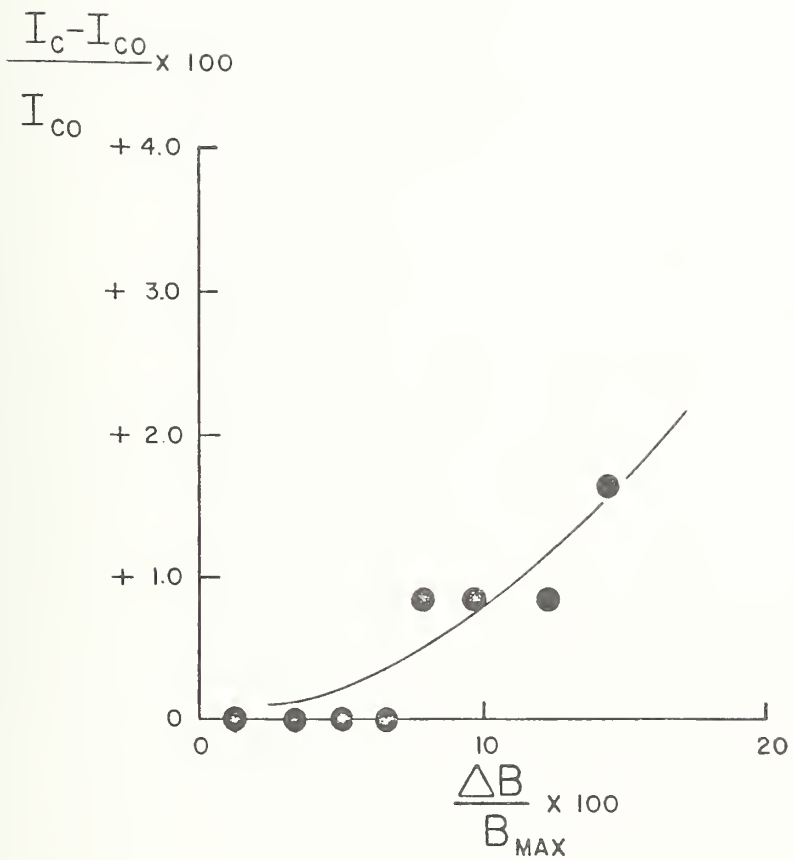

FIGURE 10: Critical Current Variation Due to Nonuniform Applied Magnetic Fields Along the Sample

Thus to reach a certain voltage level, a higher current is required in the sample as compared to a more uniform field case where more of the sample length contributes to the voltage. It is very likely that a ΔB of 15% would have a much more significant effect on a hairpin test fixture, for instance when the sample length is reduced by an order of magnitude. It appears that for the type of fixture used (noninductively wound long samples), magnetic field inhomogeneities would not be a major source of error.

2.4 EFFECT OF CONDUCTOR ORIENTATION WITH RESPECT TO THE MAGNETIC FIELD ON CRITICAL CURRENT MEASUREMENTS

It is well known that the critical current of most superconductors is greater when the magnetic field is parallel to the transport current rather than being perpendicular. The vast majority of superconducting applications utilize the conductor with the magnetic field perpendicular to the transport current and for this reason almost all the testing is performed under this condition. The tolerance for alignment inaccuracy will have an impact on both the test fixture design and the conductor mounting techniques. Obtaining data on which to base this tolerance is the purpose of this series of measurements.

2.4.1 Test Procedure

The best test fixture for the measurement of conductor/magnetic field orientation effects would be the inductively wound cylindrical configuration since it eliminated, or at least kept constant, the maximum number of other variables one of which is field homogeneity. Several samples of NbTi wire were wound with different pitches on the cylindrical mandrel. The different spiral pitches produced angles of 30^{o} (demonstrated in Figure 11), 60^{o}, 80^{o}, and approximately 90^{o} between the conductor and the magnetic field. In each case the critical current was measured at a sensitivity of 1×10^{-12} ohm·cm.

Particular care was taken during the sample mounting to insure that the orientation of the entire length of sample be uniform, including the portion soldered to the current leads.

FIGURE 11: INDUCTIVELY WOUND CYLINDRICAL TEST FIXTURE MOUNTED with the NbTi SAMPLE at 30^{0} with RESPECT to MAGNETIC FIELD

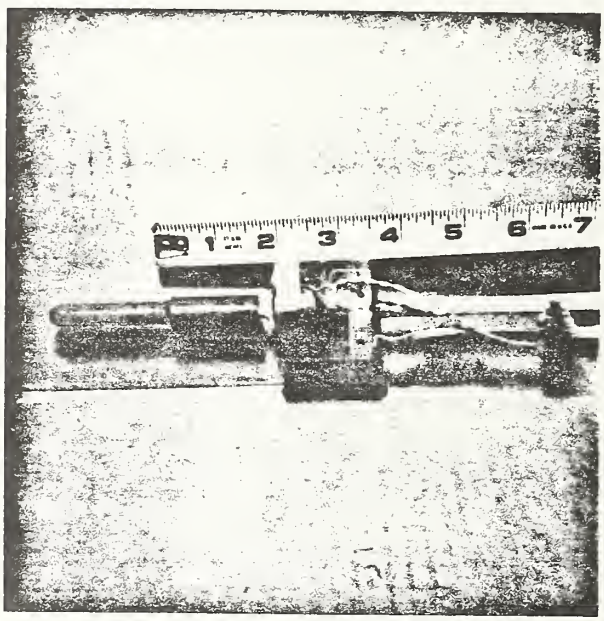

2.4.2 Test Results

The results of the critical current measurements are given in Figure 12 as a function of applied magnetic field for four different angles. The critical current increase averaged over all the magnetic fields tested is presented in Figure 13. For a 10^{o} orientation error, a 5.3% current increase is measured.

Most fixture designs can easily maintain less than 5^{o} alignment errors which should yield less than 2% critical current measurement error from this type of variation.

FIGURE 12. Critical Current vs Magnetic Field of a Typical NbTi Conductor for Several Angles with Respect to the Applied Field

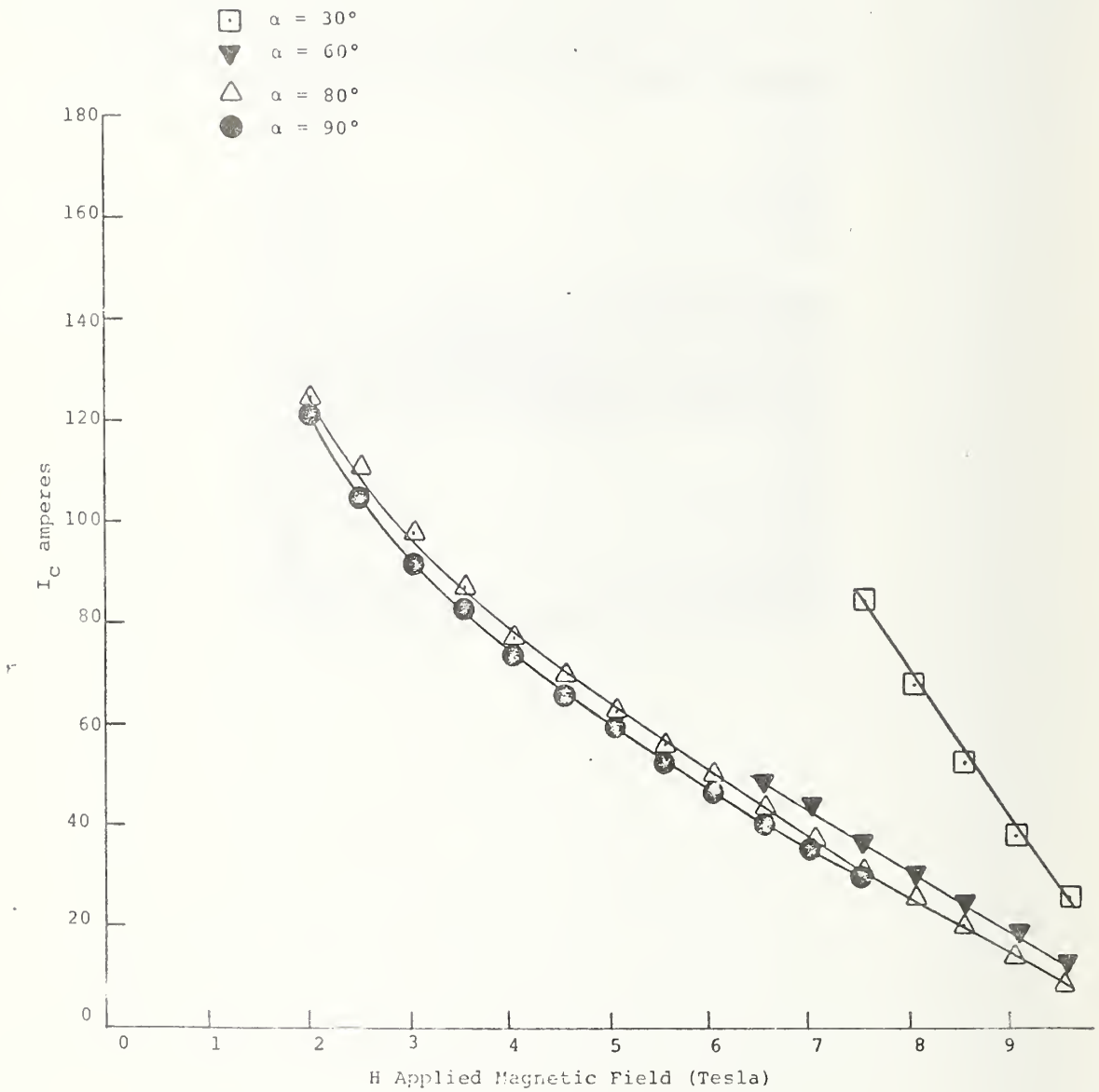

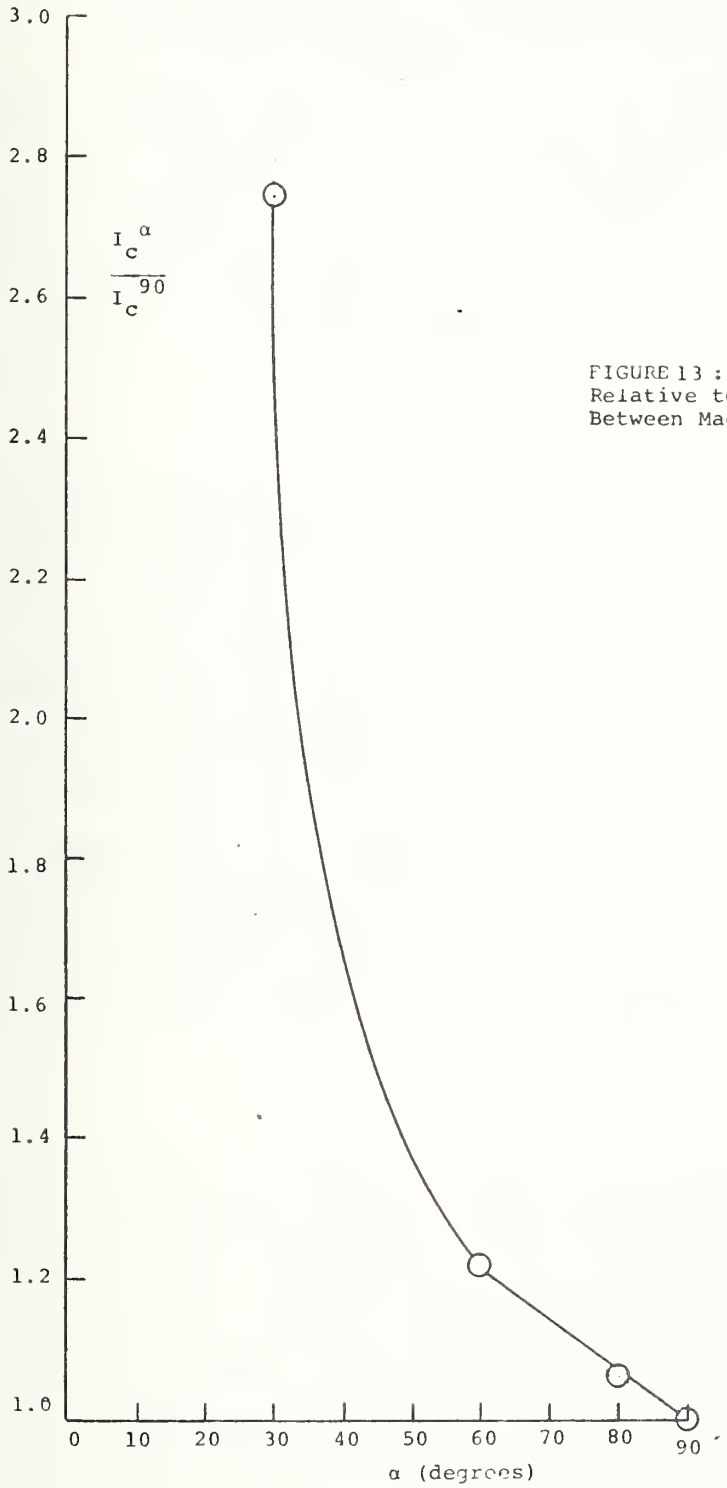

FIGURE 13 : Critical Current Ratio Relative to 90° Value vs Angle Between Magnetic Field and Conductor

2.5 EFFECTS OF IMPERFECT RECTIFICATION AND FILTERING OF AN SCR CONTROLLED CURRENT SOURCE

As the size of superconducting magnet conductors increases, so does their critical current. This natural progression has required the use of high current SCR power supplies whose output current usually contains high frequency spikes and noise to a much greater degree than the transistor power supplies used at low currents. The effect of this noise on critical current measurements is the intended goal of this section.

2.5.1 Test Procedures

Exploration of high frequency noise effects was performed on a 12 kA power supply. This power supply was primarly intended for plating applications. For the purposes of this test program modifications were made to the power supply, first, to reduce the noise level by adding a 0.9 farad capacitor bank across the terminals and, second, to increase the noise level by removing the standard filter included in the power supply. These two cases plus the unmodified configuration produced large changes in the noise level as shown in Table 9. The critical current measurement was then made with each configuration.

2.5.2 Results

Measurements were made on a NbTi conductor with an expected I_c of 7000A at 6T. These tests were limited by the performance of the test fixture. The current transfer area was insufficient for the high currents (approximately 6000A) being used and behavior usually associated with lead overheating was observed. The quench currents for Case 2 and 3 were the same (5640A) while in Case 1 the critical current was slightly

TABLE 9: Description of High Frequency Noise for Three Filtering Configurations

	Case 1	Case 2	Case 3
Peak to Peak current ripple as % of I_{DC}	110%	22%	14%
Frequency (hz)	360	360	120
Filter Configuration	none	standard	standard + 0.9 farad capacitor bank

TABLE 10: Critical Current of Cables Compared with the Critical Current of the Cable Strand

	Number of Strands	Critical Currents at 8 T		I Cable I Strand
Single Strand	-	125 A	120 A	
3 Cable	3	374 A	-	3
3^2 Cable	9	1125 A	-	9
3^4 Cable w/copper jacket	81	-	9500 A	79

higher (5760A) presumably due to instrumentation filtering saturation at these high AC signals. However, in all cases no current sharing was observed and the transition was abrupt and uncontrolled. Modification of the test fixture and further testing will be required before any evaluation of these results, relevant to the effect of noise, can be made.

2.6 SUPPORT FOR THE VALIDITY OF DETERMINING I_c (CABLE) FROM I_c (STRAND)

It was deemed appropriate to the aims of this program to present some Airco Superconductor data which sheds some light on the validity and/or feasibility of determining the critical current of a cabled conductor from a measurement of the critical current of the single strand which makes up the cable. As part of the development of the Nb_3Sn forced flow conductor, critical current measurements were made on three cable configurations using the same strand. Each cable was measured at 8 T and 4.2 K with a critical current criterion of $1x10^{-11}$ ohm·cm using:

$$A_{Ta} + Bronze + Nb + Nb_3Sn$$

The basic strand used in all the cables was similar to the wire shown in Figure 8.

The first cable is a simple three strand cable or triplet having a twist pitch of 25 mm. The second cable takes three triplets and joins them together on a 37 mm twist pitch. The third conductor is a 3x3x3x3 fully transposed cable with successive cable pitches of 25 mm, 37 mm, 75 mm and 150 mm. This cable was then compacted in a copper tube. The critical current of these three cables are given in Table 10.

In general, these measurements support the hypothesis that the cable current can be predicted from measurements made on the cable component. It may be important to note that these cables are round or square with large radii corners where the strands have not radically deformed during the cabling process. Measurements on flat cables may yield different results.

3.0 CONCLUSIONS AND RECOMMENDATIONS

We believe that the results of these tests will support the National Bureau of Standards program to develop a set of standards for superconductors. The round robin test series have been provided in such a way that they can be used easily in comparisons.

Both the measurement series on magnetic field nonuniformity and on conductor/magnetic field alignment demonstrated that they do not place intolerable demands on the test fixture design. This conclusion is only strictly valid for the types of fixtures used in each experiment.

The test program exploring the effect of current noise produced in SCR controlled power supplies should be pursued. Modifications to the test fixture can be made which will allow conclusive evidence to be obtained.

B. Intermagnetics General Corporation

THE DEVELOPMENT OF STANDARDS FOR PRACTICAL SUPERCONDUCTORS

FINAL REPORT

NBS Contract NB79RAC90025

1) Effect of Self-field on Critical Current.

2) Development of a Simple Method for Measuring the Normal State Resistivity of Composite Conductors.

IGC Report # 10-80-2

IGC Project #9576

R.E. Schwall
W.V. House
R.B. McCown
K.A. Mortensen

TABLE OF CONTENTS

List of Figures

List of Tables

1.0 INTRODUCTION

2.0 EFFECT OF SELF-FIELD ON CRITICAL CURRENT

2.1 Theory

2.1.1 Prediction of Limiting Cases From a Simple Model

2.1.2 General Theoretical Behavior

2.2 Experiment

2.2.1 High Current Conductors

2.2.2 Low Current Conductors

3.0 A SIMPLE METHOD FOR MEASURING THE NORMAL STATE RESISTIVITY OF COMPOSITE CONDUCTORS

3.1 Disucssion

3.1.1 Introduction

3.1.2 Measurement Concept

3.1.3 Measurement Procedure

3.1.4 Apparatus

3.2 Data

References

LIST OF FIGURES

2.1 Illustration of Magnetic Field Geometry in Wire

2.2 CDIF Superconductive Composite

2.3 CDIF Conductor

2.4 Fermi Energy Doubler/Saver Strand

2.5 BNL Isabelle Strand

2.6 Data From Low Current Self-field Experiment

3.1 Photo of RRR Apparatus

3.2 Typical V-I Plots from RRR Apparatus

LIST OF TABLES

2.1 Self-field Parameter ε for a Number of Commercial Conductors

2.2 Properties of CDIF Superconductive Composite

2.3 Results of High Current Self-field Effect Experiment

2.4 Low Current Self-field Results Fermi Type as Twisted

2.5 Low Current Self-field Results BNL Type as Twisted

2.6 Low Current Self-field Results Fermi Type Drawn After Twisting

2.7 Low Current Self-field Results BNL Type Drawn After Twisting

3.1 RRR Data on Various Conductors

3.2 RRR vs. Temperature Fermi Conductor

1.0 INTRODUCTION

This report is the final report under NBS PO# MB79RAC90025 issued to IGC on July 23, 1979. Under this contract, IGC performed the following tasks:

1. A theoretical analysis of the effect of self-field on the critical current of short samples of superconductive wire.
2. An experimental evaluation of the effect of self-field on the critical current of short samples of superconductive wire.
3. The design and construction of a test fixture to measure the residual resistance ratio of the stabilizer in superconductive composites.
4. The measurement of the residual resistance ratio of a number of composites using this test fixture.
5. Participation in round robin tests of critical current on superconductive samples provided by NBS.
6. Participation in the ASTM Subcommittee B1.08, efforts on Standardization of Superconductors.
7. Participation in NBS surveys concerning the generation of standards for the measurement of superconducting composites.

The first four tasks are reported in this final report. Interim reports have covered the participation in round robin tests of I_c and participation in the ASTM standardization efforts.

The work presented here represents the efforts of a number people at IGC. The initial work on the matrix residual resistance ratio measurements was performed by Dr. Mike Walker and Mr. Jack Gramm. The self-field effect theory presented in Section 2.1.2 was developed by Dr. Waylon House. The measurements of the self-field effects and matrix residual resistance ratio were performed by Mr. Karl Mortensen and Mr. Joe Clements of the IGC Conductor Development Laboratory. Dr. Robert McCown directed the design of the

residual resistance ratio apparatus and provided program management over much of the duration of the program. Direction of the experiments reported here and overall program management were the responsibility of Dr. R. E. Schwall. IGC has been pleased to participate in this significant standardization effort and hopes to continue this participation through continued membership on the AFTM Standardization Subcommittee and future work with NBS.

2.0 EFFECT OF SELF FIELD ON CRITICAL CURRENT

2.1 Theory

2.1.1 Prediction of Limiting Cases from a Simple Model

2.1.1.1 Untwisted Conductor

Consider a cylindrical conductor with uniform current density J in a transverse magnetic field B_A (Figure 2.1). At a point at radius r in the conductor the self-field is:

$$|B_S| = \frac{\mu_o J r}{2} \tag{1}$$

(MKS units are used throughout this section)

The total field $B_T(r,\theta)$ at a point in the wire is the vector sum of the applied field B_A and the self field.

$$B_T^2(r,\theta) = B_A^2 + B_S^2 - 2\, B_A\, B_S \cos(\pi/2-\theta)$$

or

$$B_T^2(r,\theta) = B_A^2 + \left(\frac{\mu_o J r}{2}\right)^2 - \mu_o J r\, B_A \sin(\theta) \tag{2}$$

The critical current density at a particular point in the wire, i.e., for a particular filament, is a function of the local field, hence (2) may be used to calculate the local critical current density $J_c(r,\theta)$.

$$J_c(r,\theta) = J_c(B_T) \tag{3}$$

If the functional form of $J(B_T)$ is known, then the overall current in the wire can be determined by integration, i.e.,

$$I_c = \int_o^R \int_{-\pi}^{\pi} J_c(r,\theta)\, r\, d\theta\, dr \tag{4}$$

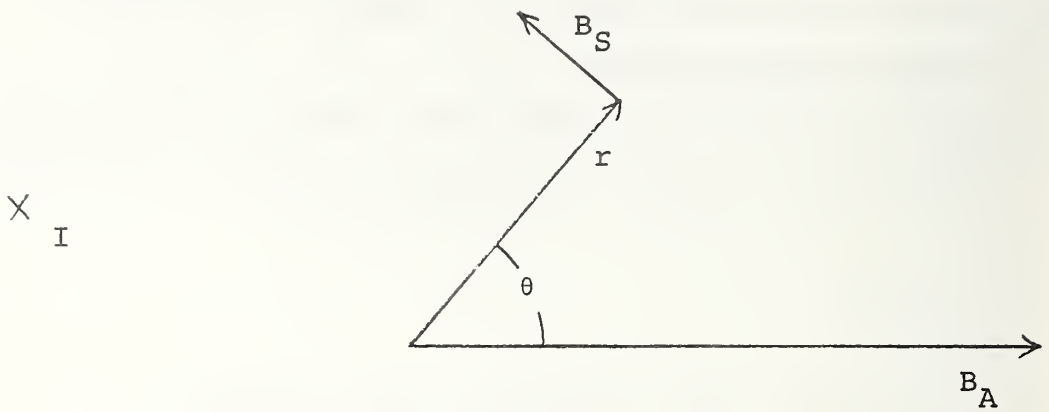

Figure 2.1 - Magnetic field geometry is used in simple model calculation of self-field effect.

By assuming a functional form for J_c (B_T) one can thus, in principle, determine the effect of the self-field directly from equation 4. There is a proliferation of models for J_c (B_T), however, and one would be hard pressed to experimentally verify any prediction that was made since changing the wire size to change the self-field will also change the intrinsic current density of the superconductor. An order of magnitude estimate of the effect is, however, quite straightforward. Equation 2 may be rewritten as

$$\frac{B_T^2}{B_A^2} = 1 - 2\varepsilon \sin(\theta) + \varepsilon^2 \qquad (5)$$

where $\varepsilon = \frac{\mu_o J r}{2B_A}$ (6)

In large conductors at low field where J_c is high, ε at the wire surface may be as large as 0.5. In commercial conductors, however, ε ranges from $\tilde{\sim}0.01$ to 0.1 at the rated operating field (see Table 2.1) and the ε^2 term will be in the range of 10^{-2} to 10^{-4}. The net effect of the ε term will depend on the functional form of J_c (B_T). If J_c $(B_T) \propto B_T^2$ then the integral over θ is zero. For other functional forms, the term is nonzero but of order ε.

The net effect of the self-field on an untwisted conductor thus depends primarily on two factors.

1) The relative magnitude of the self-field and the applied field.
2) The functional dependence of the critical current on field.

Conductor	I_c (amps)	Diameter (cm)	Operating Field (Tesla)	ε
CDIF	10583	0.518	7	0.12
GE/LCP 8T	1000	0.187	8	0.027
GE/LCP 6T	1000	0.147	6	0.045
GE/LCP 4T	1000	0.120	4	0.083
GD/LCP-H	580	0.168	8	0.017
GD/LCP-M	900	0.168	6.6	0.033
GD/LCP-L	1250	0.168	5.4	0.055
BNL	58	0.029	5	0.016
FNAL	240	0.067	5	0.029

TABLE 2.1 Self-field parameter ε evaluated at the wire surface for a number of current commercial conductors. Rectangular conductors were evaluated as rounds of equivalent cross section. ε is defined in equation 6.

In practical conductors the effect will be small and, in general, indistinguishable from other factors which affect J_c such as cold work, bend strain, etc. It should be noted however, that with a detailed knowledge of the function J_c (B_T) in the superconductor, it is possible to evaluate this effect precisely and compensate for it. In twisted conductors however, the situation is more complex.

2.1.1.2 Twisted Conductor

In the twisted conductor each filament spirals through all possible values of θ and hence the field on the filament varies from $B_A - B_S$ to $B_A + B_S$. The effect of this on the overall critical current will depend on the relative size of the current transfer length and the twist pitch. The current transfer length, in turn, depends on the matrix resistivity, the wire diameter, the measurement sensitivity and the nature of the resistive transition of the superconductive filaments themselves.

From Ekin[1] we have

$$X_{min} = (0.1N)^{1/2} \, (\rho_m/\rho^*)^{1/2} \, D \qquad (7)$$

where X_{min} = current transfer length

N = exponent describing the resistive transition of the filaments via the equation $\rho = kJ^N$

ρ_m = matrix transverse resistivity

ρ^* = equivalent resistivity defining the measurement sensitivity

D = wire diameter.

Two limiting cases $X_{min} >> \ell p$ (ℓp = twist pitch) and $X_{min} << \ell p$ may be evaluated directly.

For $X_{min} >> \ell p$ the filaments can be thought of as isolated and we have simply a weak link problem,

$$\text{i.e.,} \quad B_T = B_A + \frac{\mu_o J r}{2}$$

$$I_c = 2\pi \int_o^R J_c \left(B_A + \frac{\mu_o J r}{2} \right) r dr \qquad (8)$$

Such would be the case, for example in a very tightly twisted NbTi conductor with a full mixed matrix, i.e. Cu-Ni between each filament. It should be noted that the current transfer length X_{min} considered here is not necessarily the same as that which is involved in introducing current into a wire from an external source. In the braid used for the Isabelle accelerator magnets, for example, the wire has an outer shell of Cu-Ni alloy to reduce current transfer between strands but has a full copper matrix between the filaments. Thus the value of ρ_m in equation 7 for interfilament transfer would be that of the copper matrix while that for transfer into the strand would include the CuNi shell. X_{min} is therefore shorter for interfilament transfer.

Another possible example of the $X_{min} >> \ell p$ case is a tightly twisted multifilamentary Nb_3Sn conductor with a large amount of residual tin in the bronze.

The other limiting case of a twisted conductor is $X_{min} << \ell p$, i.e., the current transfer length long compared to the twist pitch. In this case the current can continuously redistribute among the filaments and the analysis for the untwisted conductor is applicable. Since twist pitches are usually at least 10 wire diameters and Ekin[1] has found that the current transfer resistance is immeasurably small at 10 wire diameters in copper matrix NbTi, we would expect most copper matrix NbTi materials to fall into this category. Again, however, this is a function of the particular geometry since a large diameter, high current density tightly

twisted conductor measured at a high sensitivity might not be in this limit.

In the intermediate case, i.e., $X_{min} \approx \ell p$ the analysis is more complex and has not been accomplished using this simple model.

2.1.2 General Theoretical Behaviour

2.1.2.1 Approaches

There are two basic theoretical approaches useful for describing the distribution of current density within composite conductors. The first, which has been useful in describing A.C. losses, is to minimize the ohmic power dissipation. For the case of static conditions, however, this approach results in an integral form for the equation of continuity subject to various kinds of (generally) integral constraints.

The second, in one guise or the other, attempts to solve the potential problem subject to the constraints of continuity in differential form. The latter approach is more amenable mathematically and is followed here.

Two essential views can be taken in formulating the potential problem. The first taken by Ekin[1] is to consider the resistivity ρ (or conductivity σ) a scalar variable dependent on position. In this formulation, the problem begins with two equations,

$$\vec{\nabla} \cdot \vec{J} = 0 \tag{9a}$$

$$\vec{J} = \sigma \vec{E} = \sigma \vec{\nabla} \Phi \tag{9b}$$

which yield

$$\sigma \nabla^2 \Phi = -\vec{\nabla} \Phi \cdot \vec{\nabla} \sigma \tag{9c}$$

The overall solution of equation 9 is a very formidable task. Ekin's approach is to consider two concentric cylinders of superconductor in a conducting matrix. He then solves a different equation in J. From this formulation, he is able to extract a parameter X_{min} which describes the characteristic length required for the effects of current input/output to vanish.

A second approach is to consider the conductivity as a tensor with a certain spatial dependence. This problem is solvable and some important conclusions can be drawn.

2.1.2.2 Model

The model proposed is to consider the conductivity as a tensor

$$\vec{J} = \overleftrightarrow{\sigma} \cdot \vec{E} \tag{9d}$$

The conducting composite is considered to have identical conductivity σ_1 in the (rθ) or (xy) direction and a much larger conductivity σ_3 in the Z (polar) direction. Further it is assumed that σ_3 may have (rθ) dependence. (The axis of the conductor will be taken in the Z direction).

Then

$$\vec{J} = \begin{pmatrix} \sigma_1 & 0 & 0 \\ 0 & \sigma_2 & 0 \\ 0 & 0 & \sigma_3(r\theta) \end{pmatrix} \begin{pmatrix} \frac{\partial \Phi}{\partial r} \\ \pm \frac{\partial \Phi}{\partial \theta} \\ \frac{\partial \Phi}{\partial z} \end{pmatrix} \tag{9e}$$

$$\sigma_1 = \sigma_2 \tag{9f}$$

The off-diagonal elements can be shown to vanish[2]. Clearly the choice of such a tensor is tantamount to choosing a continum model with microscopic anisotropy - much as in anisotropic problems in solid state physics. In addition spatial variation is allowed in the 3rd dimension.

2.1.2.3 Solution for a Straight Composite

Consider first the case for untwisted composite. The equation for (static) continuity gives (in cylindrical cordinates)

$$\nabla \cdot \vec{J} = \sigma_1 \left[\frac{1}{r} \frac{\partial}{\partial r} r \frac{\partial \Phi}{\partial r} + \frac{1}{r^2} \frac{\partial^2 \Phi}{\partial \theta^2} \right] + \frac{\partial}{\partial z} \left[\sigma_3(r,\theta) \frac{\partial \Phi}{\partial z} \right] = 0 \tag{10}$$

Since $\sigma_3(r\theta)$ is spatially dependent only on the coordinates normal to Z, we find

$$\frac{1}{r}\frac{\partial}{\partial r}\left(r\frac{\partial \Phi}{\partial r}\right) + \frac{1}{r^2}\frac{\partial^2 \Phi}{\partial \theta^2} + \delta(r,\theta)\frac{\partial^2 \Phi}{\partial z^2} = 0 \qquad (10)$$

where $$\delta(r,\theta) = \frac{\sigma_3(r,\theta)}{\sigma_1(}$$

is a measure of the ratio of longitudinal to transverse conductivity.

Equation 10 is separable with respect to the Z-coordinates,

$$\frac{\left[\frac{1}{r}\frac{\partial}{\partial r}r\frac{\partial}{\partial r} + \frac{1}{r^2}\frac{\partial^2}{\partial \theta^2}\right]g(r,\theta)}{\delta(r,\theta)\,g(r,\theta)} = -\frac{\partial^2 f(z)}{\partial z^2} = \pm k^2 \qquad (11)$$

Where $\pm k^2$ is the separation constant and k can be chosen positive without loss of generality. Choosing positive sign in the constant, we obtain

$$f'' + k^2 f = 0 \qquad (12a)$$

$$\left[\frac{1}{r}\frac{\partial}{\partial r}r\frac{\partial}{\partial r} + \frac{1}{r^2}\frac{\partial^2}{\partial \theta^2}\right]g(r,\theta) = k^2\,\delta(r,\theta)\,g(r,\theta) \qquad (12b)$$

Choosing the negative sign, we obtain

$$f'' - k^2 f = 0 \qquad (13a)$$

$$\left[\frac{1}{r}\frac{\partial}{\partial r}r\frac{\partial}{\partial r} + \frac{1}{r^2}\frac{\partial^2}{\partial \theta^2}\right]g(r,\theta) = -k^2\,\delta(r,\theta)\,g(r,\theta) \qquad (13b)$$

Examination of 12b and 13b show that in both cases the equation for $g(r\theta)$ appears as in an eigenvalue equation.

In point of fact, both these equations can be viewed as 2-dimensional Schrodinger equations and can be solved exactly for δ independent of θ in Laquerre Polynomials.[3]

Instead, however, consider $\delta(r\theta)$ to be a constant δ where $(r\theta)$ dependence of $\delta(r\theta)$ can be considered later as a perturbation. Then both 12b and 13b are separable in r,θ. It is easy to show[4] that with this approximation, the radial equation for 12b is the modified Bessel equation and that for 13b is the Bessel equation.

The radial equation for equation 12 b has solutions of form

$$R = h_1 I_m(r) + h_2 K_m(r)$$

and equation 13b of form

$$R = h_3 J_n(r) + h_4 Y_n(r)$$

Applying the condition of finality (R(r) finite at zero) eliminates both K and Y functions, and requiring that θ be continuous and of 2π period forces n and m to be integer.

With the assumption that the potential be finite for $r \leq ro$, and continuous in θ, the general solutions for 12 and 13 are

(14a)

$$\Phi_{K+} = \left(f_{1K} e^{iKz} + f_{2K} e^{-iKz}\right) \sum_{m=0} \left(c_{1m} e^{im\theta} + c_{2m} e^{-im\theta}\right) I_m(K\sqrt{\delta}\, r)$$

(14b)

$$\Phi_{K-} = \left(a_{1K} e^{Kz} + a_{2K} e^{-Kz}\right) \sum_{n=0} \left(b_{1n} e^{in\theta} + b_{2n} e^{-in\theta}\right) J_n(K\sqrt{\delta}\, r)$$

(14c)

$$\Phi_{K0} = (az + b) \sum_{l=0} r^l \left[d_{1l} e^{il\theta} + d_{2l} e^{-il\theta}\right]$$

(solution for K = 0)

Of course k may have a continuous or discrete spectra depending on the additional boundary conditions.

2.1.2.3.1 Radial Boundary Conditions

It is assumed that there is no current flow radially out of the composite conductor, i.e.,

$$J_r \Big|_{r=r_o} = 0 .$$

This is equivalent to the requirement that

$$\frac{\partial \Phi}{\partial r} \Big|_{r=r_o} = 0.$$

Imposing this condition on equations 14 yields

(15)

$$\Phi(r,\theta,z) = (az+b) + \sum_{n=0}^{\infty} \left(a_n e^{in\theta} + b_n e^{-in\theta}\right) \sum_{m=0}^{\infty} \left(c_m e^{\frac{X_{mn}}{\sqrt{\delta}}\frac{z}{r_o}} + d_m e^{-\frac{X_{mn}}{\sqrt{\delta}}\frac{z}{r_o}}\right) J_n\left(\frac{r}{r_o}X\right.$$

where X_{mn} is the mth root of

$$\frac{d\,J_n(x)}{dx} = 0.$$

2.1.2.3.2 End Boundary Conditions

The remaining constants in equation 15 can be determined by the end boundary conditions. These can be specified, for example, as the potential distribution at +Zo and - Zo, (or its Z-derivative there). A quite general result is obtainable using the Fourier-Bessel and Dini series.[5, 6]

The θ dependence can be dropped since it does not add any qualitatively different results to the solution. Assuming cylindrical symmetry, the solution by this means becomes

$$\bar{\Phi}(r,\theta,z) = A + B\frac{z}{z_o} + \sum_{m=1} C_m(z)\, J_o\left(\frac{r}{r_o}\chi_m\right) \tag{16}$$

where

$$A = \frac{1}{r_o^2}\int_o^{r_o} r'\left[\bar{\Phi}(r',z_o) + \bar{\Phi}(r',-z_o)\right]dr'$$

$$B = \frac{1}{r_o^2}\int_o^{r_o} r'\left[\bar{\Phi}(r',z_o) - \bar{\Phi}(r',-z_o)\right]dr'$$

$$C_m(z) = \frac{1}{r_o^2\, J_o^2(\chi_m)\sinh\left(\frac{z\chi_m}{\sqrt{\delta}}\frac{z_o}{r_o}\right)}\left[\sinh\left(\frac{\chi_m}{\sqrt{\delta}}\frac{z+z_o}{r_o}\right)\int_o^{r_o} r' J_o\left(\frac{r'}{r_o}\chi_m\right)\bar{\Phi}(r',z_o)dr'\right.$$

$$\left. - \sinh\left(\frac{\chi_m}{\sqrt{\delta}}\frac{z-z_o}{r_o}\right)\int_o^{r_o} r' J_o\left(\frac{r'}{r_o}\chi_m\right)\bar{\Phi}(r',-z_o)dr'\right]$$

and where $J'(X_m) = 0$ defines X_m

Although appearing formidable, this result is quite easily understood and significant. The term A corresponds to the mean value of the potential at Z=0 due to the imposed potentials at -Zo, +Zo. The term B corresponds to the difference between the r-averaged imposed potentials at -Zo, +Zo. Note that these terms are uniform over the radius r and are independent of δ.

The term $C_m(Z)$ is the coefficient of the radial variation of the potential as a function of Z. The functions $J_o(r_{xm}/r_o)$ form a complete set covering well-behaved functions of r.

Consequently, $C_m(Z)$ describes how the radial variation of the potential due to the electrodes (or fixture) dies out in the axial direction.

As Ekin[1] has pointed out, the exact end conditions depend on the details of the fixture. The equation for $C_m(Z)$ or $C_m(Z,\theta)$ in the extended case enables an exact calculation for this effect. In addition, this enables us to write the worst case decay constant since $X_1 < X_2$.

$$\tau = \frac{\sqrt{\delta}\, r_o}{X_1} = \frac{\sqrt{\delta}\, r_o}{3.71}$$

where the radial potential decays as $e^{-Z/\tau}$.

Clearly, 2Zo, the separation of the fixture should be ∿100 times the radius r_o to prevent interference with the measurement. (Of course, placing the voltage measuring taps equidistant from the wire midpoint can diminish these effects significantly, at least when the fixture is symmetric.)

2.1.2.3.2 Current Distribution

At a sufficient distance from the fixture, then the surfaces of equi-potential are flat planes normal to Z. Consequently the current density in this region is

$$J_r = J_\theta = 0$$

$$J_z = \sigma_3(r,\theta)\frac{\partial \Phi}{\partial z} = \sigma_3(r,\theta)\frac{B}{z_o}$$

The r,θ dependence of σ_3 can be re-introduced for it can be seen that the perturbation in **S** in equation 13b changes only the decay constants in $C_m(Z)$. In this case then the total current is

$$I_o = \int_0^{r_o}\int_0^{2\pi} J_z\, r\, dr\, d\theta = \frac{B}{z_o}\int_0^{r_o}\int_0^{2\pi} \sigma_3(r,\theta)\, r\, dr\, d\theta \quad . \tag{17}$$

2.1.2.4 Solutions for Twisted Wire

The case of a twisted composite can be treated in a way analogous to the straight composite. Consider equations 9e, 9f again, this time replacing σ_2 by a substantially larger conductivity ($\sigma_1 \neq \sigma_2$). In fact σ_2 can be allowed to have an r-dependence. Equation 10 is then modified to

$$\frac{1}{r}\frac{\partial}{\partial r} r \frac{\partial \Phi}{\partial r} + \frac{\gamma(r)}{r^2}\frac{\partial^2 \Phi}{\partial \theta^2} + \delta(r\theta)\frac{\partial^2 \Phi}{\partial z^2} = 0 \tag{10'}$$

where $\delta(r\theta)$ is now a measure of the ratio of longitudinal to radial conductivity and $\gamma(r\theta)$ is a measure of θ-angular conductivity to radial conductivity. (Note that Z separation proceeds as in the untwisted case.)

So long as the equation 10' remains an elliptical differential equation (insured by $\delta > \gamma > 1$), the qualitative form of the solution remains the same. The effect of $\gamma(r)$ on the equation for $g(r\theta)$ influences the decay constant through the boundary conditions on Jn.

The details of the actual solution are unimportant, however, since it is only the limiting case (after fixture effects have died out) which is of physical interest. In this limit

$$J_z = \sigma_3' \frac{\partial \Phi}{\partial z}$$

And the total current is (see eq. 17)

$$I_o' = \frac{B}{z_o} \int_0^{r_o} \int_0^{2\pi} \sigma_3'(r,\theta)\, r\, dr\, d\theta \qquad (17')$$

In this, the σ_3 conductivity has been primed to indicate that it is a different value from the untwisted composite. The assumption is made that the superconductor to normal conductor ratio, λ , is the same (by volume) in twisted and untwisted cases.

With this notation, the current for given potential in the twisted and untwisted cases should have the ratio

$$\frac{I_o\,(\text{twisted})}{I_o\,(\text{untwisted})} = \frac{1}{1 + \left(2n \frac{R_o}{L}\right)^2} \qquad (18)$$

where n is the number of turns in length L. This results arises simply from the difference in aspect ratio of the two cases with respect to the z-axis, i.e.

$$\sigma_3' = \frac{1}{1 + \left(2n \frac{R_o}{L}\right)^2} \cdot \sigma_3 \quad .$$

2.1.2.5 Self-field and Critical Current

A truly accurate evaluation of the effects of an applied field and a self field requires a very detailed evaluation of the specific conductor configuration. However, the simple assumption that critical field effects can be described by a thermodynamic argument leads to the approximation that ratios of critical parameters can be treated on the basis of an integrated volume.

Consider equation 17 as either the current or self or applied field increases. At some point the conductivity at r,θ reaches a value corresponding to $J_c(r\theta)$. Further increasing current or field causes additional regions to reach their J_c and so on. The details of this process may be quite obscure and in any case an ensemble approach is indicated by the long-range nature of superconductive interactions.

Thus whenever the integral in equation 17 reaches "criticality" for an untwisted sample, the integral in 17' for a twisted sample will also reach "criticality". The ratio between the two cases is given in equation 18.

For normally encountered twist pitches, this factor is $\sim 5\%$ and so may well be obscured by other effects such as the detailed structure of the composite.

2.2 Self-Field Effect: Experiments

2.2.1 High Current Conductors

As seen in Section 2.1, the self-field effect is expected to be largest in large diameter high current density conductors. In an attempt to observe the effect in such conductors, a number of tests were made using the superconducting composite from the CDIF conductor. This composite, (shown in Figure 2.2) is normally laminated into a copper core and then fabricated into a cable with extended cooling surface (Figure 2.3). For this test, however, it was used as an unstabilized composite with the characteristics shown in Table 2.2.

In view of the high cost of test fixtures for such high current tests, we chose to use an existing test fixture at the Francis Bitter National Magnet Laboratory (FBNML) to perform our tests. The fixture, which was built to perform 12 simultaneous short sample tests, consists of 4 circular copper plates each $\tilde{\sim}$ 3.2 cm thick separated by phenolic insulators.

Each plate holds 3 samples and the apparatus is assembled so that the samples are electrically in series. The normal short sample test is performed by placing two plates symmetrically around the midplane of a Bitter solenoid and measuring the voltage across all 6 samples simultaneously. The voltage taps on the samples are then 1.2 cm apart giving a sensitivity of $\sim 2 \times 10^{-11}$ Ω-cm at 1 μv sample voltage and 8 kA current.

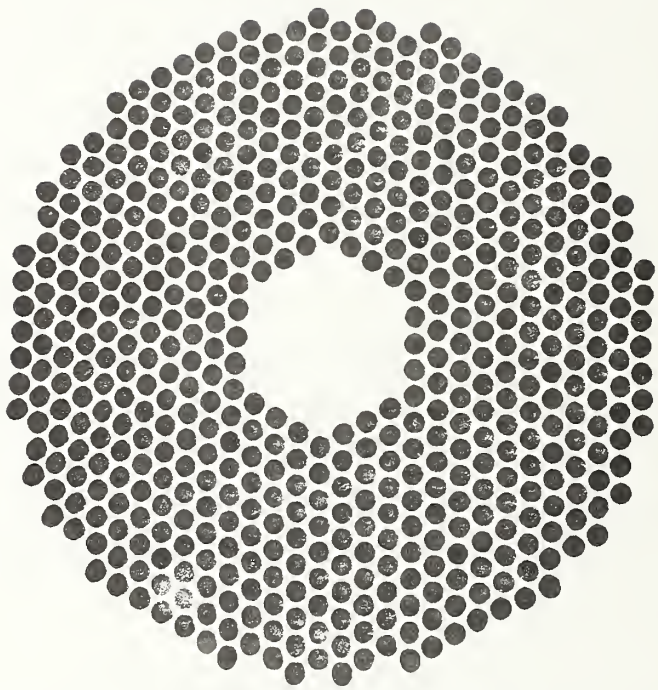

FIGURE 2.2 - CDIF SUPERCONDUCTIVE COMPOSITE USED IN HIGH CURRENT SELF-FIELD EXPERIMENT.

FIGURE 2.3 - CDIF CONDUCTOR INCORPORATING THE COMPOSITE OF FIGURE 2.2.

Composite Diameter	0.518 cm
Cu:Sc Ratio	1:1
Nb-Ti Filament Number	198
Nb-Ti Filament Diameter	240 μm
Critical Current	10583 A @ 7T

Table 2.2 Characteristics of conductor used in high current self-field experiment. Actual conductor used had slightly lower I_c due to lack of final size heat treatment.

For the self-field experiment, one 60 cm long sample was placed in each plate. Three sets of voltage taps spaced at 1.1 cm, 3.9 cm and 42 cm were installed in the copper near the sample using existing holes. The samples were soldered to the copper plate along their entire length using pure indium.

The 4 samples tested were produced by twisting adjacent pieces of CDIF composite with twist pitches of 2.5 cm, 5.0 cm and 10.0 cm. The 4th sample was untwisted. These twist pitches represent 5, 10 and 20 wire diameters.

Two trips were made to the Magnet Lab to run the experiment. On the first trip the SCR power supply used to supply current to the samples failed and no data was obtained. On the second trip, critical current data was obtained at field of 7.46 and 7.01 T on all four samples. A total of 16 runs were made with 3 sets of voltage taps monitored on each run.

Data was recorded using the MIT data acquisition system that is normally used for the CDIF short sample tests. In this system, three voltage signals are fed through 10 Hz bandwidth amplifiers with a gain of 1000 to a Biomation 4 channel transient recorder. The 4th channel is used to record sample current. All signals are recorded as a function of time as the sample current is ramped linearly from zero with the background magnetic field held constant. The current is dropped to zero after the sample critical current is reached and the data stored in the Biomation. Memory is read out to an X-Y recorder as 3 voltage vs. current traces.

The quality of data obtained in this experiment was variable. Noise on the various voltage channels ranged from $\sim$ 2 μv p-p to $\sim$ 20 μv p-p. All channels were susceptible

to random noise spikes and occasional large amplitude long time constant surges. The combined effect of these was to render some of the data useless and to reduce the overall sensitivity of the experiment to an equivalent resistivity of 2×10^{-11} Ω-cm. All the data obtained from the voltage taps spaced 42 cm apart showed a large resistive component indicating incomplete current transfer and thus was not used in the analysis.

A summary of the data obtained using the 3.9 cm voltage tap separation is given in Table 2.3. Although there appears to be a systematic variation of critical current with twist pitch, this was found to be due to variations in the magnetic field at the assumed equivalent sample locations. In the final two runs of this experiment, the untwisted and 2.5 cm twist pitch samples were both run with the sample located on the magnet midplane and the currents were identical to within the resolution afforded by the system noise.

Subsequent examination of the Bitter magnet by FBNML personnel indicated that the coil was shorted between plates above the midplane and was producing a non-homogeneous field.

We thus conclude that for a short sample test of a copper matrix NbTi sample where the sample is imbedded in a large area of stabilizer, the current redistribution through the sample-stabilizer assembly is such that there is no appreciable effect of twist pitch on the critical current measured at a sensitivity $\gtrsim 10^{-11}$ Ω-cm.

H = 7.46 Tesla

Twist Pitch (cm)	I_c $\sim 10^{-11}$ Ω-cm	I_c Quench
Untwisted	7650 amps	7700 amps
	7600	7700
2.5 cm	7880	8080
	7900	8100
5.0 cm	7850	7980
	7880	7950
10.0 cm	8200	8280
	8250	8300

H = 7.0 Tesla

Untwisted	8700	8700
	8750	8750
2.5 cm	9080	9180
5.0 cm	8750	9000
10.0 cm	9300	9300

H = 7.0 Tesla Sample on Magnet Midplane

Untwisted	8800	8850
2.5 cm	8750	8890

Table 2.3 - Results of High Current Self-field Effect Experiment. Each Twisted Sample was Run Twice at 7.46 T and Once at 7.0 T.

2.2.2 Low Current Conductors

Following the essentially negative result of the high current measurements a series of high sensitivity measurements were made on long samples of low current wire. The samples were fabricated of conductor currently in production at IGC for the Fermi Energy Doubler/Saver Accelerator (Figure 2.4) and for the Isabelle Accelerator at BNL (Figure 2.5). A section of each conductor was removed from the production cycle prior to the final twisting operation and cut into three lengths, each $\approx$ 80 cm long. One length of each sample was measured untwisted and the other two were twisted by hand to varying twist pitches and then measured.

The test sample in each case was a 5 turn single layer spiral wound on a phenolic holder. The sample was potted in wax and measured in the bore of a 10 T Nb_3Sn tape solenoid. Current was supplied by two IGC 180M power supplies operated in parallel and voltage was measured by a micro-voltmeter and recorded versus current on an X-Y recorder. The active sample length between voltage taps was $\sim$ 70 cm.

Data quality on this experiment was quite good (see Figure 2.6) with peak to peak noise usually about 500 nV. Data was evaluated at 10^{-12} Ω-cm for fields from 1 to 8 T and at 10^{-13} Ω-cm from 1 to 4 T on the BNL wire. The Fermi data extends from 4T to 8T reflecting the maximum available current of 360 amps. (Tables 2.4 & 2.5)

It is seen that there is a definite decrease in critical current when the conductor is twisted and that this effect is larger in the Fermi material than in the BNL material, as would be expected by the relative values of ε (see Table 2.1). The decrease in critical current does not, however, show the expected progression with magnetic field, i.e., the effect does not grow larger as the field is reduced. This indicates that the critical current change is perhaps caused by some effect other than self-field. To eliminate the possibility of dimensional changes which could have occurred during the twisting operation, the previously tested samples were

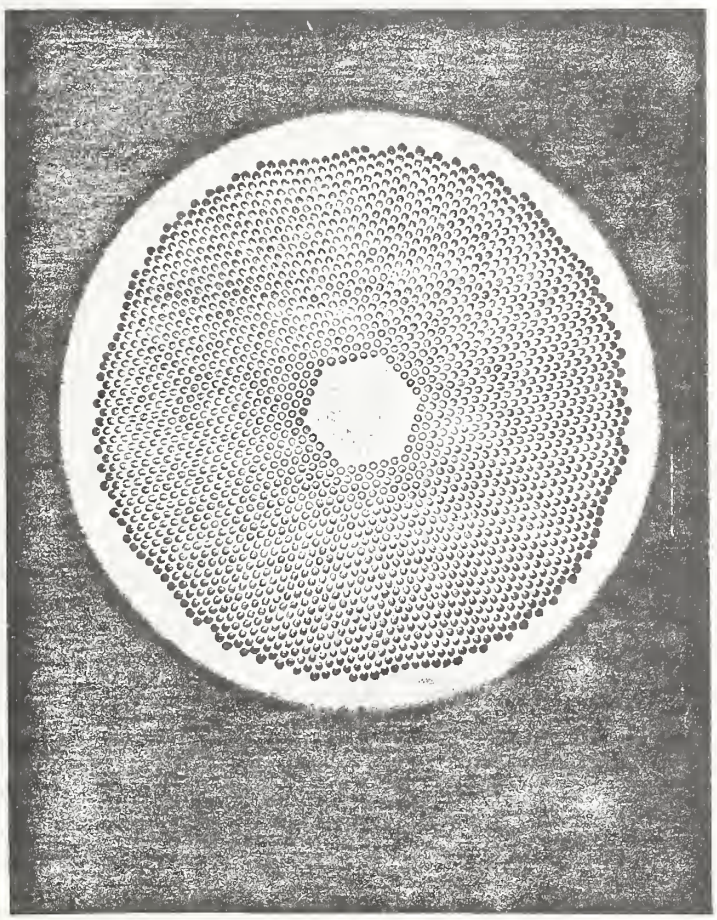

FIGURE 2.4 - FNAL ENERGY DOUBLER/SAVER TYPE STRAND USED IN THE LOW CURRENT SELF-FIELD EXPERIMENTS.

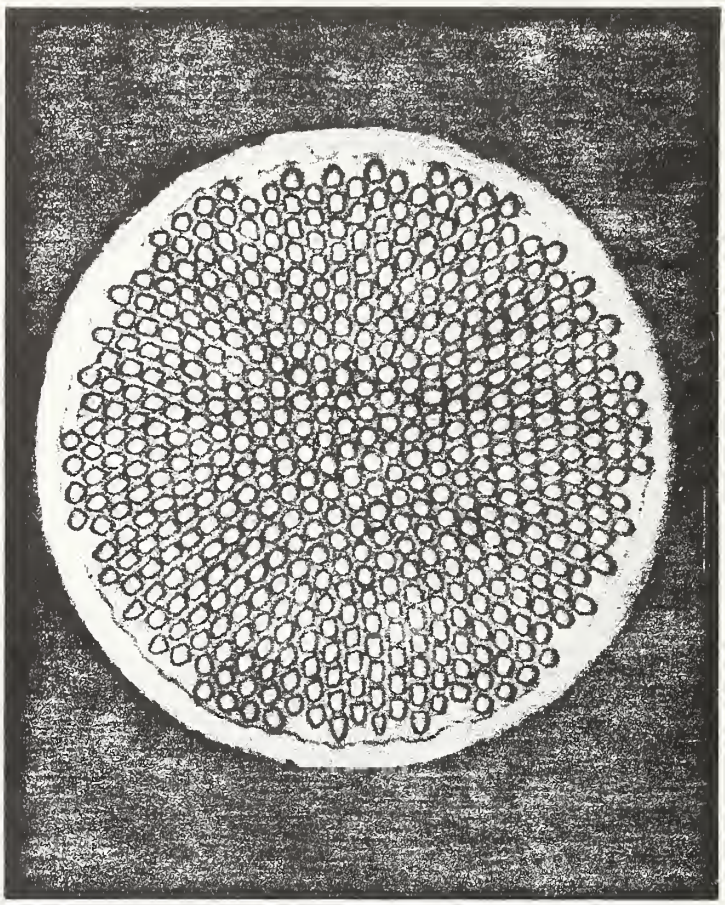

FIGURE 2.5 - BNL ISABELLE TYPE STRAND USED IN THE LOW CURRENT SELF-FIELD EXPERIMENTS.

Figure 2.6 - Data from low current self-field experiment.

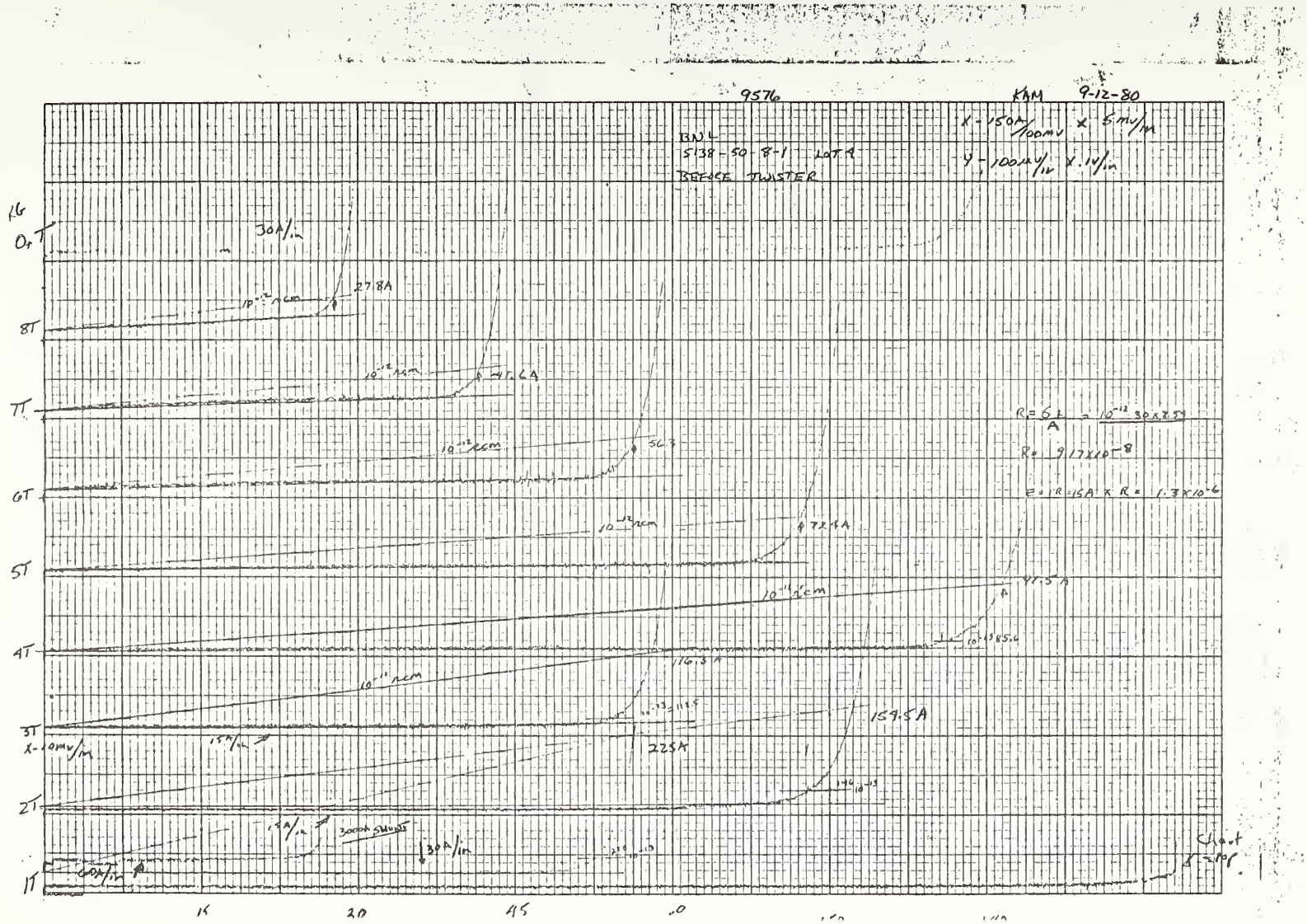

SENSITIVITY 10^{-12} Ω-cm

H (Tesla)	Untwisted I_c (amps)	0.32cm Twist I_c (amps)	0.32cm Twist ΔI_c (%)
8	115.5	98.3	14.9
7	168	143.3	14.7
6	219	187.5	14.4
5	277.5	235.5	15.1
4	339	289.5	14.6

TABLE 2.4 Critical current of FERMI type conductor as twisted. ΔI_c is I_c change upon twisting.

Sensitivity: 10^{-12} Ω-cm

H (Tesla)	Untwisted I_c (Amps)	1 cm Twist I_c (Amps)	1 cm Twist ΔI_c (%)	0.16 cm Twist I_c (Amps)	0.16 cm Twist ΔI_c (%)
8	27.8	26.6	4.3	24.8	10.8
7	41.6	39.8	4.3	38.3	7.9
6	56.3	54.8	2.6	52.5	6.8
5	72.4	70.9	2.1	67.5	6.8
4	91.5	89.3	2.4	89.5	6.1
3	116.3	113.3	2.6	108.8	6.4
2	154.5	144.8	6.3	138.8	10.2
1	225	211.5	6.0	207.8	7.6
Sensitivity: 10^{-13} Ω-cm					
1	85.6	84	1.8	80.3	6.2
2	112.5	106	5.8	100.5	10.7
3	146	135	7.5	129	11.6
4	210	199	5.2	194	7.6

Table 2.5 Critical Current of BNL Type Conductor as Twisted For Different Twist Pitches. ΔI_c is I_c Change Upon Twisting.

drawn through the dies which are normally used after the production twisting operation to insure a uniform cross section. The samples were remeasured and the results are shown in Tables 2.6 & 2.7. Again there is a definite reduction in the critical current upon twisting and the effect becomes larger as the wire is twisted more tightly and as the field is lowered. It scales, however, much more slowly than ε indicating that if a self-field effect is present, it is not adequately described by the simplistic model used in Section 2.1.1. It is difficult, however, to postulate a mechinism which would explain the observed behaviour. Most phenomonen which degrade critical current such as non-uniform reduction in filaments or non-uniform strain in filaments, have an effect which is predominate at high fields, and in this data the effect is larger at the low fields. At this point, we would therefore say that there does exist a degradation of the critical field in NbTi superconductor wires upon twisting which can tentatively be ascribed to self-field effects in the absence of a more satisfactory explanation. It is obvious, however, that considerably more experimental and theoretical work would be necessary to unambigously establish this effect and to quantify it in such a manner that it could be properly taken into account in the design of short sample tests.

SENSITIVITY 10^{-12} Ω-cm

H (Tesla)	Untwisted I_c (Amps)	0.5 cm Twist I_c (amps)	0.5 cm Twist ΔI_c (%)	0.3 cm Twist I_c (amps)	0.3 cm Twist ΔI_c (%)
8	87	72.8	16.3	72.8	16.3
7	123	108	12.4	105	14.8
6	160.8	141.8	11.8	134.3	16.5
5	198	127	10.6	165	16.7
4	241	202	16.0	200	16.9
3	296	252	15.0	245	17.1

TABLE 2.6 Critical current of FERMI type conductor drawn after twisting. ΔI_c is I_c change upon twisting.

H (Tesla)	Untwisted I_c (amps)	1 cm Twist I_c (amps)	1 cm Twist ΔI_c (%)	0.16 cm Twist I_c (amps)	0.16 cm Twist ΔI_c (%)
		SENSITIVITY 10^{-12} Ω-cm			
8	23.7	23.3	1.7	22.0	7.2
8	35.8	35.3	1.4	32.8	8.4
6	48.4	47.3	2.3	44.6	7.9
5	61.9	60.8	1.8	57.2	7.6
4	78.0	76.5	1.9	71.3	8.6
3	97.7	85.3	2.5	89.6	8.3
2	128	124.5	2.7	116.7	8.8
1	184.4	176.3	4.4	168.3	8.7
		SENSITIVITY 10^{-13} Ω-cm			
4	72.8	69.9	4.0	66.2	9.1
3	90.7	88.5	2.4	83.9	7.5
2	118.5	115.5	2.5	105	11.4
1	170.6	165	3.3	154.6	9.4

TABLE 2.7 Critical current of BNL type conductor drawn after twisting ΔI_c vs I_c change upon twisting.

3.0 A SIMPLE METHOD FOR MEASURING THE NORMAL STATE RESISTIVITY OF COMPOSITE CONDUCTORS

3.1 Discussion

3.1.1 Introduction

Measurement of the resistivity ratio of the stabilizer in composite superconductors, although simple in concept, can be difficult or complicated in practice. The problem is associated with the ability to fix the conductor temperature within reasonable limits at some low level above its transition temperature. Immersion in liquid hydrogen is ideally suited to this purpose for most practical superconductors, but liquid hydrogen is not always available and the safe handling of it is a serious problem.

Dangling the conductor in a helium-filled dewar at a sufficient height above the helium level to insure that the superconductor is normal can work, but the temperature of a long length of conductor may be uncertain.

3.1.2 Measurement Concept

The temperature is stabilized by "pinning" the conductor between liquid helium as a thermal sink and current leads as a thermal source, while the voltage drop across a short section of it is measured using relatively high current for adequate sensitivity. The temperature range within the measured section is monitored using gold-iron and chromel thermocouples spaced above and below the measured section.

3.1.3 Procedure

Although the procedure described below has been empirically derived, it seems to have a wide range of applicability. It has been used to measure the resistivity ratio of the copper component

of multifilamentary NbTi-copper superconductors, and is should be readily applicable to other types of superconductors as well.

3.1.3.1 Mounting the Sample

The conductor is mounted on a holder which hangs vertically in a helium dewar and is immersed at its lower end in liquid helium. The top end of the conductor is soldered to a terminal capable of carrying 50 Amperes at room temperature. The total conductor length should be 14½" long when mounted on the holder shown in Figure 3.1. The circuit is completed by soldering the conductor to a second terminal at the lower end.

Voltage taps from twisted-pair leads are soldered to the conductor using No. 36 wire at the center of the conductor and separated by one inch. This spread is precisely measured. Five mil diameter gold-iron and chromel thermocouples are soldered to the sample at points ½" above and below the voltage taps, with particular care to insure that they are thermally grounded by the solder to the sample. Cold reference junctions are located at the bottom of the probe, which will always be in liquid helium for the measurement. The thermocouple leads are taken directly from the probe to differential floating input terminals without plugs or connectors to minimize extraneous thermal EMF's.

3.1.3.2 Instrumentation

The instrumentation consists of three microvoltmeters, an x - y recorder, and a DC current source. Two of the meters are used to monitor the thermocouple EMF's. The third meter must have a chart recorded output voltage and is used to record the voltage drop across the conductor test length. V is plotted vs. I on the x - y recorder using the chart recorder voltage output from the microvoltmeter to drive the "y" input and the voltage drop across an appropriate current shunt to drive the "x" input.

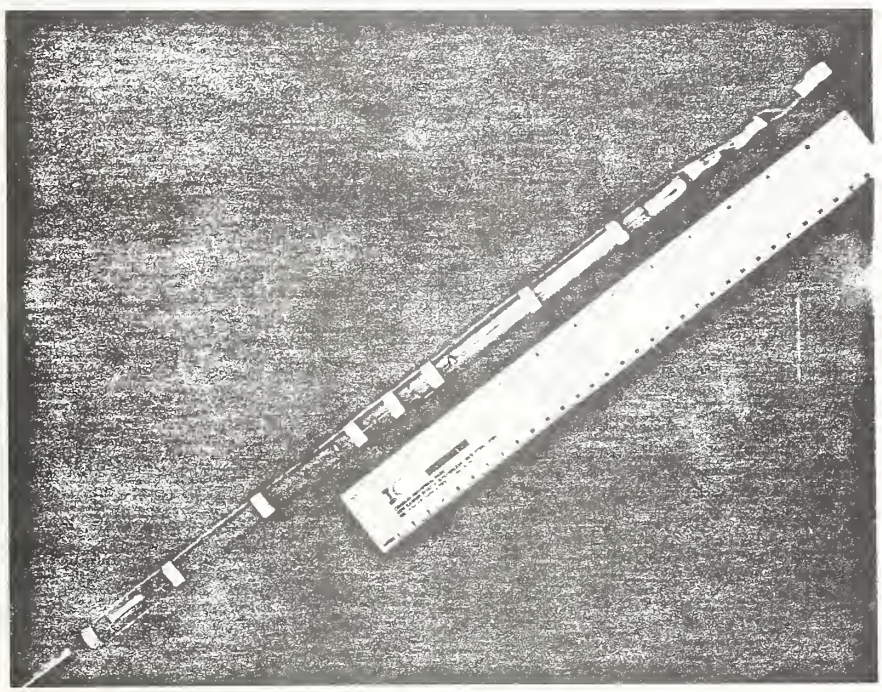

FIGURE 3.1A - LOWER END OF RRR APPARATUS. THERMOCOUPLE REFERENCE JUNCTIONS ARE TO RIGHT OF PICTURE.

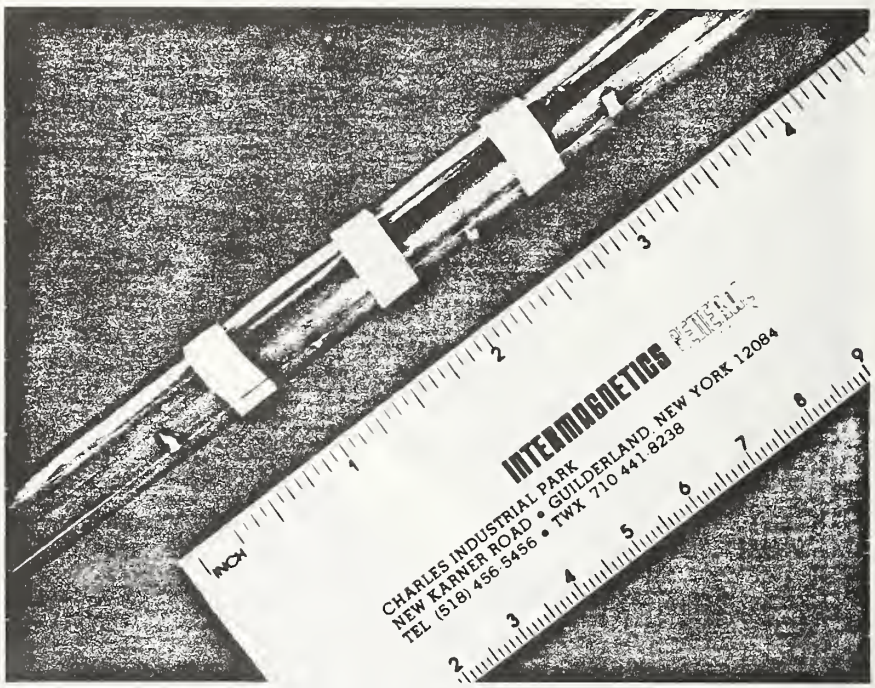

FIGURE 3.1B- DETAILS OF VOLTAGE TAPS AND THERMOCOUPLE ATTACHMENT TO SAMPLE.

3.1.3.3 Measurement of Resistance Near Room Temperature

Immerse the sample in a stirred alcohol bath which is held at 0°C by a surrounding ice-water bath. Record the bath temperature. Record voltage vs. current with I varying from I=0 to I=∿25 Amperes for .049" diameter conductor, and smaller maximum current for smaller wire. The measurement should be repeated using different ramp rates for the currents. The data should be logged, noting any non linearities and hysteresis in the traces.

3.1.3.4 Measurement of Resistance Near 10°K

(1) Immerse the probe in helium until the thermocouple EMF's are constant and approximately zero, then zero both of the thermocouple microvoltmeters. Mark the helium level by the lack of change in the thermocouples as the sample is moved vertically.

(2) Lift the sample until the lower thermocouple indicates approximately 10°K. Verify that the upper thermocouple temperature is less than 15°K. Be sure that the cold junctions of the thermocouples remain in the liquid helium. Record the helium level from the probe end. Record both thermocouple readings.

(3) Record voltage vs. current from I = 0 to I = 25 Amp (or less). Hold the current at maximum I and verify that the thermocouple temperatures are less than 15°K. Vary the I sweep rate and repeat the above measurement. The temperature is expected to shift as a function of I. If this shift causes an appreciable change in the chart recorder slope, then the measurement of R can be taken point by point as a function of average temperature between the two thermocouples. In general the resistance measured at the lowest temperature that is still above the superconductor Tc will be most relevant.

3.1.3.5 Resistance and Resistivity Ratios

(1) RRR' (T_R, $\bar{T}_L$): The ratio of the resistance measured at T_R and $\bar{T}_L$ gives directly the Resistance Ratio.

(2) RRR' (T, $\bar{T}_L$): To convert the measured ratio to represent the ratio for some standard temperature near room temperature, the Gruneisen relation is used;

$$\rho \propto TG(\theta/T)$$

where

$$G(\theta/T)=(\theta/T)^{-4}\int_0^{\theta/T}\frac{s^5 ds}{(e^s-1)\ (1-e^{-s})}$$

with θ = 330K for copper for the most common conversion, from 273K to 300K we have RRR' (273, TL) = 0.899 RRR' (300K, TL).

(3) Both of the above are measures of resistance ratio. To determine the resistivity ratio for the stabilizer component of the superconductor wire, the room temperature resistivity of the superconducting alloy or compound may have to be taken into account and the fractions of each component must be known.

$$RRR_{cu}\ (T, \bar{T}_L) = RRR_{tot}\ (T, \bar{T}_L) - \frac{R_{cu}\ (T)}{R_{sc}\ (T_L)}$$

Where: RRR_{cu} (T, $\bar{T}_L$) is the ratio of the copper resistance at T to that at $\bar{T}_L$.

RRR_{tot} (T, $\bar{T}_L$) is the ratio of the composite resistance at T to that at $\bar{T}_L$.

R_{cu} (T) is the resistance of the copper at T

R_{sc} (T_2) is the resistance of the superconductor at $\bar{T}_L$

We assume $\bar{T}_L > T_C$ so that the superconductor is in the normal state. We also assume that R_{sc} (T) >> R_{cu} (T).

3.1.4 Apparatus

The basic test apparatus is illustrated in the detailed construction blueprints included in this report as Attachment A*. It consists of an epoxy glass or phenolic sample holder with two high conductivity copper current contacts mounted on the end of a 0.5" diameter stainless steel tube. Leads for sample current, sample voltage and thermocouple voltage are routed through the tube. The phenolic holder is slotted to contain the sample and all leads within a 0.5" diameter circle. This allows the entire apparatus to be introduced into a helium storage dewar via an O ring sealed "quick connect" fitting without venting the helium to air.

The thermocouple junctions themselves are potted in epoxy in holes cut in the phenolic and thermal contact to the samples is made via copper foil tapes which are soldered to the sample and to the junctions. This arrangement provides protection for the junctions and still yields good thermal contact to the wire. It was found that a solder bond of a thermocouple to the sample was essential for accurate temperature measurement. Other methods of attaching the thermocouple, such as clamping or spring-loaded pressure contacts resulted in measurement of a temperature more characteristic of the surrounding helium than of the sample itself.

The apparatus described here represents a third generation in the evolution of this measurement technique at IGC. Two previous pieces of equipment were built and used for varying lengths of time, and experience with them contributed to the design of the present facility. The current design can be, we believe, easily duplicated in any low temperature laboratory, and, if sufficient interest exists, can be offered by IGC as a commercial product.

* Editor's note - The blueprints are not included in this NBSIR. Interested persons should contact the authors.

3.2 Data

The apparatus was tested by measuring a variety of wires and by measuring RRR of a single wire at several temperatures by changing the position of the holder in the helium dewar. A typical set of V-I plots obtained on the apparatus is shown in Figure 3.2.

Data on 4 different wires ranging in RRR from ∿1.2 to 113 are presented in Table 3.1. The results compare quite well with measurements from other sources.

In Table 3.2, data on a second sample of FNAL is presented as a function of temperature. It appears that the resistivity is slightly temperature dependent in the 11° to 17°K range as would be expected from data on pure copper.

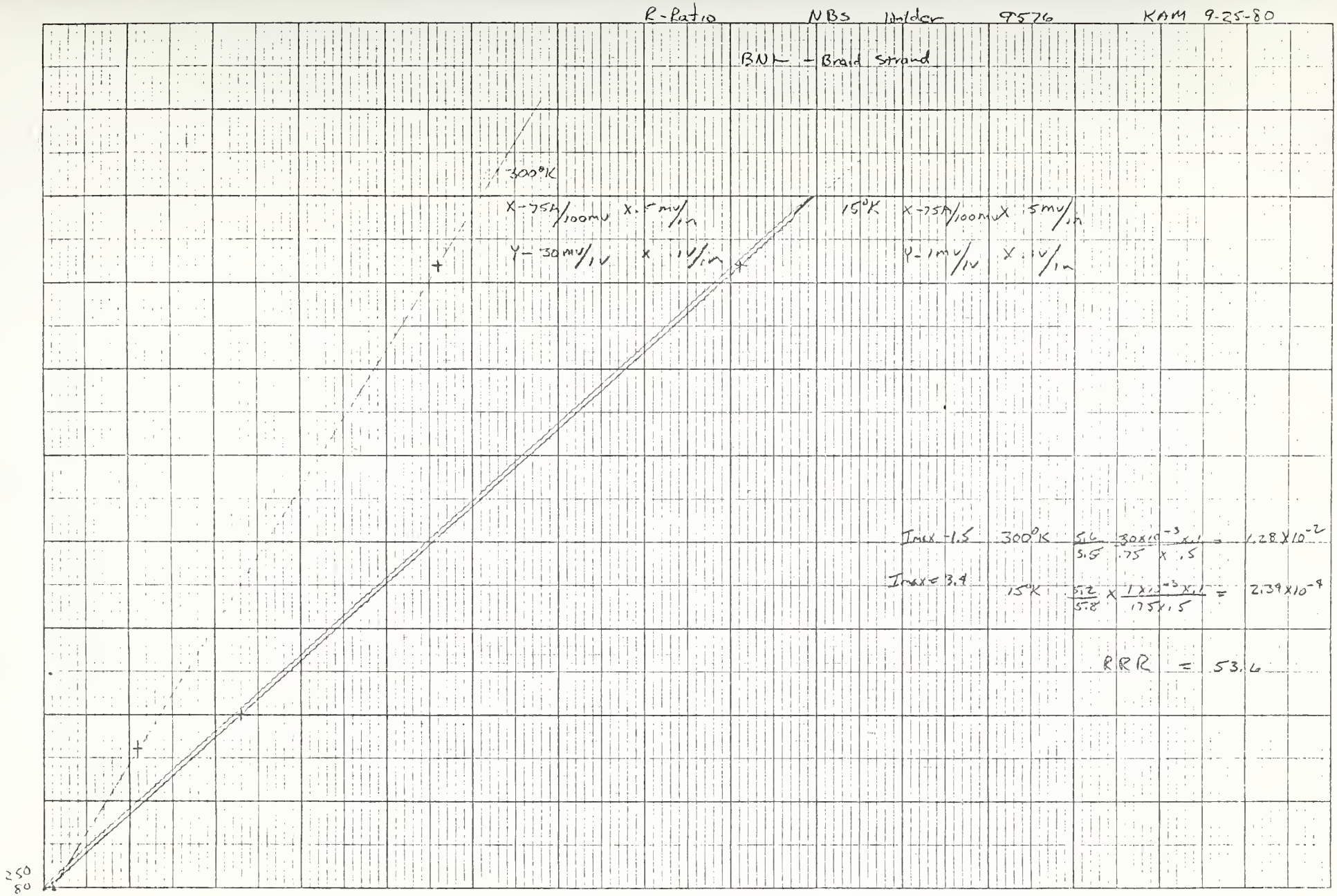

Figure 3.2 - Data from RRR Apparatus

Conductor	Dia. (inches)	TL (K)	Imax (300K) (A)	Imax (TL) (A)	RRR
BNL Isabelle	.0117	15	1.5	3.4	53.6
Full Cu-Ni Matrix	.010	14	1.2	1.2	1.19
FNAL - as twisted	.027	14	3.4	12	36.6
FNAL #1 final product	.027	14	4	12	113

TABLE 3.1 - RRR Data Obtained with NBS Test Fixture.

TL (K)	RRR
9.5	superconducting
11	120
12	120
14	118
17	115

TABLE 3.2 - RRR data on FNAL #2 final product for different temperatures TL.

REFERENCES

1) J.W. Ekin, J Appl Phys 49 3406 (1978, J Appl Phys 49 3410 (1978).

2) J.C. Maxwell, A Treatise on Electricity and Magnetism, 3rd Ed. Dauer 1954 p. 445.

3) J. W. Huang, A. Kozycki, Am. Jour. Phys. 47, #11, p. 1005.

4) N. N. Lebedev, Special Functions and Their Applications, Dover 1972, p. 98.

5) G. P. Tolstov, Fourier Series, Prentice Hall 1962, p. 197.

6) G. N. Watson, A Treatise on the Theory of Bessel Functions, Cambridge Univ. Press, London 1962.

C. Magnetic Corporation of America

DEVELOPMENT OF CRITICAL CURRENT MEASUREMENT STANDARDS

FINAL REPORT

Prepared for

U.S. Department of Commerce
NATIONAL BUREAU OF STANDARDS
Boulder, Colorado

Under Contract No. NB79RAC90026

Prepared by

MAGNETIC CORPORATION OF AMERICA
179 Bear Hill Road
Waltham, Massachusetts 02154

Principal Investigator:
Z. J. J. Stekly

Investigators:
H. R. Segal
K. F. Hwang

NBS-02

LIST OF FIGURES

Figure Number

2.2-1 Straight sample holder.

2.2-2 Noninductive sample holder.

2.2-3 U-shaped sample holder.

2.3-1 Variation in critical current as a function of electric field sensitivity.

2.3-2 Variation in critical current change as a function of heat flux. Results obtained using voltage/length criterion.

2.3-3 Variation in critical current change as a function of heat flux. Results obtained using equivalent resistivity criterion.

2.3-4 Critical current as a function of measurement criterion.

2.3-5 Short sample performance of round-robin NbTi at 1 mv/cm.

2.3-6 Short sample performance of round-robin Nb_3Sn tape at 1 mv/cm.

2.3-7 Short sample performance of round-robin multifilamentary Nb_3Sn at 1 mv/cm.

3.3-1 Current transfer measurements. Effect of removing some copper from current contacts.

3.3-2 Current transfer into CuNi matrix cable.

LIST OF TABLES

Table Number

2.1-1 Group 1 samples.

2.1-2 Group 2 samples (cable).

2.1-3 Group 3 samples (round robin).

2.3-1 Critical currents of Group 2 samples.

2.3-2 Conductor performance as a function of sample holder.

2.3-3 Short sample performance of round robin NbTi.

2.3-4 Short sample performance of round robin Nb_3Sn tape.

2.3-5 Short sample performance of round robin multifilamentary Nb_3Sn.

3.1-1 Current transfer samples.

ABSTRACT

This report on U. S. Department of Commerce Contract Number NB79RAC90026 deals with the development of standards for critical current measurements. The two tasks investigated were: (1) The Determination of Critical Current of Short Samples as a Function of Transition Criterion, and (2) Analysis of Current Transfer from Sample Holder to Sample. The samples used in the critical current measurements included both NbTi and Nb_3Sn. Critical currents were measured using the equivalent resistivity criterion with sensitivities ranging from 10^{-7} Ω-cm to 10^{-12} Ω-cm and using the electric field criterion with sensitivities of 1 mV/cm to 100 nV/cm. Current transfer measurements were performed on monolithic conductors with critical currents greater than 1,000 amps and on a CuNi-matrix cable. The results of the program are that no single measurement standard and no single test holder are suitable for all types of critical current measurements, and that sample holders must be designed with sufficiently large copper current contacts in order to minimize current transfer effects.

I.0 INTRODUCTION

Although superconductivity was discovered almost seventy years ago and although applied superconductivity is approximately twenty years old, at the present time there are still no defined standards for the basic superconductivity parameters (critical field, critical temperature, and critical current). There can easily be a 50% difference in the critical current of a sample depending upon the measuring technique. In addition, in most reports on critical current measurements, the evaluation criterion is not mentioned. In order to assist the National Bureau of Standards (NBS) in the development of standards for superconductivity parameters the Magnetic Corporation of America (MCA) has undertaken a program to investigate critical current measurements. Testing was performed on approximately twenty samples using three types of test fixtures. Critical current measurements were made using two evaluation criteria (electric field and resistivity) and various sensitivities.

With the results of the tests on those samples, including three round-robin conductors supplied by NBS to MCA and the other contractors, recommendations are made on the establishment of evaluation criteria and standardized sample holders. As an additional guide in the design of test fixtures, testing was performed to determine current transfer properties from the sample holder into the superconductor. Recommendations are made on means of improving the current transfer characteristics. In the following section the results of the short sample tests are discussed. Descriptions of the experimental equipment including the various test fixtures are included. In Section 3 the current transfer tests are described. The effect of modifying the amount of copper on the current contacts is shown. In Section 4 the conclusions of the program and recommendations for the establishment of tests standards are made.

2.0 Short Sample Measurements

The majority of the work performed during this program involved the measurement of the critical current of approximately twenty samples. The samples varied in their diameters, copper-to-superconductor ratios, and superconducting material. The measurements were made using three different sample holders, each sample holder using a different length conductor in a different configuration. The tests were made at various magnitudes of external magnetic field and at various sensitivities. The critical current was determined in terms of electric field and equivalent resistivity.

2.1 Description of Samples

Three groups of samples have been tested. The first group consisted of 15 samples of multifilamentary, copper stabilized NbTi. The wire diameter varied from .020 cm to .109 cm and the copper-to-superconductor ratio ranged from 1.25 to 5.5. The specification of the samples in that group are listed in Table 2.1-1. These samples were chosen to demonstrate the influence, if any, of copper current density, matrix resistance, heat flux, etc., on the critical current of superconductors. It was hoped that by careful analysis of the critical current at different measurement criteria for the various samples, a single fundamental measuring technique might be formulated for all short sample testing. In order for that to be possible the relationship between the critical current and the other sample parameters must be understood. For example, suppose short sample critical current measurements are made using a criterion of 10^{-12} Ω-cm equivalent resistivity. The resistivity of the copper stabilizer in a typical conductor in an external field of 7 tesla is approximately 5×10^{-8} Ω-cm. Therefore, for typical samples the resistivity measured at 10^{-12} Ω-cm is due almost exclusively to the superconductor. It is thus conceivable

TABLE 2.1-1 GROUP 1 SAMPLES

DIAMETER (cm)	Cu/SC	NO. OF FILAMENTS
.020	1.25	367
.028	1.25	367
.041	1.25	367
.064	1.25	367
.020	1.6	180
.051	1.6	180
.028	1.8	2178
.064	1.8	2200
.020	3.0	121
.028	3.0	361
.051	3.0	121
.061	3.0	121
.086	3.0	2772
.109	4.0	84
.100	5.5	114

that the critical current measurements could be independent of the amount of copper in the conductor. This hypothesis could be tested by determining the critical current of samples with identical amounts of NbTi but with varying amounts of copper. It is for such reasons that the chief variables of the Group 1 samples are copper-to-superconductor ratio and wire diameter.

With the samples chosen in Group 1 it is not possible to hold all the variables constant while varying only the amount of copper. This is due to the fact that the critical current density varies with the amount of cold work reduction. As the diameter of a given type of wire increases, its critical current density decreases. In order to have a few conductors with a fixed amount of superconductor which would behave identically in each of the samples while having a variable amount of copper, a second group of samples was made. The three samples listed in Table 2.1-2 each consist of a strand of identical multifilamentary NbTi. In the second sample of the group the superconductor is cabled with a single strand of copper wire, and in the third sample the superconductor is cabled with two strands of copper wire. In this way the superconductor of all three samples will be identical and only the amount of copper will vary.

Finally, Group 3 consists of samples sent to us by NBS to be evaluated in round-robin testing. The three samples consist of multifilamentary NbTi, multifilamentary Nb_3Sn, and Nb_3Sn tape. A description of each sample is listed in Table 2.1-3.

2.2 Description of Equipment

Samples were tested on three sample holders. Since part of the goal of this program is to aid in the establishment of a standard test fixture it was hoped that a comparison of the results obtained from different sample holders might lead to a preference in geometry.

TABLE 2.1-2 GROUP 2 SAMPLES (CABLE)

SUPERCONDUCTOR				COPPER		OVERALL Cu/SC
Sample Number	Number Of Strands	Strand Dia. (cm)	Cu/SC	Number of Strands	Strand Dia. (cm)	
C1	1	.028	1.25	0		1.25
C2	1	.028	1.25	1	.018	3.06
C3	1	.028	1.25	2	.018	4.90

TABLE 2.1-3 GROUP 3 SAMPLES
(ROUND ROBIN SAMPLES)

MATERIAL TYPE	CROSS SECTION
Multifilamentary NbTi	0.53 x 0.68mm
Nb_3Sn Tape	2.3 x 0.2mm
Multifilamentary Nb_3Sn	0.7mm diameter

The first sample holder accommodates four straight samples each up to 3.5 cm long. A photograph of the sample holder is shown in Figure 2.2-1. This sample holder was originally built to test reacted Nb_3Sn samples. The straight sample shape permits the Nb_3Sn to be reacted in the simplest geometry and mounted with a minimum amount of handling. This sample holder was designed for use in a dewar with an inner diameter of less than 4 cm. Because of the short sample length this holder is suitable only for conductors with very short current transfer lengths. In addition, the current through the sample should be limited to less than 100A in order to minimize the joule heating at the current contacts. This point is discussed further in the next section of this report.

For systems with a larger magnet bore, a similar sample holder could be built to handle longer and higher current samples. With the present system a distance between voltage taps of 1 cm is about the largest reliable length. In order to ensure that each sample is placed in the central field region the samples are attached to a phenolic support tube which may be raised or lowered through a quick connect in the top plate of the holder. The sample holder is made out of phenolic. Small grooves are machined into the sample holder to help in the alignment of the samples. The samples are held rigidly in place during testing by a coating of vacuum grease. Because of the simple geometry the mounting of samples is extremely fast and convenient. With this sample holder, as well as the other two to be described, one current lead is common to all the samples. The total number of current leads is therefore N+1, where N is the number of samples in a sample holder.

A second sample holder designed for use in a small bore magnet is shown in Figure 2.2-2. Three noninductively wound samples can be mounted on each sample holder. The length of each sample is approximately 75 cm and

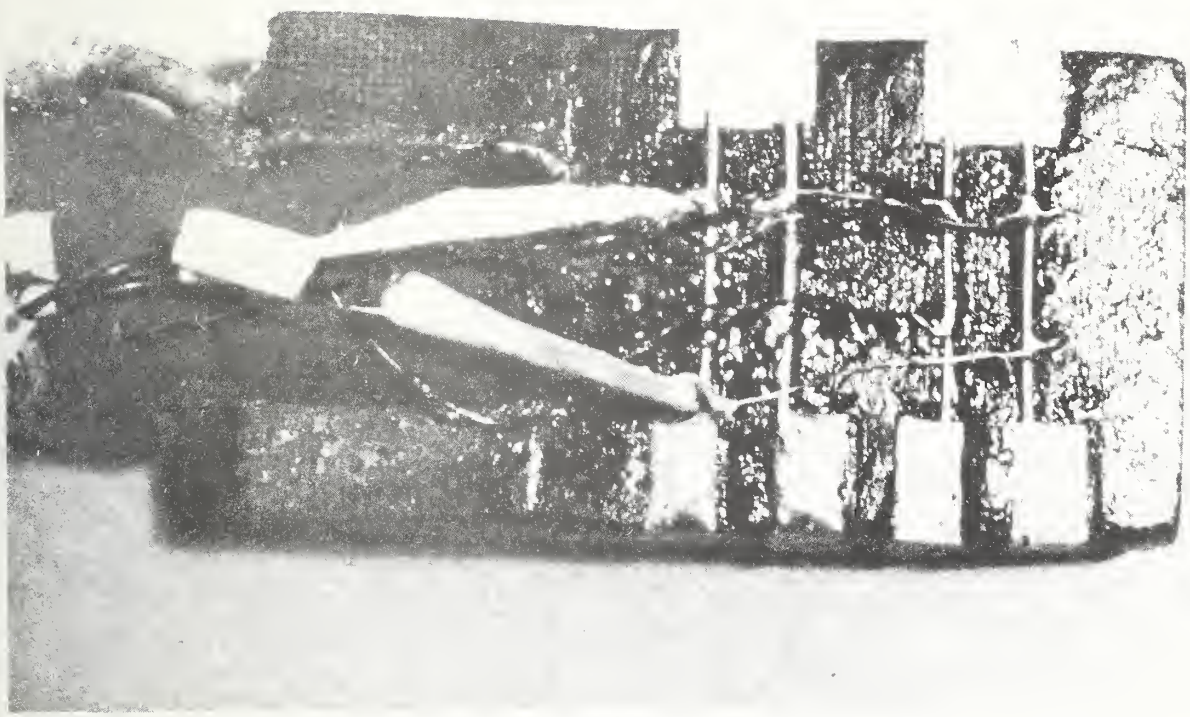

Straight Sample Holder

Figure 2.2-1

Non-inductive Sample Holder

Figure 2.2-2

a typical distance between voltage taps is 40 cm. Grooves are machined in the phenolic sample holders to accommodate samples up to .150 cm in diameter. Each sample is held in place with two to three pieces of lacing cord. The samples are prevented from moving during testing by a coating of vacuum grease. Just as for the straight sample holder, each sample can be located in the central field by sliding the support tube through a quick connect on the top plate. Because of the limited helium capacity of the dewar, sample current is restricted to 100A.

The third sample holder is shown in Figure 2.2-3. The samples are U-shaped and approximately 35 cm long. Three samples can be mounted to the holder. The maximum current that can be carried is 850A. As with the other sample holders, conductor motion is prevented by coating the samples with vacuum grease. This sample holder is designed to fit into a magnet with a bore of 7.6 cm. Because of the curvature of the bottom of the sample holder, only a very small portion of the sample is perpendicular to the magnetic field. Because of the variation in sample orientation with respect to field direction, this sample holder is most suited for less sensitive measurements such as quench currents, rather than for measurements in which there is significant current sharing between the superconductor and the copper stabilizer. The current contact region is 8 cm long on each end of the sample.

Terminal voltage versus current (V-I) characteristics were obtained for all samples. The current was generally supplied by a 100A 10V Hewlett Packard power supply. For samples that carried more than 100A, a 500A 10V supply was used. The current was measured using an external shunt. The output of the voltage taps was fed into a Keithley microvoltmerer. The amplified output of the microvoltmeter was the input to the X-axis of an

U-shaped Short Sample Holder

Figure 2.2-3

X-Y recorder, and the potential difference across the shunt was the input to the Y-axis. With this experimental setup it was possible to measure sample voltages as low as 0.1 μV. Critical current measurements were made at MCA using a 7.5 cm diameter, 7 tesla, superconducting magnet and at the Francis Bitter National Magnet Laboratory at MIT. The magnetic field was supplied by a 15 tesla, 5.4 cm bore, water-cooled Bitter coil.

2.3 Results and Analysis

The V-I characteristics of the three groups of samples described in Section 2.1 have been measured as a function of applied field and voltage sensitivity. In addition to measuring the quench current of each sample the critical current was measured using electric field and equivalent resistivity criteria. With electric field used as the evaluation condition critical currents were determined for a range of sensitivity from 1 mV/cm. Maximum sensitivity was between 1 μV/cm and 0.1 μV/cm, depending upon the particular sample and sample holder. When resistivity was used as the evaluation criterion, measurement sensitivity ranged from 10^{-7} Ω-cm to 10^{-11} Ω-cm or 10^{-12} Ω-cm.

It was originally planned to test the samples in Group 1 at fields of 3 tesla to 7 tesla. However, it was observed that at low fields there was little variation in critical current as a function of the measurement standard. This can be seen in Figure 2.3-1 for a sample with a copper-to-superconductor ratio of 1.25. In that figure for fields less than 7 tesla there is less than a 10% reduction in critical current as the measurement criterion is varied from 1 mV/cm to 0.1 μV/cm. For samples with higher copper-to-superconductor ratios the reduction is somewhat larger. However, for a sample with a wire diameter of 0.06 cm and a copper-to-superconductor ratio of three, the decrease in critical current at 7 tesla is only 11%

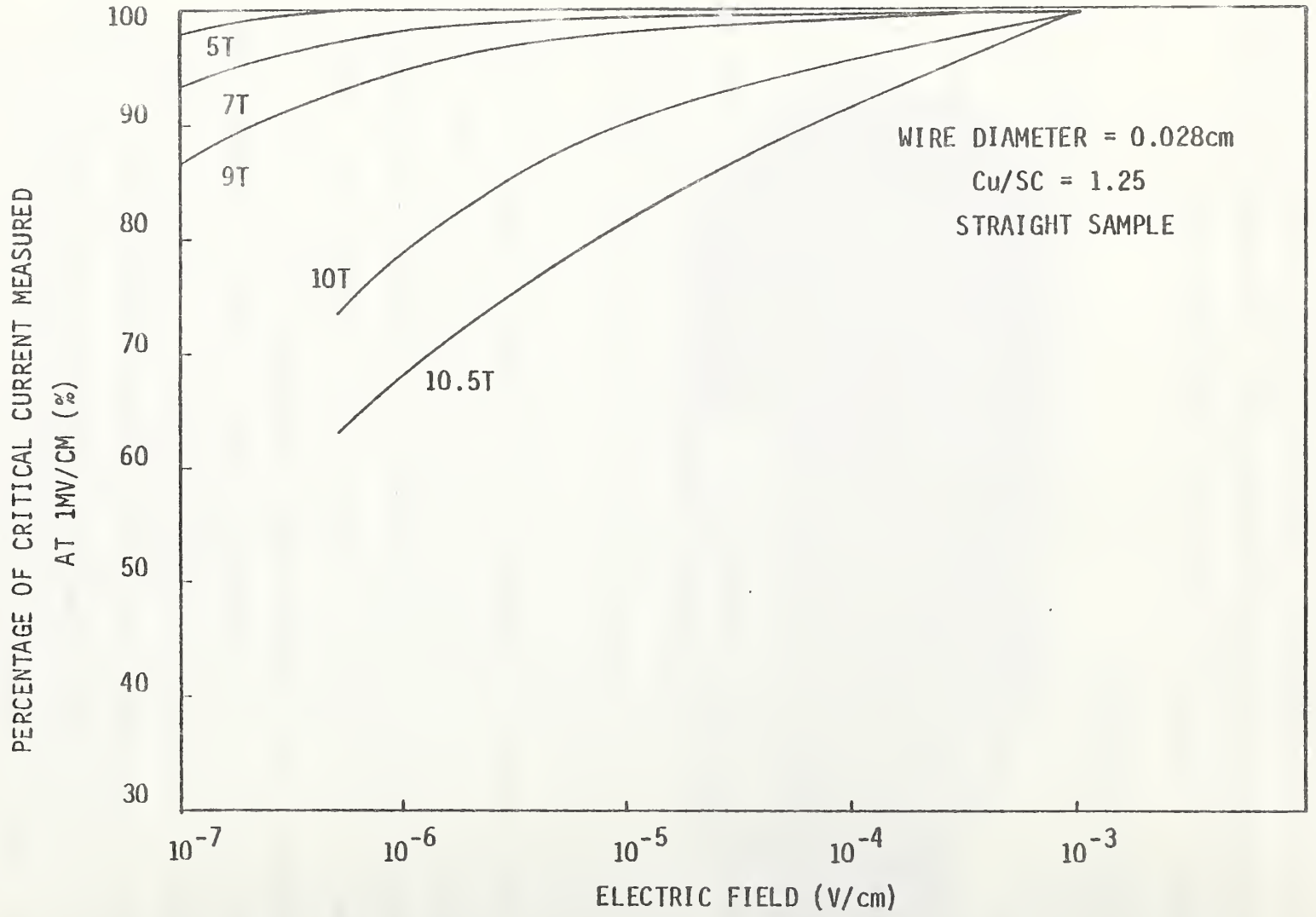

FIG. 2.3-1 VARIATION IN CRITICAL CURRENT AS A FUNCTION OF ELECTRIC FIELD SENSITIVITY

as the measurement criterion is increased four orders of magnitude from 1 mV/cm to 0.1 μV/cm. In order to maximize the difference in critical current with sensitivity it was decided to vary the magnetic field between 7 tesla and 10.5 tesla instead of between 3 tesla and 7 tesla. It should be pointed out, however, that the small variation in critical current with sensitivity up to 7 tesla implies that there is a good deal of freedom in the definition of critical current in that range. Although it is not common to measure critical currents in NbTi superconductors at 10.5 tesla at a temperature of 4.2K, this is in many ways equivalent to measuring the critical current at a lower field of a sample with a high copper-to-superconductor ratio. At least some of the variation of critical current with measurement standard can be related to the joule heating in the conductor. Low critical currents at high fields result in joule heating that is comparable to that of low field high current conductor having a high copper-to-superconductor ratio. For example, a typical critical current density at 10.5 tesla is 1×10^4 A/cm^2. If all of the current would transfer to the stabilizer in a conductor with a copper-to-superconductor ratio of 1.8, the copper current density would be 5,500 A/cm^2.

On the other hand, at 7 tesla a typical superconductor current density of 1×10^5 A/cm^2 would require a copper-to-superconductor ratio of 18 in order to have the same stabilizer current density. Therefore, testing samples at high field values seems to be a reasonable method of simulating results for high copper-to-superconductor ratio conductors.

The change in critical current with measuring sensitivity varied significantly as the sample, magnetic field, copper-to-superconductor ratio, and wire size were varied. For example, a sample with a 0.0635 cm diameter and a copper-to-superconductor ratio of 1.25 exhibited only a 3.8% decrease in critical current as the sensitivity was varied from 1 mV/cm to 0.2 μV/cm

at a field of 7 tesla. On the other hand, there was a 54% decrease in critical current in a 0.020 cm diameter wire with a copper-to-superconductor ratio of 1.6 when the sensitivity was varied from 1 mV/cm to 0.5 μV/cm when the external field was 10 tesla.

The critical current data obtained using an electric field standard were analyzed in order to understand the variation in performance with measuring sensitivity. For example, it would be advantageous to be able to predict the performance of a conductor at a high measuring sensitivity based on the quench current results. Attempts were made to find a good correlation of the data with one of the significant parameters of the experiment. The best fit of the data occurred when the decrease in critical current with sensitivity was plotted as a function of heat flux. In Figure 2.3-2 the percentage decrease in critical current from 1 mV/cm to 0.1 μV/cm sensitivity is plotted as a function of heat flux at 1 mV/cm sensitivity. NbTi samples from all three groups and at various magnetic field are included in the data. The solid lines represent an envelope of the data points. The heat flux is calculated assuming 100% wetted surface area. In fact, the samples were coated with a thin layer of vacuum grease to prevent motion. The influence of the grease on the heat flux will account for some of the scatter in the data. For the conductors tested in the straight sample holder, conduction cooling through the ends will also cause scatter in the data. In view of these considerations the data points tend to be situated on a common curve. It is thus possible to estimate the performance of a sample at 0.1 μV/cm sensitivity from the short sample data at 1 mV/cm sensitivity.

A similar study was performed on results using equivalent resistivity as a criterion. It was hoped that resistivity might be a more fundamental

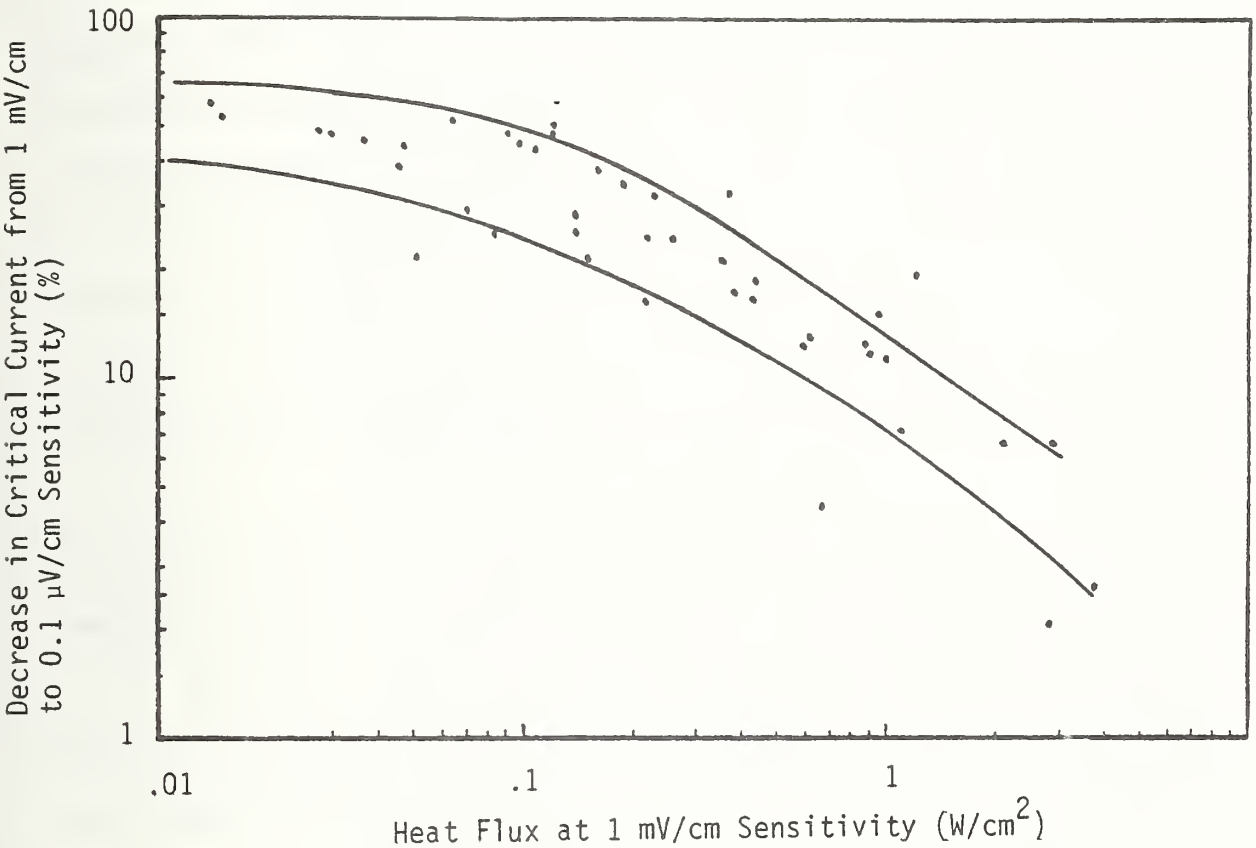

Fig. 2.3-2 Variation in Critical Current Change as a Function of Heat Flux. Results obtained using Voltage/Length Criterion

standard than electric field. For example, consider a conductor with a copper-to-superconductor ratio of 1.25, a copper residual resistance ratio of 100, and an applied magnetic field of 7 tesla. At an equivalent resistivity of 10^{-11} Ω-cm, the resistivity of the superconductor is 17,000 times smaller than that of the copper. Since almost all of the current will flow through the superconductor one might expect that the results are independent of copper-to-superconductor ratio and are, therefore, intrinsic to the superconductor. Even at an equivalent resistivity of 10^{-10} Ω-cm the total resistance of the copper is 1,400 times greater than that of the superconductor. The experimental results shown in Figure 2.3-3 are very similar to those for electric field. In that figure the decrease in critical current with a four order of magnitude increase in sensitivity is plotted along the ordinate and the heat flux at 10^{-8} Ω-cm sensitivity is plotted along the abscissa. The spread of data is approximately the same for the two cases.

It is clear, based on the results of Figure 2.3-2 and Figure 2.3-3, that the change in critical current with sensitivity is inversely related to the heat flux. This is true even when only a small fraction of the transport current is flowing through the copper stabilizer. In order to verify that the critical current at all measuring sensitivities is dependent on the amount of copper stabilizer and the size of the conductor, the samples in Group 2 were tested. These samples have identical amounts of superconductor and cold work reduction. The amount of copper and the wetted surface area are the only variables. In Table 2.3-1 the critical currents of the samples are listed for various magnetic fields, evaluation criteria, and sensitivities. From these results it can be seen that the critical current increases as the copper-to-superconductor ratio increases. In other words, the amount of copper and the amount of cooling are important influences on the critical current. For the criteria used, the critical current is not a function only of the amount of superconductor.

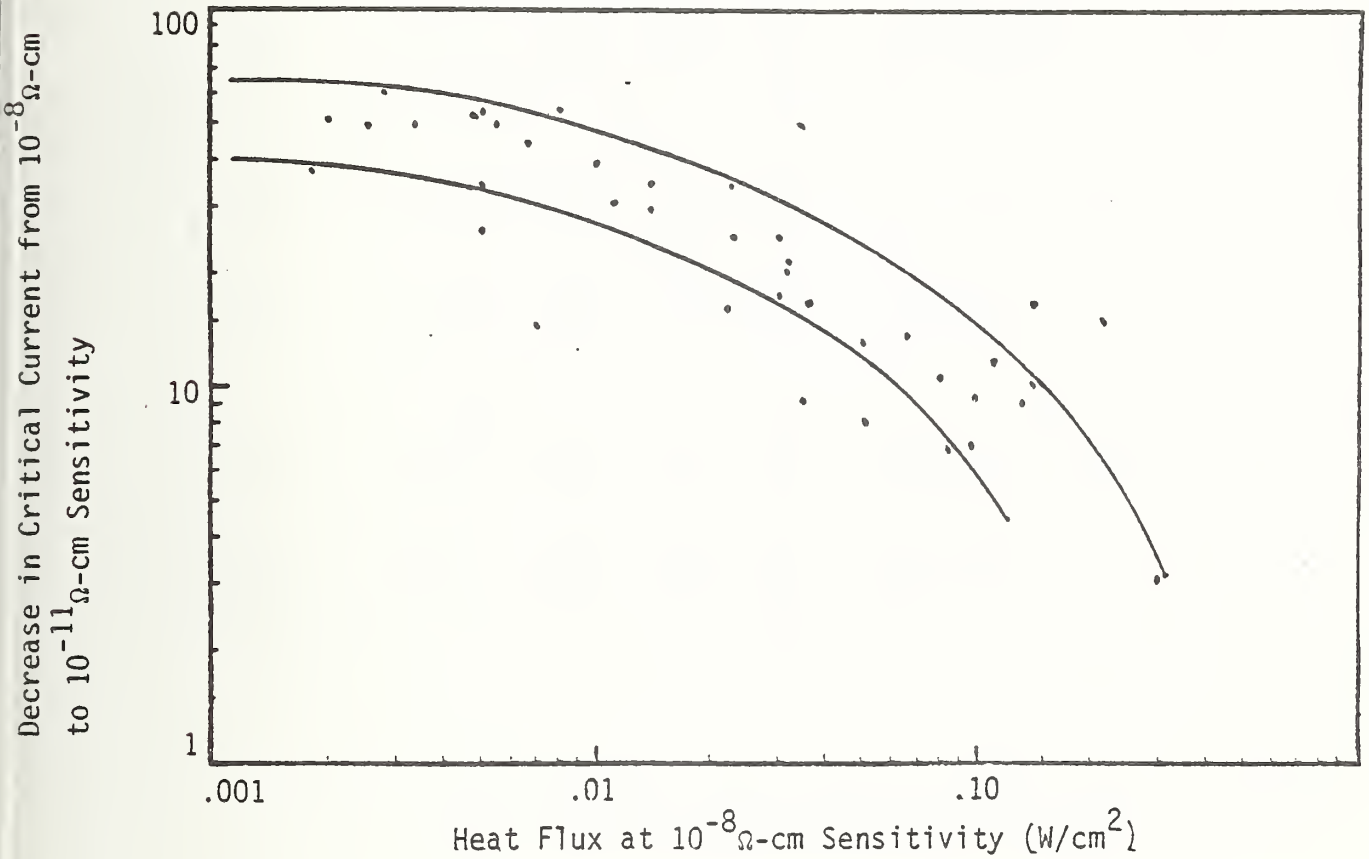

Fig. 2.3-3 Variation in Critical Current Change as a Function of Heat Flux. Results obtained using Equivalent Resistivity Criterion.

TABLE 2.3-1 CRITICAL CURRENTS OF GROUP 2 SAMPLES

Sample Number	Cu/SC	Sensitivity	Critical Current (Amps)			
			7T	9T	10T	10.5T
C1	1.25	100μv/cm	33.2	16.6	7.9	4.4
		.1μv/cm	31.2	14.7	5.6	2.1
		$10^{-8}\Omega$-cm	33.4	16.8	8.3	4.4
		$10^{-11}\Omega$-cm	31.6	15.4	5.7	2.0
C2	3.06	100μv/cm	36.2	18.9	10.4	6.2
		.1μv/cm	32.0	15.0	6.1	2.5
		$10^{-8}\Omega$-cm	36.4	18.0	10.0	5.2
		$10^{-11}\Omega$-cm	33.0	14.0	6.1	2.0
C3	4.90	100μv/cm	36.6	19.9	12.2	4.2
		.1μv/cm	32.0	15.2	6.8	2.7
		$10^{-8}\Omega$-cm	37.5	19.9	11.0	3.9
		$10^{-11}\Omega$-cm	33.6	15.2	6.6	2.4

In Figure 2.3-3 only the change in critical current between 10^{-8} Ω-cm and 10^{-11} Ω-cm is plotted. In Figure 2.3-4 the critical currents at intermediate sensitivities are shown for a sample with a wire diameter of 0.041 cm and a copper-to-superconductor ratio of 1.25. For comparison the critical current measured at 10^{-6} V/cm and 10^{-7} V/cm is also presented. It can be seen that at 7 tesla and at 9 tesla the critical current is almost constant between 10^{-8} Ω-cm and 10^{-10} Ω-cm sensitivity. Reductions in critical current begin to become significant only at 10^{-11} Ω-cm. For many applications (e.g., most epoxy-filled intrinsically stable magnets) it is not necessary to know the critical current at the high sensitivities. On the other hand, for some magnets, such as for NMR applications where low level losses become important, the critical current must generally be known at 10^{-12} Ω-cm to 10^{-14} Ω-cm sensitivity. To a certain extent it is possible to extrapolate short sample curves like these in Figure 2.3-4. However, particularly at the higher fields the variation in critical current is very rapid as a function of sensitivity, and it would be difficult to obtain a reliable extrapolation.

On the other hand, because of difficulties in measuring voltages lower than 0.1 μV it is not practical to increase the sensitivity of the measurement when testing very short samples. The best solution would be to use a sample holder consisting of a small spool of noninductively wound wire. For example, with a measuring sensitivity of 1 μV one can detect a signal of 1 nV/cm across a 10 meter long sample. While such a sample holder is not convenient for a typical short sample test it would be extremely useful for certain applications where high measuring sensitivity is required.

An important consideration in measuring critical currents is the consistency of measurements made with different sample holders. In order to

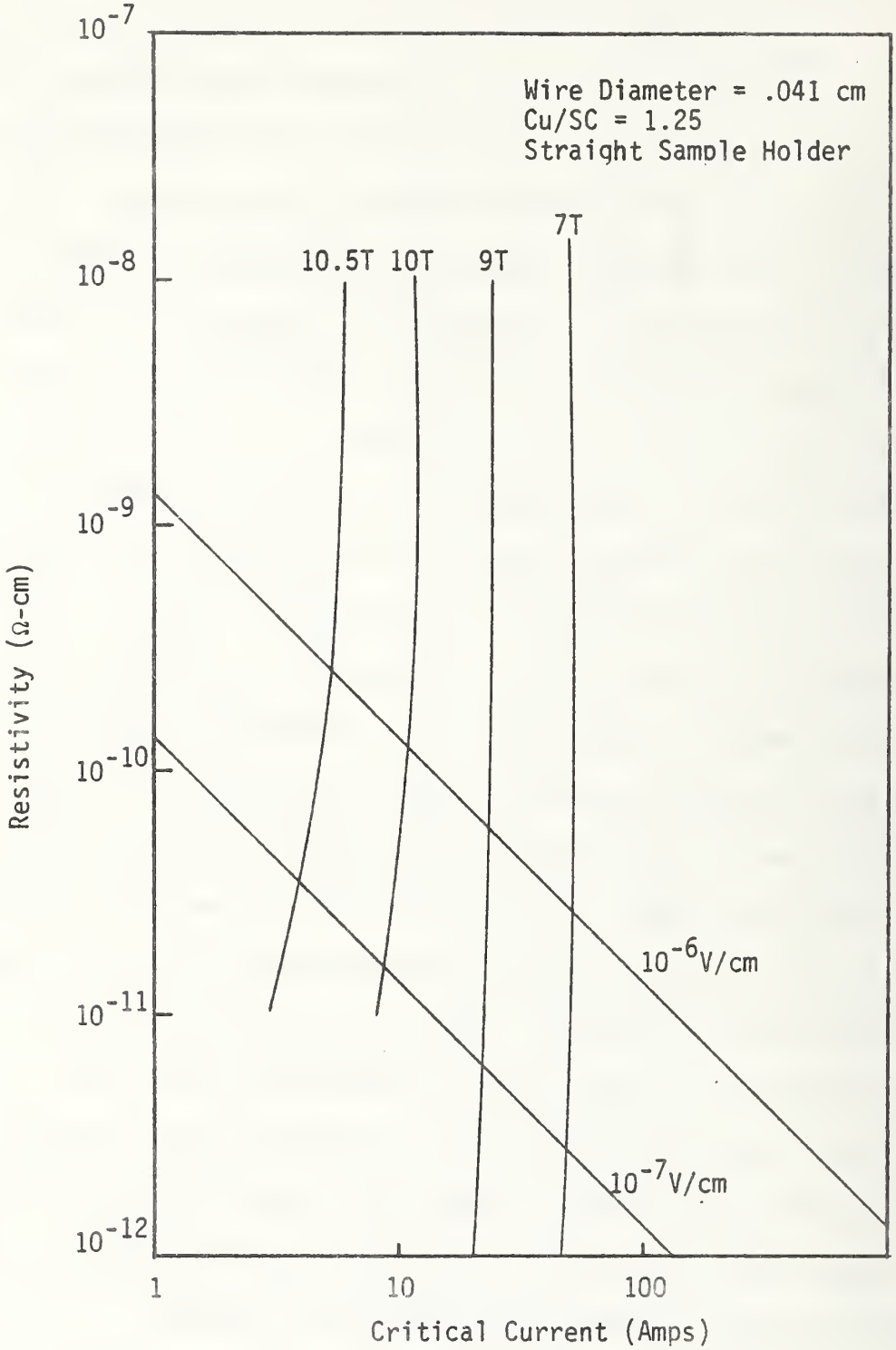

Fig. 2.3-4 Critical Current as a Function of Measurement Criterion

study this effect two approaches were used: (1) samples were tested using three different sample holders available at MCA, and (2) three round-robin samples supplied by NBS were tested. The three sample holders have been described in Section 2.2. The two most significant differences among the sample holders are the sample geometries and lengths. Sample shapes are straight, U-shaped, and noninductively wound spiral. Sample lengths vary from 3.5 cm to 1 meter. The straight sample holder and the noninductive sample holders were designed for use below 100A. For the noninductive sample holder the voltage drop across the current leads limits the current to 100 amps when used with a 10 volt power supply. Although larger currents can be passed through the straight sample holder the results above 100A tend to be unreliable. Therefore, in order to make a good comparison among the various sample holders, critical currents were generally limited to 100A or less. Since the U-shaped sample holder is designed for use in a magnet with a maximum central field of 7 tesla, the comparison measurements were made at low fields only. In general, the agreement in critical currents as measured in the three sample holders was quite good. Typical results are presented in Table 2.3-2. The maximum variation between any two measurements is 7%. Similar tests made with only the U-shaped and straight sample holders at higher fields yielded similar results.

It was possible to make a partial comparison of sample holder performance with one of the round-robin samples. In Figure 2.3-5 and Table 2.3-3 the short sample performance of the multifilamentary NbTi sample is presented. At 9 tesla the noninductive and straight sample results varied by 7% from one another. Although it was possible to obtain results from the straight sample holder at currents above 100A, they were not expected to be reliable. In the figure the large difference between the U-shaped and straight samples can be seen.

TABLE 2.3-2 CONDUCTOR PERFORMANCE AS A FUNCTION OF SAMPLE HOLDER

Critical Currents @7 Tesla, 4.2K Measured At 1mv/cm Sensitivity

Sample Description		Critical Current (Amps)		
Wire Diameter (cm)	Cu/SC	U-Shaped Sample	Straight Sample	Non-Inductive Sample
.0508	3.0	54	55	55
.0508	1.6	104	99.5	--
.041	1.25	54	50.4	52.5

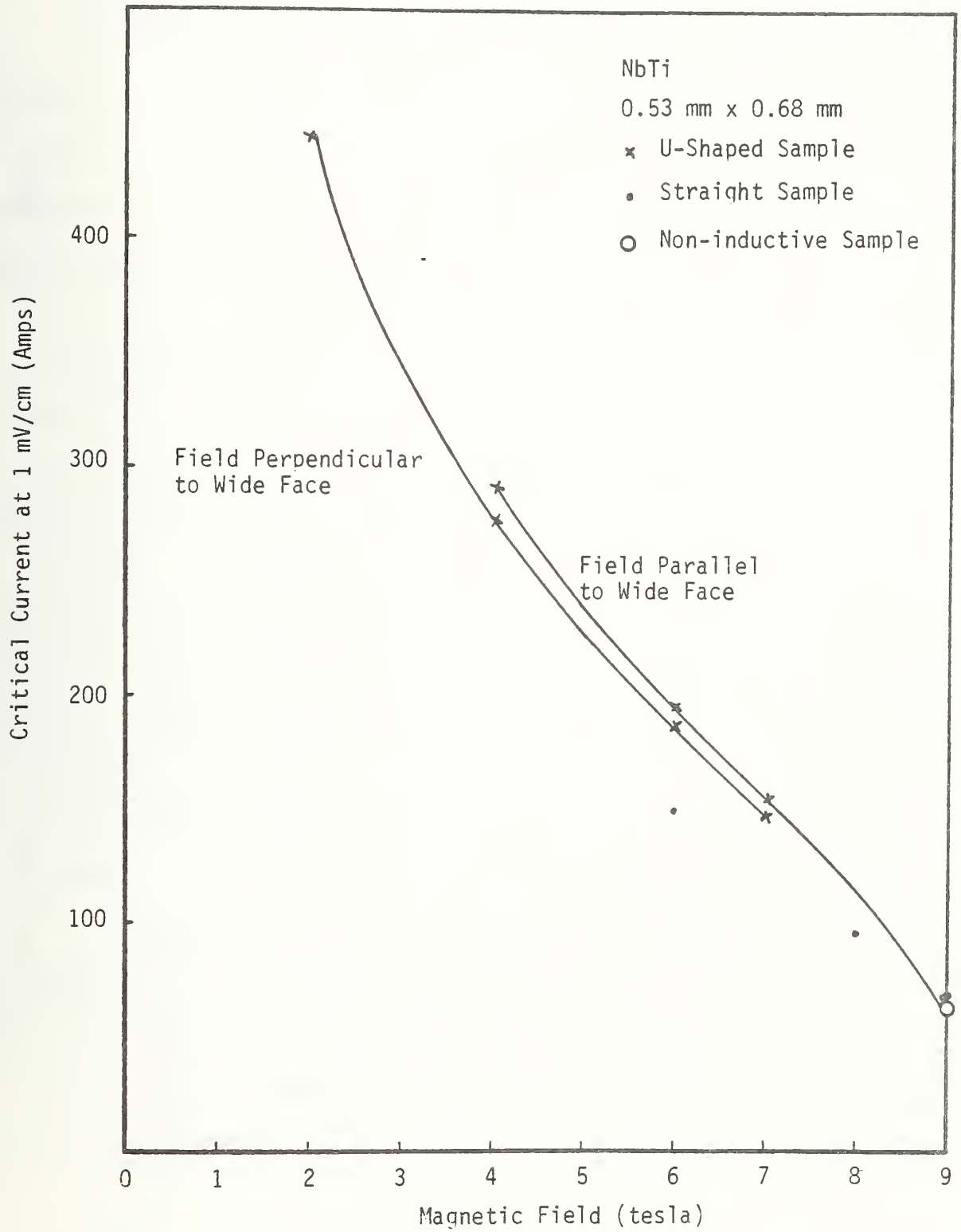

Fig. 2.3-5 Short Sample Performance of Round Robin NbTi

All of the samples in Groups 1 and 2 were round. In Group 3 two of the samples are rectangular. Consequently the mounting orientation of those samples is an additional parameter in the round-robin measurements. For the NbTi sample the aspect ratio is 1.28. However, even for such a low aspect ratio there is a 5% to 6% difference in critical current between the two measurements. It is extremely important, therefore, that the orientation of samples be reported for all rectangular short sample measurements. A list of the critical currents of the NbTi sample for various sensitivities and sample holders is presented in Table 2.3-3.

Sample 2 in the round-robin series is a Nb_3Sn tape. Again, the orientation of the sample is important. For fields up to 7 tesla, measurements were made using the U-shaped sample holder. When mounted in that sample holder the wide face of the tape is perpendicular to the field in the region in which the conductor voltage is measured. At fields above 7 tesla the straight sample holder is used, and the face of the tape is parallel to the magnetic field. In Figure 2.3-6 the short sample results measured at 1 mV/cm are shown. It can again be seen that at currents above 100 amps the straight sample holder is unreliable. In the case of this sample at 8 tesla the current may be underestimated because of current transfer problems as well as because of joule heating at the contact points. A complete listing of short sample performance of the Nb_3Sn tape is given in Table 2.3-4.

The final round-robin sample was multifilamentary Nb_3Sn. Because the sample was heat treated in a straight length it could be tested only in the straight sample holder. Critical currents are shown in Figure 2.3-7 for fields from 8 tesla to 12 tesla at 1 mV/cm sensitivity. The critical currents at

TABLE 2.3-3

CRITICAL CURRENT OF SAMPLE 1 (MULTIFILAMENTARY NbTi-0.53mm x 0.68mm)

	U-SHAPED SAMPLE HOLDER							STRAIGHT SAMPLE HOLDER				NON-INDUCTIVE SAMPLE HOLDER	
	MAGNETIC FIELD PERPENDICULAR TO WIDE FACE				MAGNETIC FIELD PARALLEL TO WIDE FACE			MAGNETIC FIELD PARALLEL TO WIDE FACE				MAGNETIC FIELD PARALLEL TO WIDE FACE	
SENSITIVITY	2T	4T	6T	7T	4T	6T	7T	6T	8T	9T	10T	8T	9T
1mv/cm	443A	275A	186A	148A	291A	196A	155A						
100μv/cm								148A*	96A	66.5A	34A	99.5A	61.5A
10μv/cm									95.8A	65.8A	32.6A	98.8A	
1μv/cm								146A*	95A	65.5A	29.2A	98.8A	
.5μv/cm								146A*	95.5A	63.5A	28.0A	98.8A	
.2μv/cm								145.5A*	95.5A	61.0A	25.4A		
0.1μv/cm								145.5A*	95.5A	59.0A	23.6A		
10^{-8}Ω-cm									95.8A	66.3A		99.5A	61.5A
10^{-9}Ω-cm								148A*	96.0A	65.8A	34.0A	99.5A	
10^{-10}Ω-cm								147A*	95.8A	65.5A	32.6A	98.8A	
10^{-11}Ω-cm								146A*	95.0A	61.0A	29.0A	98.8A	
10^{-12}Ω-cm									94.5A		23.5A		

*Measurements above 100A on straight sample holder are underestimated

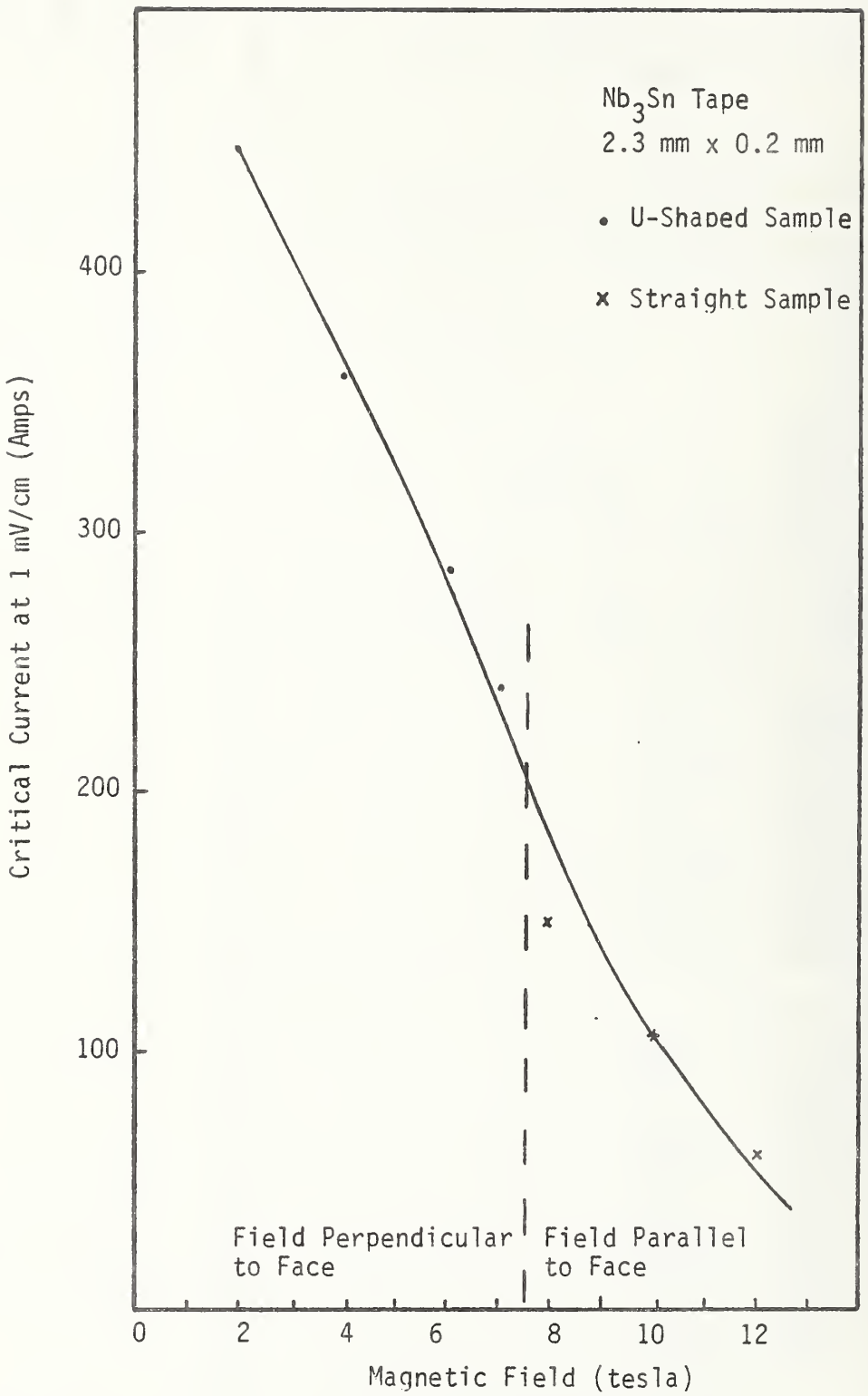

Fig. 2.3-6 Short Sample Performance of Round Robin Nb_3Sn Tape

FA 5230

TABLE 2.3-4

CRITICAL CURRENT OF SAMPLE 2 (Nb_3Sn TAPE)

	U-SHAPED SAMPLE HOLDER (MAGNETIC FIELD PERPENDICULAR TO WIDE FACE)				STRAIGHT SAMPLE HOLDER (MAGNETIC FIELD PARALLEL TO WIDE FACE)		
	2T	4T	6T	7T	8T	10T	12T
1mv/cm	445A	360A	285A	239A	150A*	105A	
100μv/cm					150A*	104A	60A
10μv/cm					149A*	100A	53A
1μv/cm					148A*	96A	50.5A
.5μv/cm					148A*	94A	47.5A
.2μv/cm						92A	
10^{-7}Ω-cm						100A	
10^{-8}Ω-cm					150A*	100A	55A
10^{-9}Ω-cm					149A*	98A	55A
10^{-10}Ω-cm					148A*	96A	50A
10^{-11}Ω-cm							45A

*Measurements above 100A on straight sample holder are underestimated

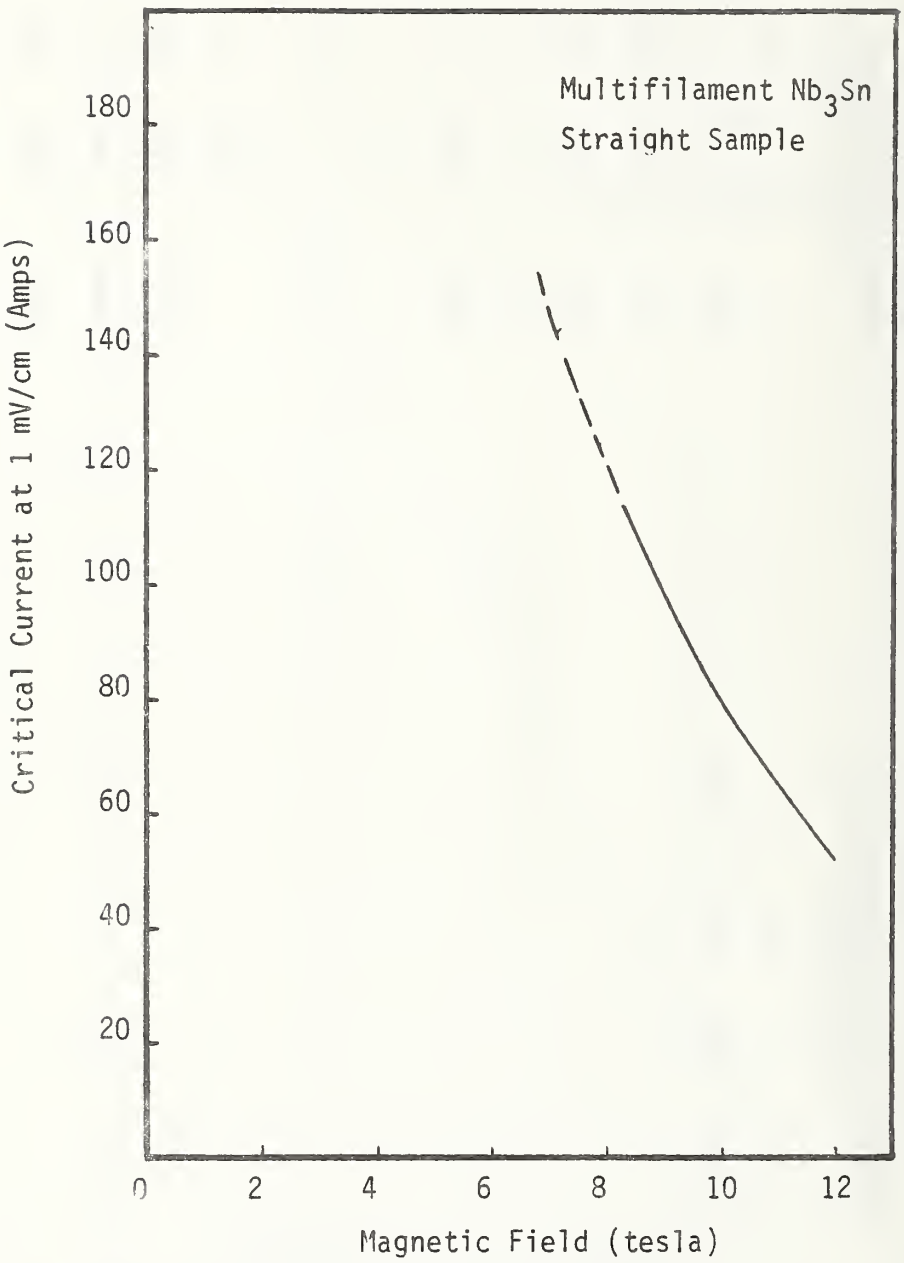

Fig. 2.3-7 Short Sample Performance of Round Robin Multifilamentary Nb_3Sn

other sensitivities are listed in Table 2.3-5. It can be seen from that table that the decrease in critical current with increasing measuring sensitivity is greater for this sample than it is for the NbTi samples discussed earlier in this section. For example, at 10 tesla and 10^{-8} Ω-cm resistivity the heat flux of a 0.7 mm conductor is 0.075 W/cm^2 for a current of 80 amps. Based on the results in Figure 2.3-3 for NbTi, the decrease in critical current from 10^{-8} Ω-cm to 10^{-11} Ω-cm sensitivity is between 8% and 18%. However, for the Nb_3Sn sample the decrease in critical current when the sensitivity is increased from 10^{-8} Ω-cm to 10^{-10} Ω-cm is 32%. It thus appears that the curves generated for NbTi are not applicable to Nb_3Sn. It would be useful if attempts were made to develop similar curves for Nb_3Sn.

3. Current Transfer Measurements

The second task of this program was to study current transfer between the sample holder and the test conductor. The importance of this task is apparent from some of the measurements reported in the previous section. The straight sample holder was designed to use very short samples at low currents. When currents greater than 100 amps were put through a sample, the critical current measurements were frequently underestimated. This was undoubtedly due to joule heating at the current contacts and current transfer problems. Within the scope of this program the important questions in studying current transfer are: (1) what length of conductor is necessary to give reliable data, and (2) what are the requirements of the current contacts on a sample holder?

3.1 Description of Samples

Six samples were tested in this program phase. A description of the conductors are given in Table 3.1-1. With the exception of the cabled conductor and the .081 cm x .163 cm conductor, all the samples were capable

TABLE 2.3-5

CRITICAL CURRENT OF SAMPLE 3 (MULTIFILAMENTARY Nb_3Sn)
(STRAIGHT SAMPLE HOLDER)

	6T	8T	10T	12T
1mv/cm	173A*	120A*	80A	52A
100μv/cm	172.8A*	117A*	77.5A	51A
10μv/cm	165A*	110A*	72.5A	46A
1μv/cm	88A*	65A	45.5A	30A
.5μv/cm		42A	30A	22.5A
10^{-8}Ω-cm	173A*	119A*	80A	51.5A
10^{-9}Ω-cm	172.8A*	116A*	77.5A	47A
10^{-10}Ω-cm	150A*	92A*	54A	29.5A

*Measurements above 100A on straight sample holder are underestimated

TABLE 3.1-1 CURRENT TRANSFER SAMPLES

Dimensions	Cu/SC	Number of Filaments	Twist Pitch (cm)
.157 cm x .315 cm	5	672	2.5
.210 cm diameter	1.25	361	2.5
.318 cm x .210 cm	1.8	180	2.5
.183 cm x .183 cm	2.6	132	2.5
.081 cm x .163 cm	5	672	2.5
7 Strand Cable .035 cm dia. strand	*	54/strand	0.5

*CuNi matrix. CuNi/SC = 2.5

of carrying currents of at least 1,000A. Those monolithic samples had copper-to-superconductor ratios ranging from 1.25 to 5. The cabled conductor was composed of seven strands. It was chosen for these tests because the matrix was made of CuNi instead of copper. Previously published experimental results[1] have indicated that current transfer lengths in copper-stabilized NbTi are extremely small and difficult to detect. The CuNi matrix material would be expected to have a much larger current transfer length than a similar conductor with copper. In fact, current transfer problems in some other CuNi matrix superconductors at MCA have been solved only by soldering high purity copper to the test conductor.

3.2 Description of Equipment

Two sample holders were used for these tests. One was the U-shaped sample holder described in Section 2.2. The other was a U-shaped sample holder used specifically for high current samples. The sample holder has been used to measure critical currents up to 5,000A. The sample length is approximately 45 cm long. The ends of the samples are soldered into 13 cm long OFHC channels which are soldered to 1.27 cm diameter OFHC copper rods. The rods are connected to vapor-cooled leads. The advantage of soldering the sample into a channel instead of directly to the copper rod is that the extra copper cross section and cooling surface of the channel aids in the current transfer. The sample holder is designed to fit into the bore of a 7.6 cm diameter superconducting magnet. The sample is held in place with stainless steel ties, vacuum grease, and a two-piece phenolic jacket that fits around the sample. Each sample holder was fitted with five pairs of voltage taps to be attached to the sample. Two or three pairs of voltage taps were attached to the section of the conductor in contact with

---

[1]See, for example, J.W. Ekin and A.F. Clark, "Current Transfer in Multifilamentary Superconductors. II. Experimental Results", J. Appl. Phys. Vol 49, p 3410 (1978).

the sample holder. The remaining leads were distributed along the test portion of the short sample. The voltage signals were detected with a nanovoltmeter and X-Y recorder. Two power supplies were available for use in testing. One was a 10,000A 10-volt Saban power supply, and the other was a 500A 10-volt Electronic Measurements supply.

3.3 Results and Analysis

Current transfer measurements were performed on the six samples previously described. Because of the low copper-to-superconductor ratio of most of the samples and because of the high matrix resistance of the cabled sample, the test currents were kept below the quench values in order to eliminate sample burnout. In addition, because of excessive noise pickup in the nanovoltmeter from the 10,000A supply it was decided that the maximum sensitivity would be achieved through the use of the 500A supply. The accuracy of the experiment was not hampered in any way by the limitation in current since flux flow resistivity predominates over the current transfer effects near the critical current. In general, there was no detectable signal along the test length (the length between the current contacts) of any of the NbTi samples mounted as described in the previous section. It was possible to measure resistivities to 10^{-11} Ω-cm or 10^{-12} Ω-cm. In every case a pair of voltage taps was positioned one centimeter apart and directly adjacent to the current contacts. This was the case for samples mounted in either sample holder. Signals were, however, occasionally detectable along the current contact regions. For example, when the .152 cm x .315 cm sample was mounted in the high current sample holder there was an equivalent resistivity of 3.2×10^{-11} Ω-cm in the first centimeter of conductor adjacent to the current contacts. In the next 12 cm the average resistivity was 8.0×10^{-12} Ω-cm, and in the last centimeter of contact the resistivity dropped to approximately 1.6×10^{-12} Ω-cm.

In order to estimate the effect of the sample holder on the measurements the same sample was remounted on the sample holder without the copper channels. The sample was soldered directly to the 1.27 cm diameter copper rods. The result was that the removal of some copper greatly increased the current transfer effects. In the first centimeter of the contact area the resistivity was 1.9×10^{-10} Ω-cm, and at the end of the contact area the resistivity is 5×10^{-11} Ω-cm. In Figure 3.3-1 a comparison is made of the current transfer resistivity along the sample with and without the copper channel. It can be seen that at all points along the conductor for which a voltage was detectable the current transfer resistivity is approximately an order of magnitude higher for the case in which the copper channel was removed from the sample holder. The results shown in Figure 3.3-1 were obtained in an external magnetic field of 5 tesla. The measurements obtained at 3 tesla and at 7 tesla were identical within the experimental uncertainty.

The one conductor that is not copper stabilized is the seven strand cable with a CuNi matrix. Each cable strand has a diameter of .035 cm. The critical current of each strand is 42 amps at 3 tesla. If such a small conductor were copper stabilized one would not expect to detect current transfer resistance. Any effects are due to the high resistance matrix. The sample was mounted in the lower current U-shaped sample holder. The results which are again independent of external field are shown in Figure 3.3-2. It can be seen that the current transfer region extends past the end of the current contacts and is still measurable in the middle of the sample. It is clear that the short sample characteristics of this sample cannot be measured accurately with this sample holder and mounting procedure. In the past it has proven very effective to solder a copper strip to the conductor to shorten the current transfer region in CuNi matrix conductors.

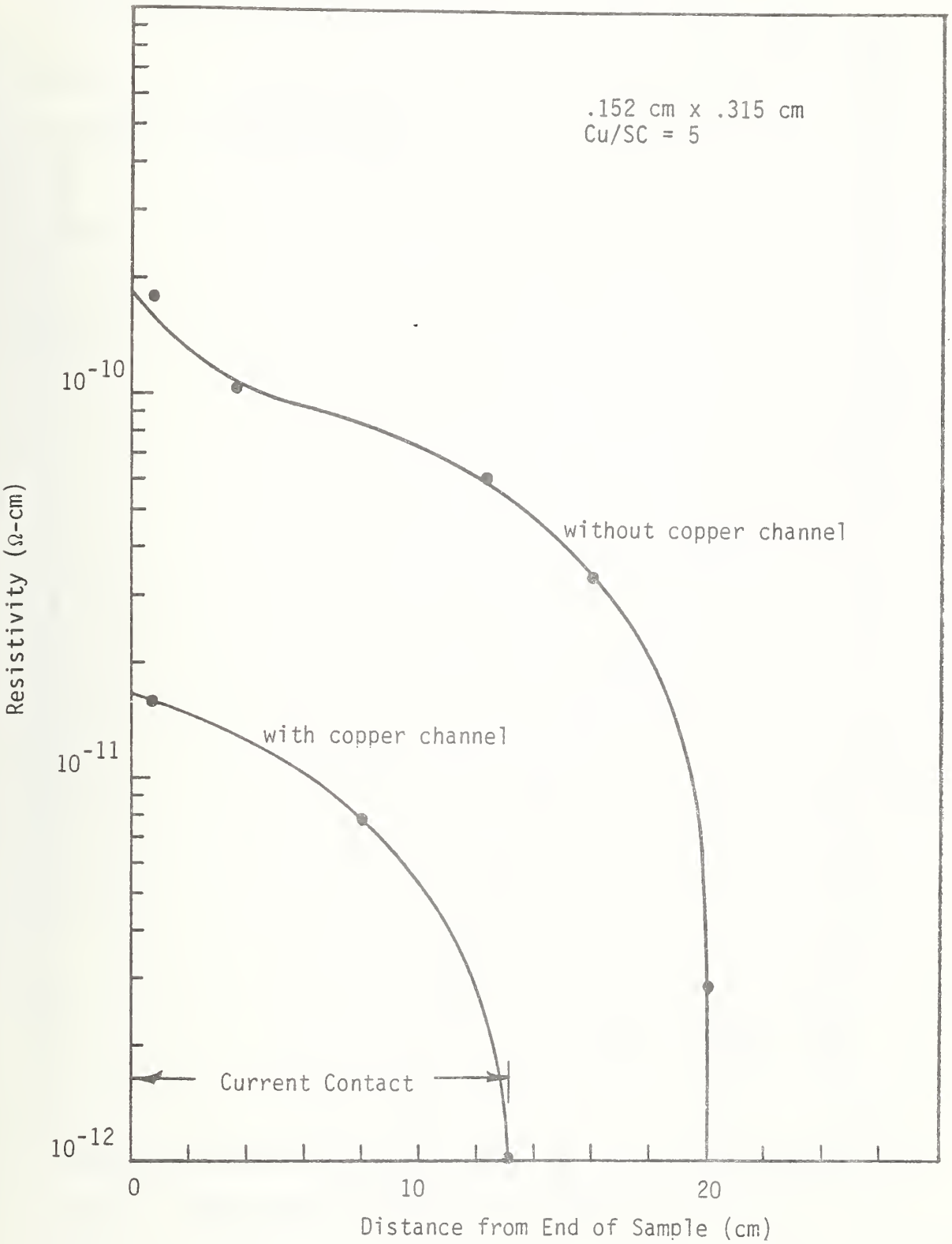

Fig. 3.3-1 Current Transfer Measurements. Effect of Removing Some Copper from Current Contacts

FA 5260

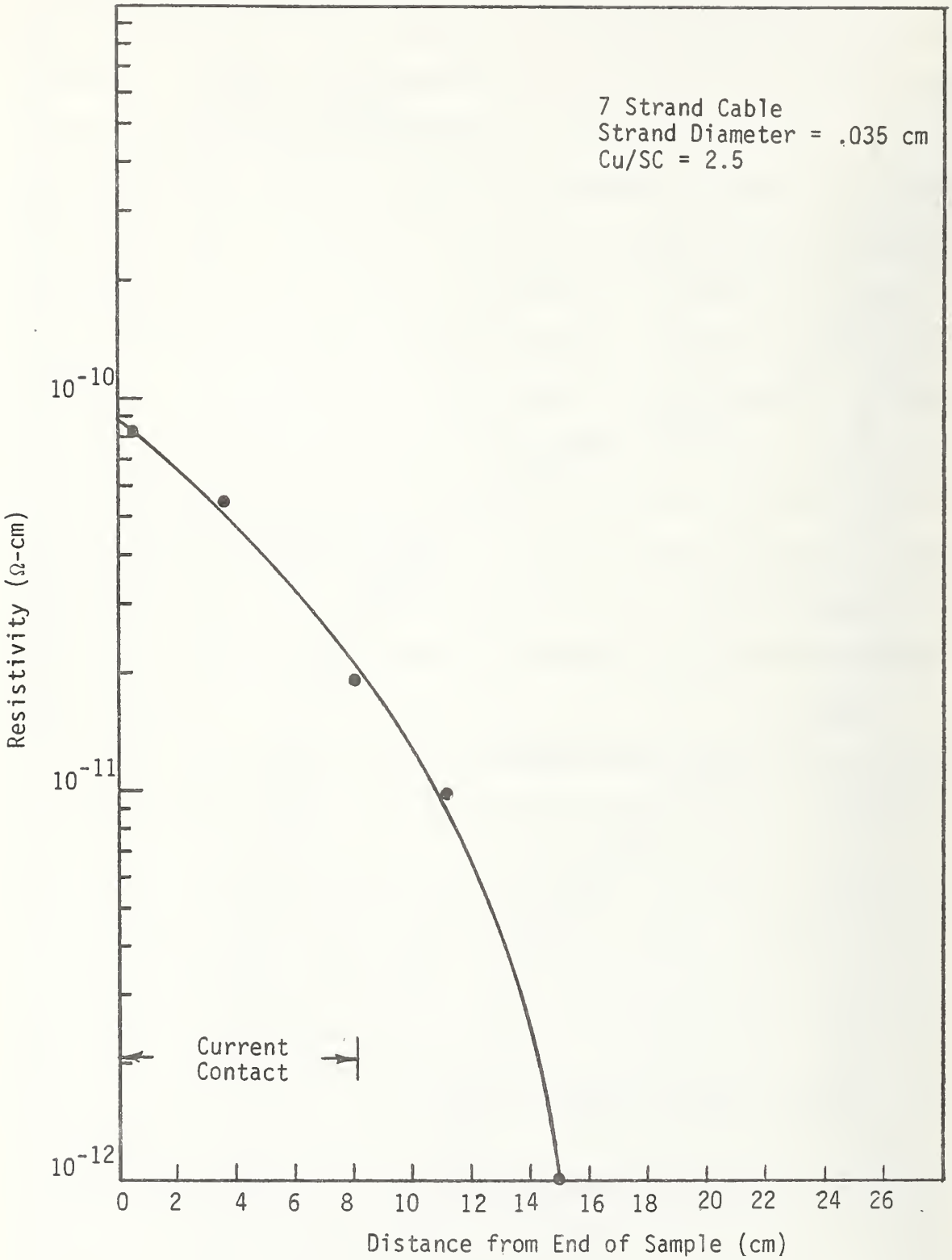

Fig. 3.3-2 Current Transfer into CuNi-Matrix Cable

FA 5259

4. Conclusions and Recommendations

It was originally hoped that on the basis of this program a single measuring procedure and sample holder could be recommended for adoption as a test standard. After the completion of this work it becomes clear that no single procedure or test apparatus is suited for all types of samples. The sample holder and measurement standard that are most suited for a conductor such as that used for the Fermilab Doubler Magnets is not necessarily practical for measuring the critical currents of a high resistivity matrix superconductor or of a conductor requiring very low losses.

For many applications such as intrinsically stable magnets not run in a persistent mode the quench current is a satisfactory measurement of the critical current. These measurements are easy to perform with a minimum of instrumentation. Many different configurations of sample holder can be used. The samples can be mounted very quickly and multiple sample test fixtures are very practical. It is also straightforward to estimate the critical current at a higher sensitivity if that should be of interest. Although it would be worthwhile to have a standard established for this type of measurement, that standard need not be very rigorous. An uncertainty in measurement of at least 5% should be acceptable for this type of test.

On the other hand, if the same conductor is to be used in a coil with a persistent switch and if the magnet decay rate is extremely low, then it is essential to define the critical current at a very low resistivity or electric field. Depending upon the details of the magnet, critical currents might need to be defined in the 10^{-12} Ω-cm to 10^{-14} Ω-cm range. In order to measure such low values it is necessary to use a very long sample. For example, a small noninductively wound coil with up to 10 meters of test conductor might be needed. Because of the extra equipment (e.g.,

a microvoltmeter or nanovoltmeter) that is needed for the measurement, and because the mounting and the testing of the samples will be slower than those of a quench measurement, it is recommended that this type of measurement be made only when high sensitivity results are needed. It should not be adopted as the standard for routine measurements.

Sample holders must be designed to assure that all the current has transferred into the sample, outside of the region in which the test signals are detected. Although it was observed that current transfer can be improved by soldering additional copper to the sample for testing, this is not as satisfactory a solution as having a test holder with a very long current transfer region. This is due to the fact that the amount of copper in a conductor can affect its critical current. It is possible to design a sample holder with a sufficiently large sample contact area to ensure reliable measurements. The improvement in current transfer measurements has been noticed when extra copper was added to the current contact areas.

Based on all of these measurements it seems clear that two or three types of sample holders are needed in order to test all types of conductors. A similar number of measuring standards are needed as well. It is hoped that the results of this program will contribute to the development of those standards.

ACKNOWLEDGMENTS

Most of the high field critical current measurements were made by the authors at the Francis Bitter National Magnet Laboratory at Massachusetts Institute of Technology. We would like to thank the Magnet Laboratory staff for their assistance in our effort.

We would like to thank Joseph Pileeki, Sileshi Woldemariam, and Rene Chouinard for help in performing short sample tests.

We would also like to acknowledge many helpful discussions with Dr. F. R. Fickett at the National Bureau of Standards, Boulder, Colorado.

D. Supercon, Inc.

FINAL REPORT

to

National Bureau of Standards

Boulder, Colorado

under

Contract Number NB79RAC90024

From

Supercon, Inc.
9 Erie Drive
Natick MA 01760

Introduction

Towards the effort by the National Bureau of Standards to standardize measurement practices for practical superconductors, Supercon, Inc. has accomplished the following:

1. A determination of the variations in critical current, I_c, from composite superconducting wire that is similarly processed.

2. A determination of the relative stabilities of superconducting wires.

3. A determination of the effect of filament uniformity on the I_c and stability of superconducting wire.

4. Participation in NBS and ASTM on-going activities.

Powell and Clark[1] provide a workable definition of critical current as the "electrical current below which an ideal superconductor may exist in the superconducting state at a specified temperature, magnetic field strength, and other specified external conditions". The four terminal electrical resistance method generates a current versus voltage function which can be interpreted in a variety of ways to determine the value of the critical current. The most common criteria are based on voltage, power or resistivity; these are also described by Powell and Clark[2].

Experimental Work

Testing by the four terminal electrical resistance method is fairly straightforward. Minimum component requirements are a DC power supply with variable output and a known volts/amp outlet for monitoring; a calibrated electromagnet capable of accepting a sample and its cryogenic envelope through its bore; a recording device capable of plotting current versus resulting voltage. Standard practice includes the calibration of the recording device with a voltmeter, and a test run using a sample of known critical current.

Many test configurations are currently in use for superconducting wire. The easiest tests, and those requiring the least amount of superconductor, are the straight sample and hairpin tests. We have found these tests most useful in surveying large numbers of samples, comparing samples of a broad range experiment to narrow the field of variables, and the testing of A15 and other brittle superconductors requiring reaction in the geometrical form of the test to reduce strain of handling. Hairpin and straight samples lend themselves particularly well to the design of multiple sample probes; see Figure 1.

Longer samples of wire are usually bifilar wound to cancel out the self field of the sample and inductance from the magnet. The samples are either wound as a solenoid or a pancake, the solenoid being

preferred for round wire and any test in a small bored magnet, and the pancake for conductors that are either very bulky or have a high aspect ratio, and in facilities where very large bored magnets are available. See Figure 2.

A number of production variables affect the correlation between short (< 10 cm) and long (> 1 M) sample test results. We use this difference and consider it along with the value of the critical current. The amount of degradation from a short to a long sample corresponds to relative filament integrity, most useful in the examination of multifilamentary wire for assessment of the severity of its processing. This kind of evaluation is based primarily on engineering experience and would be difficult to quantify. In general, short samples are for screening, either for production uniformity or production variable testing, and long samples are used to better project end use performance.

There are prevailing conditions at the Francis Bitter National Magnet Laboratory which limit the precision of data collection. This is a large facility with water cooled copper magnets capable of serving up to four experiments simultaneously. Some magnet noise is always picked up by the voltage taps, but noise can increase substantially with the field changes of other investigators. A six pole bessle filter on the voltage taps is used to reduce the low frequency noise which, on a

bad day can amount to as much as 200 u V, but on a good day may be less than 10 u V. Considering these limitations, we have confidence in measurements of voltage changes greater than 20 u V and interpret our data accordingly. Practical sample sizes, equipment precision, and power supply noise also limit the sensitivity of the I-V plots. A voltage of 100 u V is an effective resistivity of 2×10^{-9} (ohm cm) for a .5mm diameter short sample carrying 100 amps. A three meter sample of the same material will have an effective resistivity of 6×10^{-12} (ohm cm). We have chosen 10^{-12} (ohm cm) resistance as the criterion for critical current for these long samples and 10^{-8} (ohm/cm) the criterion for the short samples.

Many factors influence the current carrying capacity of a superconductor. The amount of superconductor, the number, size, and shape of the filaments, the reduction schedule and heat treatments, and the chemical composition of the alloy. This last variable is controlled by the manufacturer's specification to the producer: if the specifications are too tight, the cost is increased. The chemistry of the superconductor, therefore, varies from lot to lot. We have received more than one billet from a lot and in surveying a large amount of I_c data have found that current density measurements from the billets of one lot vary consistently with those of billets from a different lot. See Figure 3. The effect of specific elements is beyond the scope of this study.

With any composite extrusion there are areas of non-uniformity at the nose and tail of the resulting bar due to "end effects". With single core composites of copper around niobium titanium, the superconductor can take on a "dog-bone" shape which, if drawn to wire, will have varying ratios of copper to superconductor, see Figure 4. A judicious cropping of the extruded rod eliminates gross irregularities, but slight variations along the length of the wire will remain. Two simple methods for determining ratio of copper to superconductor are: measure the diameter before and after a nitric acid etch and take a ratio of the areas, or weigh a length of composite wire before and after etching and calculate the ratio while factoring in the difference in densities.

Short samples from six consecutive pieces of Cu-NbTi wire approxinately 30,000 ft long were tested for critical current and subsequently weighed and etched to find the volume percent of superconductor in each. The results are plotted in Figure 5; the relation is linear, as would be expected.

A survey of I-H tests from 26 billets processed similarly shows the variations from billet to billet due to differences in chemistry as explained above, minor changes in ratio, and improvements in quality control. See Figure 6.

There are as many definitions of the stability of a superconductor as there are uses for them. Most of them depend considerably on design parameters of the device such as electrical, thermal, and magnetic insulation, and fluid dynamics, which cannot be controlled by the wire manufacturer. But there is a need to be able to compare wires and therefore to define relative stability.

In the current versus voltage curve of a multifilamentary wire, there is a region of current sharing. This means not all of the current is passing through a superconductor. The onset of this phenomena is defined as the critical current; the voltage will rise as more current is passed through the wire until the voltage "takes off" and displays resistance comparable to a normal conductor. The detectable voltage found in this current sharing region can be useful in monitoring the performance of a device as a warning signal that the conductor is nearing its limit.

Some ways of comparing wire have been suggested: reporting currents at two resistance levels, i.e., 10^{-12} ohm cm and 10^{-11} ohm cm, or two voltage levels, 10^{-7} and 10^{-6} V/cm. For this study, a similar approach was taken. The definition combines two previously defined parts of the I-V curve[3], I_c (as defined by the resistivity criterion of 10^{-12} ohm cm) and the I_t (the "take off" current), by finding their difference as a ratio to the critical current, $I_t - I_c / I_c$. The result could be reported with the critical current as a per cent current sharing margin, and as such could be compared with similar conductors.

This analysis was done for some multifilamentary superconducting wires of varying copper to superconductor ratios and number of filaments. The results can be found in Table 1. It should be noted that the conductors have different current densities due to difference in reduction schedules and heat treatments; an attempt to keep all parameters constant would be very time consuming and expensive.

The per cent current sharing margin increases with increasing copper content (see Figure 7), with increasing numbers of filaments (see Figure 8), and with decreasing filament size (see Figure 9). This is as would be expected, for all of these functions either increase the surface area of the filaments or the amount of copper around them, both of which improve the heat transfer characteristics of the composite. All results are from tests at 8 Tesla.

The method of comparing the current sharing characteristics just described is easily adapted to normal I-H testing procedures. The reproducibility of the result is limited by that of the take-off current measurement.

In the extrusion of a multifilamentary composite just as with a monofilament composite, there are regions of non-uniform cross-section. In multifilament wire, many more types of non-uniformity are possible. Examples of non-uniform filament patterns are: out of

round filaments, over-sized center filaments, (typical of the nose of an extrusion), and undersized center filaments (typical of the tail of an extrusion).

Six non-uniform wires were processed and tested for critical current and per cent current sharing, and were weighed and etched to determine copper content, see Table 2. Their cross sections were examined and are found in Figure 10. Since all samples were processed identically, comparison of their current densities is important to distinguish differences due to changes in the ratio of copper to superconductor from any effects of non-uniformity. None of the mildly distorted wire produced significant changes in the current density; their differences in critical current are proportional to their differences in superconductor content. A slight difference can be seen in the current density of the highly distorted sample, Number 6. The per cent current sharing margin is not affected.

References

1. R. L. Powell and A. F. Clark; "Definitions of terms for practical superconductors 2. Critical parameters", Cryogenics 19 3 (1979) p 140.

2. ibid.

3. D. T. Read, J. W. Ekin, R. L. Powell, and A. F. Clark; "Definitions of terms for practical superconductors 3. Fabrication, stabilization, and transient losses"; Cryogenics 19 6 (1979) pp 327-332.

List of Figures

Figure 1 Short sample multi ple test probe

Figure 2 Long sample test probes

Figure 3 I_c vs per cent superconductor for different lots

Figure 4 Typical composite extrusion shape

Figure 5 I_c vs per cent superconductor for six consecutive lengths

Figure 6 I_c vs billet at two fields

Figure 7 Per cent current sharing vs copper content

Figure 8 Per cent current sharing vs number of filaments

Figure 9 Per cent current sharing vs filament size

Figure 10 Non-uniform cross sections of 54 filament wire

List of Tables

Table 1 Current sharing of multifilament wire

Table 2 Current capacity of non-uniform wires

Table 1

I.D. No.	Volume % S. C.	No. of Filaments	(Mils) Size of Filaments	% Current Sharing Margin at 8 T.
2770	51.5	517	1.0	2
2791	37.4	54	1.0	12
2620	26.7	54	1.0	33
2260	42.0	294	1.0	24
2720	28.8	48	4.8	19
2792	34.6	54	1.6	11
2793	34.9	54	1.2	11
2794	35.5	54	1.9	10
2795	35.4	54	2.4	5

Table 2

I.D. No.	Volume % S.C.	Current Density/% Current Sharing Margin 9T		8T		7T	
2951	36.3	557	5	856	5	1182	2
2952	36.3	533	4	911	3	1223	2
2953	38.2	542	7	788	10	1098	5
2954	40.8	520	7	786	6	1052	3
2955	41.5	535	11	856	4	1106	5
2956	36.4	488	6	759	2	1030	3

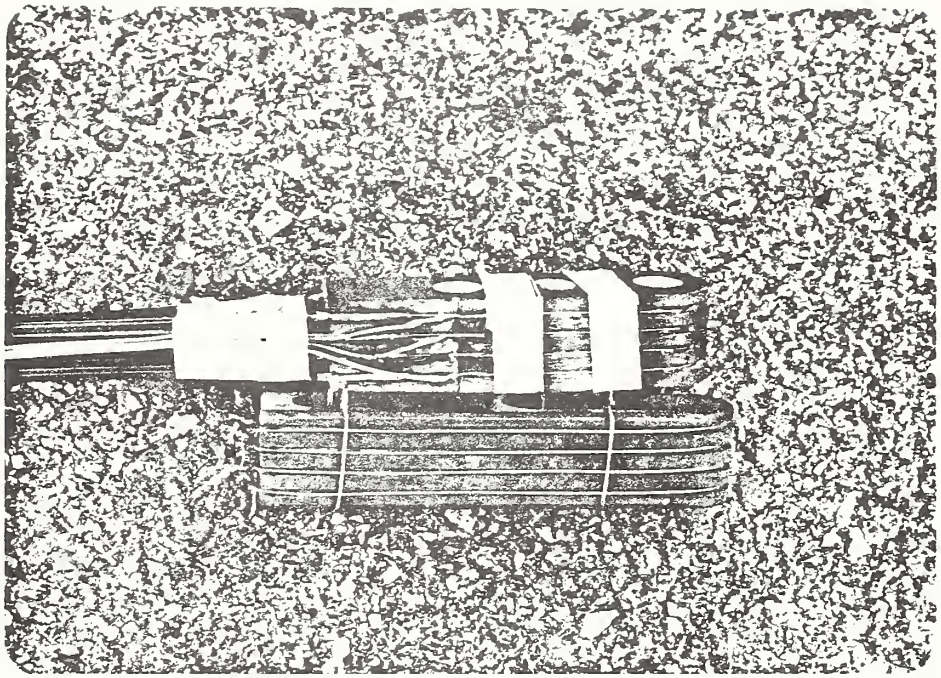

figure 1

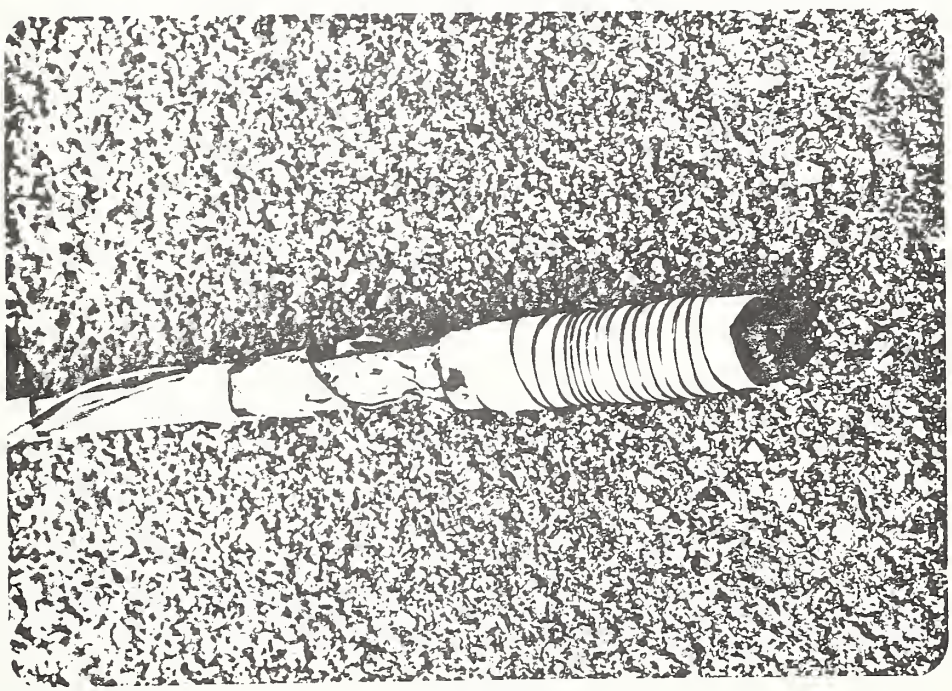

figure 2

figure 3

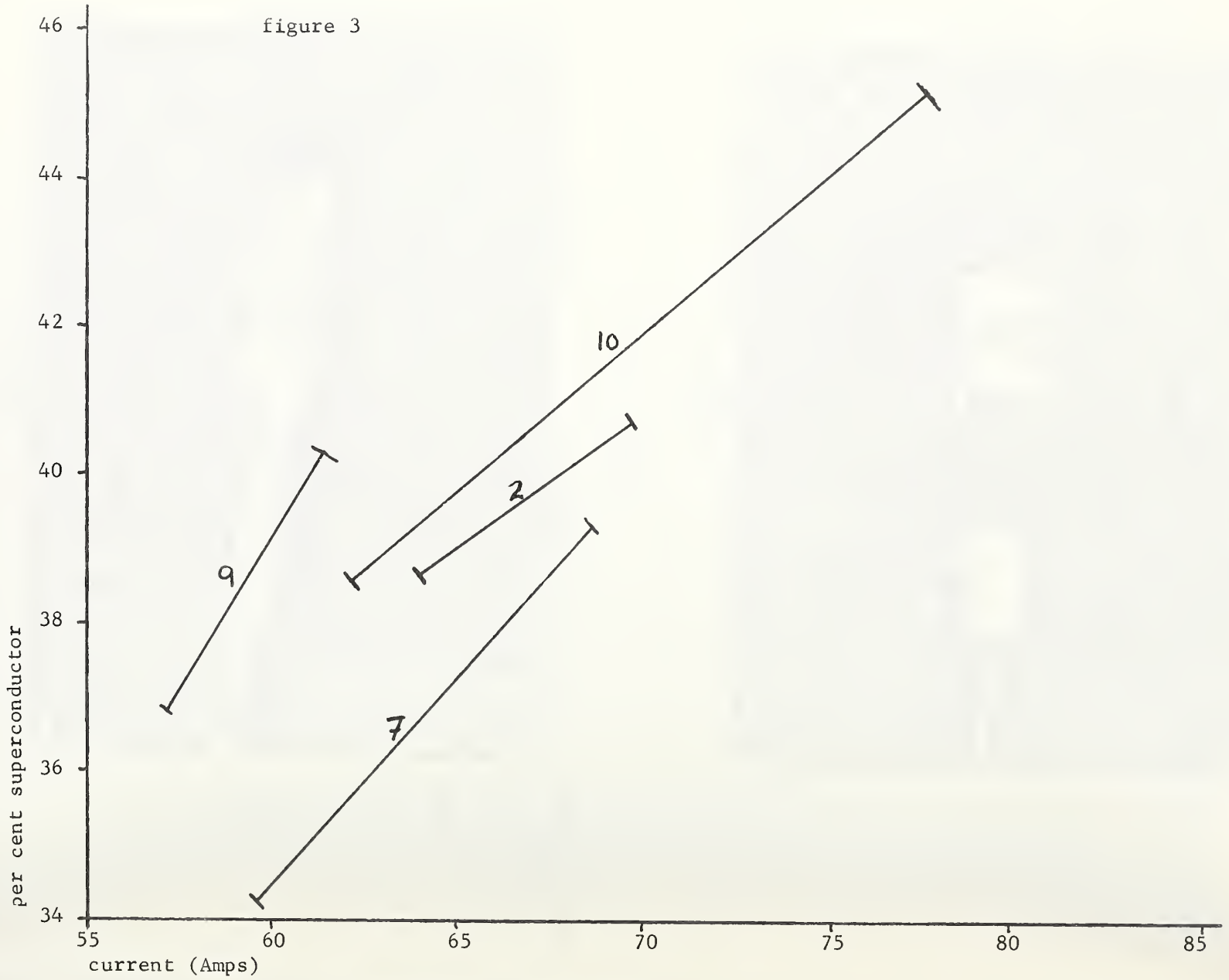
46
44
42
40
38
36
34
per cent superconductor
55
60
65
70
75
80
85
current (Amps)
10
2
9
7

figure 6

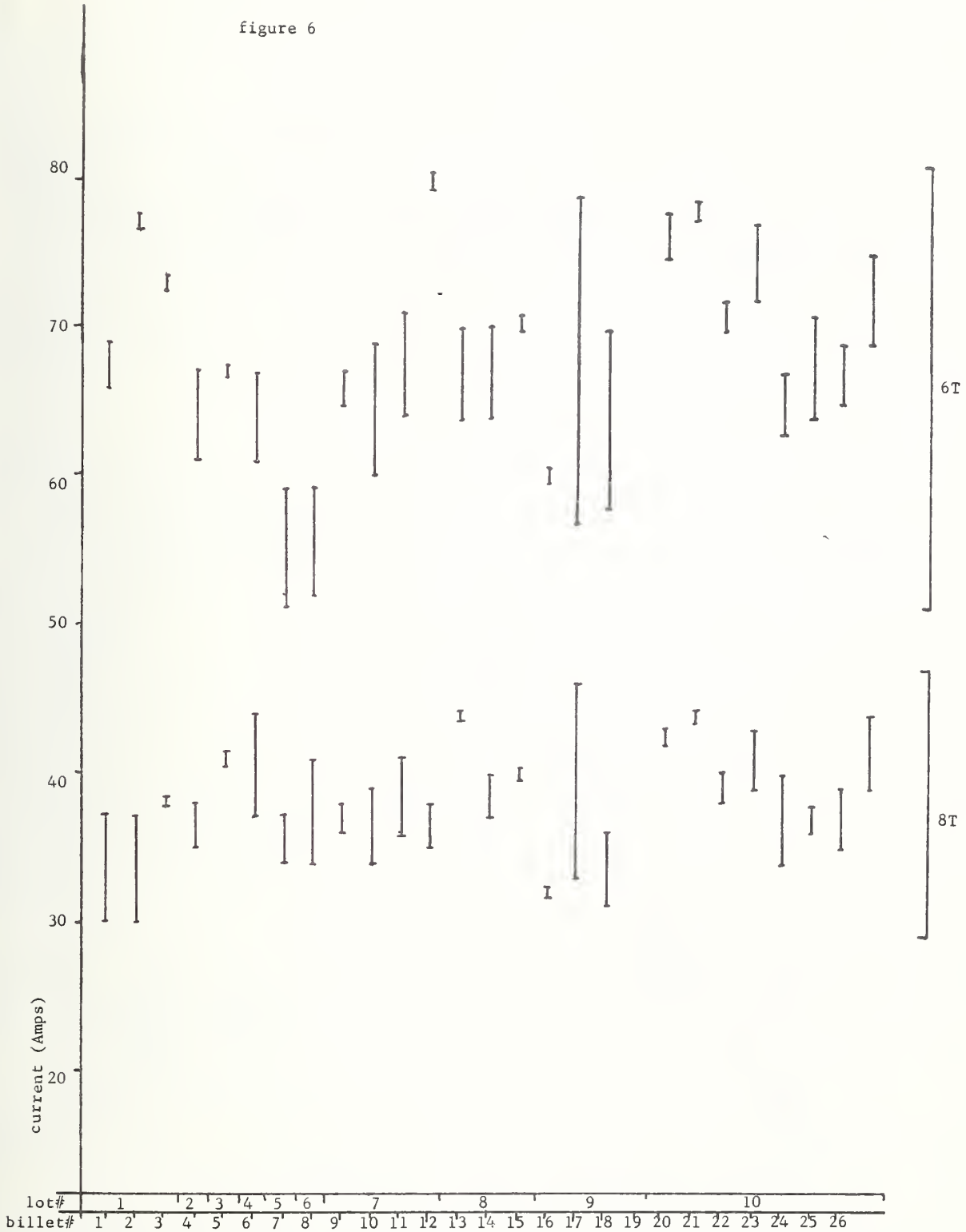
80
70
60
50
40
30
20
current (Amps)
6T
8T
lot#
1
2
3
4
5
6
7
8
9
10
billet#
1 2 3 4 5 6 7 8 9 10 11 12 13 14 15 16 17 18 19 20 21 22 23 24 25 26

figure 4

figure 5

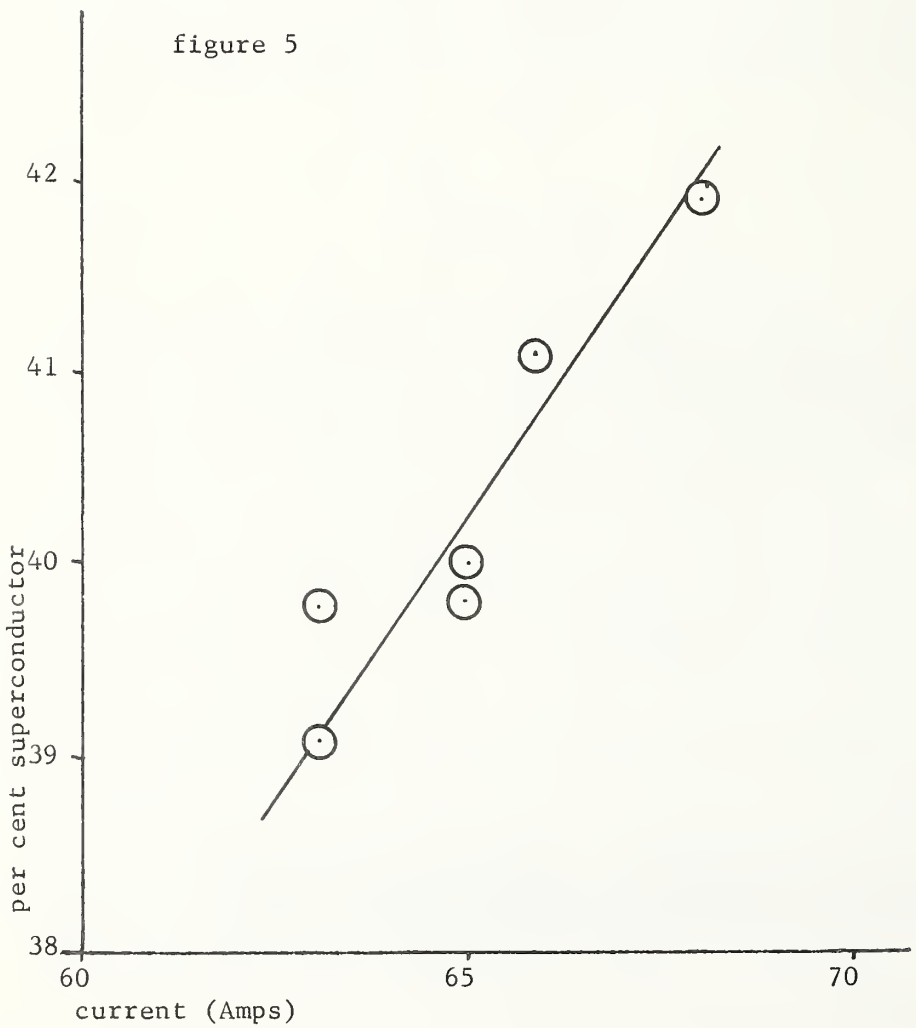

figure 7

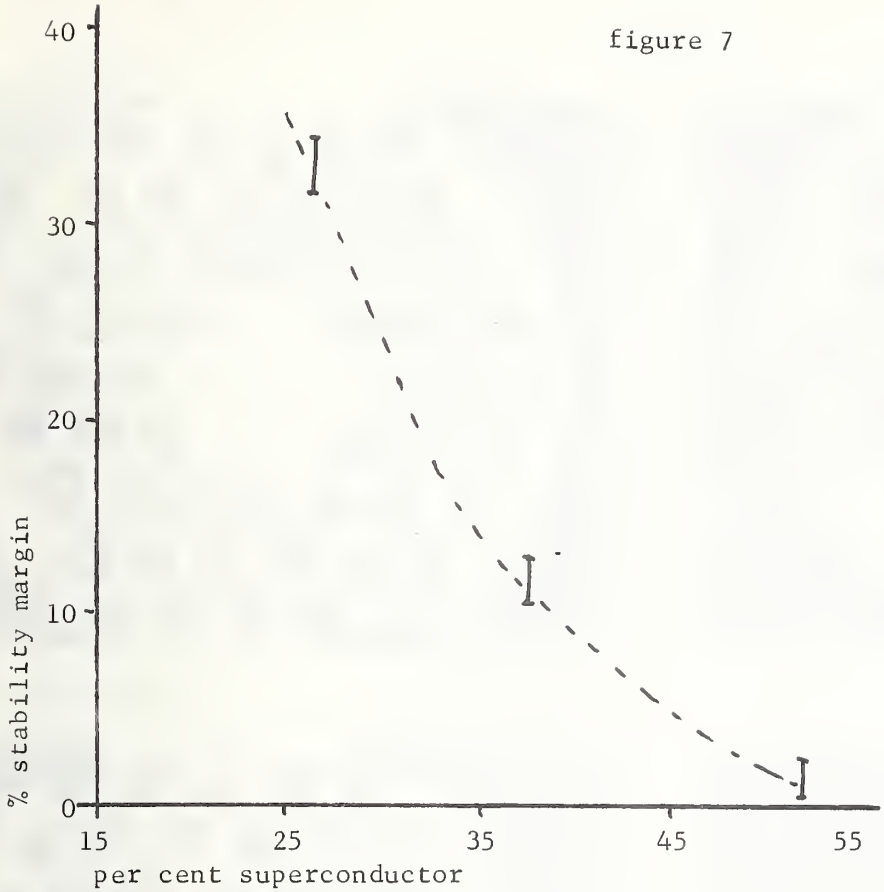

figure 8

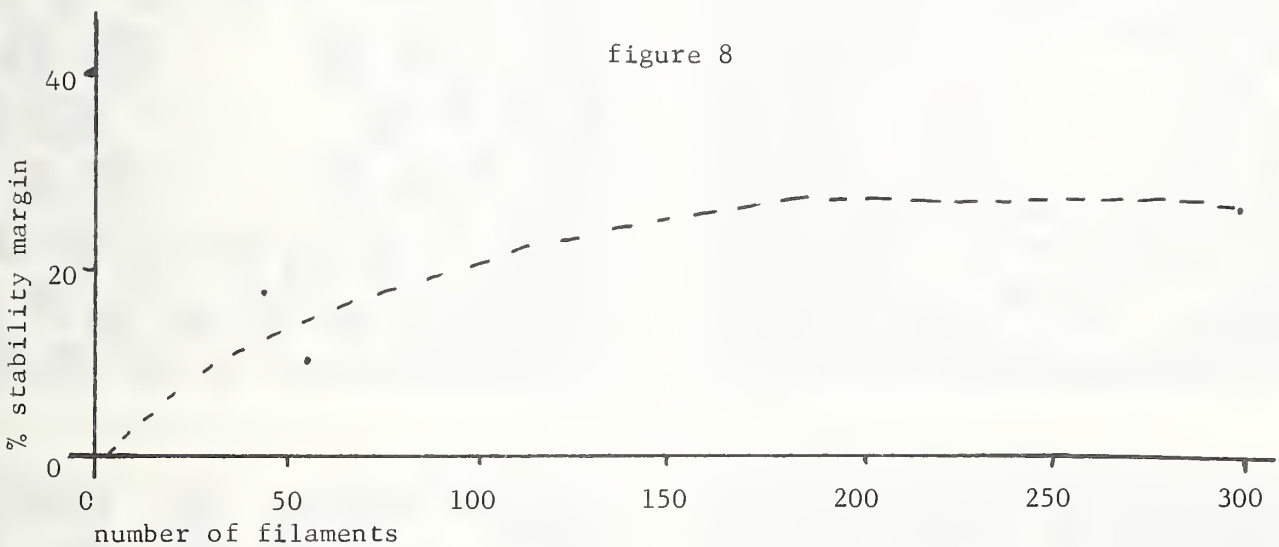

figure 9

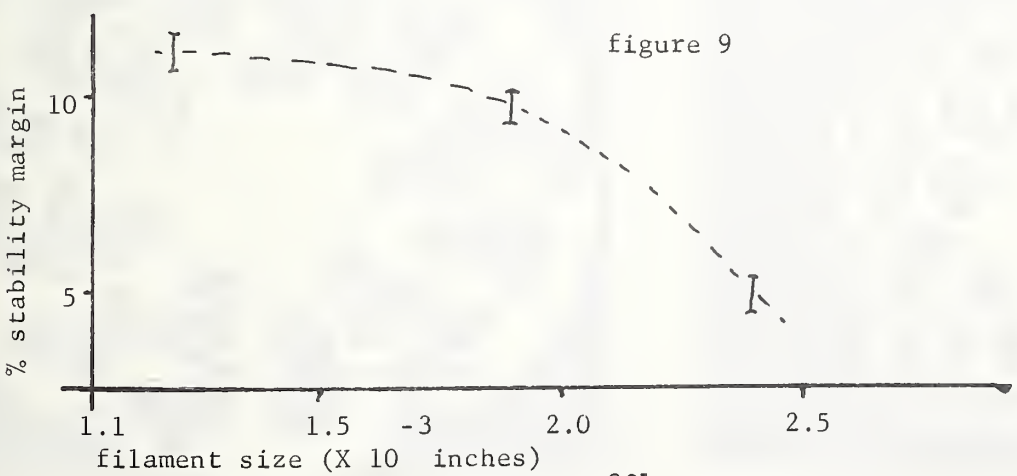

Figure 10

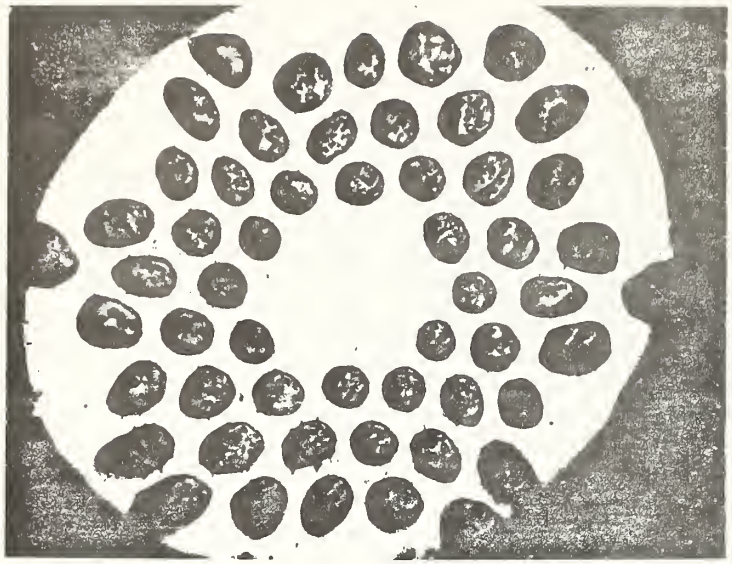

2951

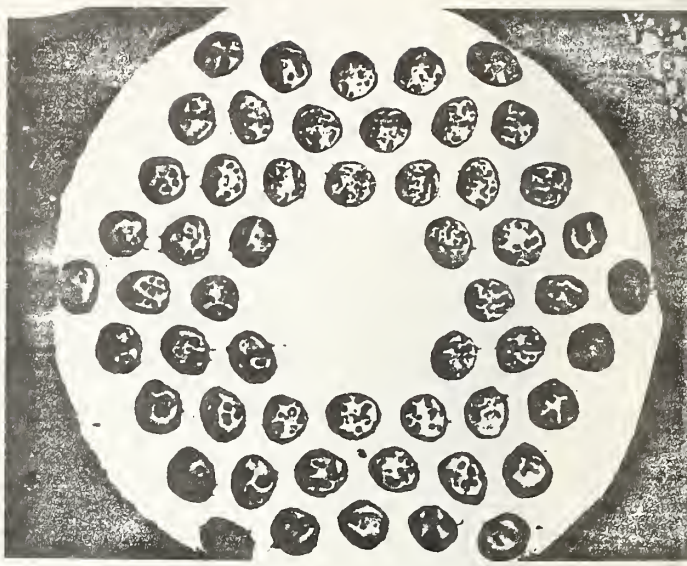

2952

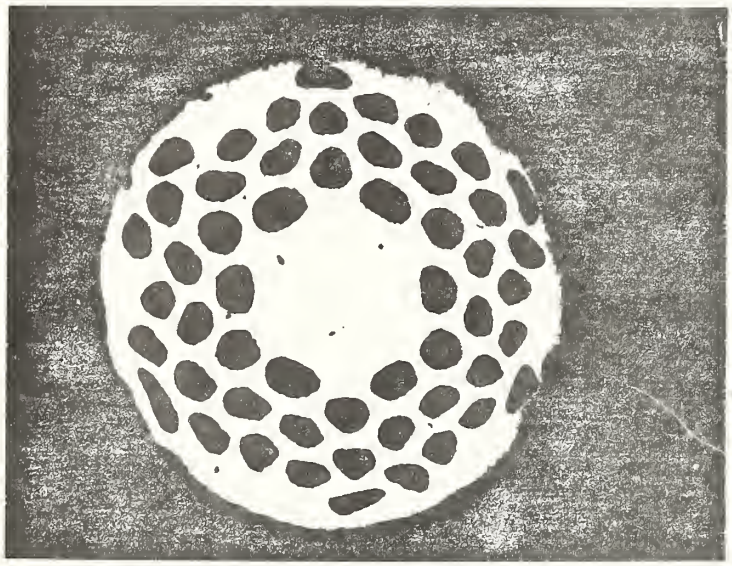

2953

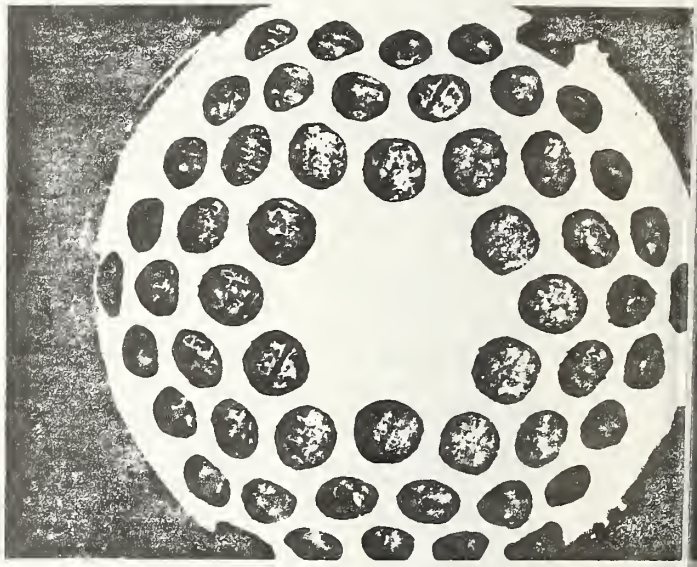

2954

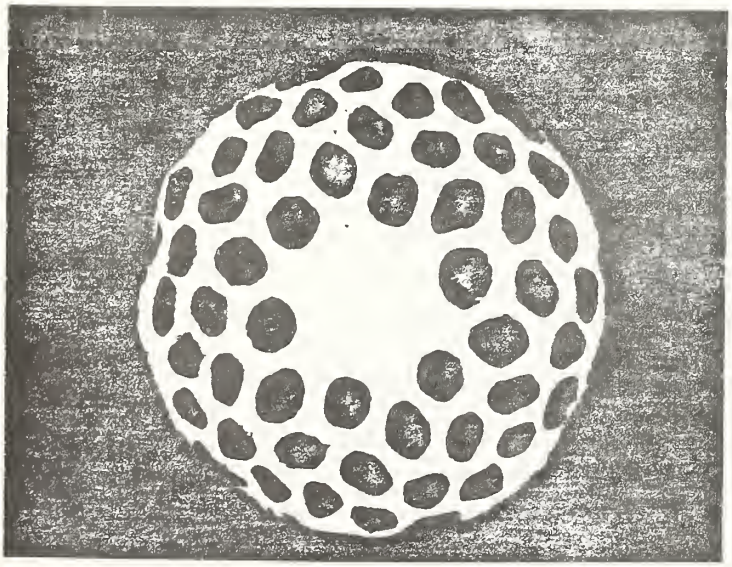

2955

2956

VI. REFERENCES

[1] F. R. Fickett and A. F. Clark, "Development of Standards for Superconductors, Annual Report FY 79," NBSIR 80-1629 (December 1979).

[2] F. R. Fickett, S. B. Kaplan, R. L. Powell, R. Radebaugh, and A. F. Clark, "Definitions of Terms for Practical Superconductors: 4. Josephson Phenomena," Cryogenics 20, 319-325 (1980).

[3] M. N. Wilson, Rutherford Lab. Report SMR/1, Chilton, Oxfordshire, England, 1977 (unpublished).

[4] J. W. Ekin, "Critical Transfer in Multifilamentary Superconductors. I. Theory," J. Appl. Phys. 49, 3406-3409 (1978).

[5] L. Dresner, "Distribution of Current Among the Filaments of a Multifilamentary Superconductor Close to the Input Leads," Cryogenics 18, 285-288 (1978).

[6] J. W. Ekin, A. F. Clark, and J. C. Ho, "Current Transfer in Multifilamentary Superconductors. II. Experimental Results," J. Appl. Phys. 49, 3410-3412 (1978).

[7] L. F. Goodrich and J. W. Ekin, "Lap Joint Resistance and Intrinsic Critical Current Measurements on a NbTi Superconducting Wire," Proc. 1980 Applied Superconductivity Conference, IEEE Trans. on Mag. (to be published).

[8] G. Fujii, J. W. Ekin, R. Radebaugh, and A. F. Clark, "Effect of Thermal Contraction of Sample Holder Material on Critical Current," Adv. in Cryog. Eng. 26, Plenum Press, New York (1980) p. 589.

APPENDIX A

PUBLICATIONS AND PRESENTATIONS

Major publications and presentations resulting from the research performed under this program during FY 80 are listed here. Copies are available from NBS.

F. R. Fickett, S. B. Kaplan, R. L. Powell, R. Radebaugh, and A. F. Clark, "Definitions of Terms for Practical Superconductors: 4. Josephson Phenomena," Cryogenics 20, 319-325 (1980).

F. R. Fickett and A. F. Clark, "Development of Standards for Superconductors," Proc. 8th Int. Cryo. Eng. Conf. (ICEC8), IPC Science and Technology Press (1980) pp. 494-498.

L. F. Goodrich and J. W. Ekin, "Lap Joint Resistance and Intrinsic Critical Current Measurements on a NbTi Superconducting Wire," Proc. 1980 Applied Superconductivity Conference, IEEE Trans. Mag. (to be published).

G. Fujii, "Present Practices in Japan for the Measurement and Definition of Various Superconducting Parameters," Tech. Report of ISSP, Ser. A, No. 1063 (July 1980).

G. Fujii, J. W. Ekin, R. Radebaugh, and A. F. Clark, "Effect of Thermal Contraction of Sample-Holder Material on Critical Current," Adv. Cryo. Eng. 26, Plenum Press, New York (1980) p. 589.

R. Radebaugh, G. Fujii, D. T. Read, and A. F. Clark, "A Standards Program for AC Losses in Superconductors," Proc. XVth International Congress of Refrigeration (1980).

H. R. Segal, Z. J. J. Stekley, and T. A. DeWinter, "Development of Critical Current Measurement Standards," Proc. 1980 Applied Superconductivity Conference, IEEE Trans. Mag. (to be published).

F. R. Fickett and A. F. Clark, "Standards for Superconductors," Proc. 1979 Mech. and Mag. Energy Storage Contractors' Review Meeting, Conf-790854 (December 1979).

F. R. Fickett and L. F. Goodrich, "NBS Superconductor Standardization Program," Proc. 7th Int. Conf. on MHD Electrical Power Generation (June 1980) (to be published).

G. Fujii, M. A. Ranney, and A. F. Clark, "Thermal Expansion of Nb_3Sn and V_3Ga Multifilamentary Superconducting Cables, Fiberglass-epoxy and Cotton-phenolic Composite Materials," Jap. J. Appl. Phys. (to be published).

G. Fujii and J. W. Ekin, "Effect of Compressive Strain on the Critical Current of Multifilamentary Nb_3Sn and V_3Ga," (in preparation).

APPENDIX B

STAFF AND CONTACTS

A significant amount of the work on this program was done under subcontract to NBS. We list here both the NBS staff and the technical contacts for the various contractors.

National Bureau of Standards, Electromagnetic Technology Division, Boulder, CO 80303. Ph. (303) 497+EXT, FTS 320+EXT.

F. R. Fickett (PI) x3785

A. F. Clark (PI) x3253

L. F. Goodrich x3143

Airco Superconductors, 600 Milik Street, Carteret, NJ 07008. Ph. (201) 541-1300.

P. Sanger

C. Rosen

Intermagnetics General Corporation, P. O. Box 566, Guilderland, NY 12084. Ph. (518) 456-5456.

R. Schwall

R. McCown

Magnetic Corporation of America, 179 Bear Hill Road, Waltham, MA 02154. Ph. (617) 890-4242.

H. Segal

B. Strauss

Supercon Inc., 9 Erie Drive, Natick, MA 01760. Ph. (617) 655-0500.

W. Larson

K. Stohlman

APPENDIX C

MINUTES

ASTM SUBCOMMITTEE B01.08 ON SUPERCONDUCTORS

Held October 2-3, 1980
La Posada Inn, Santa Fe, New Mexico
(In conjunction with the 1980 Applied Superconductivity Conference)

SUMMARY

The meeting was called to order at 5:00 pm October 2, 1980 by the chairman, Al Clark, who outlined the tasks to be accomplished at the meeting to the 33 attendees (list attached). These were: 1) a presentation and discussion of the results of a survey of test methods and a round robin test of superconductor critical current, 2) presentation of draft standards for definitions and three critical current tests, and 3) the majority of the time to be spent by the task groups modifiying the draft standards into working standards to be submitted to the subcommittee for approval. All the tasks were accomplished with the exception that the critical current test standard needs further modification as directed by the subcommittee. The subcommittee also strongly recommended that a standard reference material for superconductor tests be generated and that work begin immediately on the problems of ac loss measurements in superconductors.

SURVEY AND ROUND ROBIN RESULTS

The results of a mail survey of test methods and specifications and of a series of round robin tests were presented by Fred Fickett of NBS. The survey indicated that more understanding is needed of transfer voltage, stress, and power supply effects on critical current measurements and that it is necessary to specify sample mounting techniques and to develop accurate magnetic field measurement. In general, specific values for various criteria, sensitivity limits, and most other aspects of the measurement were not agreed upon. The survey served well as the basis for the draft standards preparation.

The round robin tests were performed by the four superconducting wire manufacturers on identical sets of three different conductors: a NbTi multifilamentary wire, a Nb_3Sn multifilamentary wire, and a Nb_3Sn tape. A "critical current" value at several magnetic fields was requested, but no other instructions were provided. Variations on the order of 30% were found for all materials with no consistency. The subcommittee felt this was cause enough to proceed with vigor!

For information Fred Fickett also presented a list of 16 areas in which research has been done by the wire manufacturers and the National Bureau of Standards (sponsored principally by the Department of Energy) on parameters that can effect a critical current measurement. This information was used as a resource by the task groups in development of the draft standards.

PRESENTATION OF DRAFT STANDARDS

A draft set of definitions of terms related to standards for practical superconductors was presented by Steve St. Lorant who had created the draft based upon four articles published by NBS in Cryogenics, the Compilation of ASTM Standard Definitions, and his own input and that from several of his colleagues. The subcommittee decided that these definitions should only include terms usable in the critical current standard with others to be added as needed.

Three separate draft standards for critical current were presented by Bob Schwall, Bill Fietz, and Loren Goodrich. The subcommittee decided to combine the measurement standards for the various geometries (e.g. straight, hair-pin, and coil) into one test with three variations and use the most generic of the drafts as a basis for discussion and modification.

The meeting was adjourned at 10:00 pm to reconvene at 8:30 am on October 3, 1980 to work in task groups on the drafts and incorporate the modifications from the evenings discussions.

TASK GROUP MODIFICATIONS

The two task groups met the following morning, the one on definitions chaired by Steve St. Lorant and the one on critical current chaired by Bob Schwall.

The set of definitions was cut and edited, added to and clarified until a workable set of definitions was agreed to by the task group. These will be retyped and submitted to the subcommittee for approval by mail.

The task group on critical current measurements was faced with an almost impossible job of going through the more than 50 detailed parts of the draft standard, but did remarkably well. Those areas where consensus was not achieved in short order were left to be resolved later. These were assigned to the NBS staff for further evaluation. The next version of the draft standard is to be circulated by mail for comment in late October. A discussion of the open questions will accompany the draft as will comments relating to specific objections.

After a joint discussion of the results the meeting adjourned about 11:30 am.

Al Clark
Electromagnetic Technology Div.
National Bureau of Standards
Boulder, CO 80303

Bob Wolf
CERN
Geneva, Switzerland

K. J. Best
Vacuumschmelze GMBH
Postfach 109
D-6450 Hanau 1
West Germany

J. D. Thompson
Los Alamos Scientific Lab.
P-10, MS-764
Los Alamos, NM 87545

Harvey Segal
Magnetic Corporation of America
179 Bear Hill Road
Waltham, MA 02154

Kate Stohlman
Supercon, Inc.
9 Erie Drive
Natick, MA 01760

M. J. Superczynski
Naval Ship R&D Center
Annapolis, MD 21402

Don Waltman
Naval Ship R&D Center
Annapolis, MD 21402

F. McDonald
Naval Ship R&D Center
Annapolis, MD 21402

B. Zeitlin
Intermagnetic General Corp.
P. O. Box 566
Guilderland, NY 12084

L. F. Goodrich
Electromagnetic Technology Div.
National Bureau of Standards
Boulder, CO 80303

C. E. Oberly
Air Force AFAPL/POD-1
Wright-Patterson AFB, OH 45433

H. Riemersma
Westinghouse Electric Corp.
Churchill Boro
Pittsburgh, PA 15235

Max Swerdlow
AFOSR/NE
Bldg. 410, Rm. C213
Bolling AFB
Washington, DC 20332

Jack Ekin
Electromagnetic Technology Div.
National Bureau of Standards
Boulder, CO 80303

Thomas Luhman
Brookhaven National Lab.
Upton, NY 11973

Don Beard
Office of Fusion Energy
Department of Energy
Washington, DC 20545

Bill Fietz
Oak Ridge National Lab.
P. O. Box Y
Bldg. 9204-1, MS-14
Oak Ridge, TN 37830

Phil Sanger
Airco Superconductors
600 Milik Street
Carteret, NJ 07008

Moyses Kuchnir
FERMILAB
P. O. Box 500
Batavia, IL 60510

R. N. Randall
Supercon, Inc.
9 Erie Drive
Natick, MA 01760

Bruce Strauss
Magnetic Corporation of America
179 Bear Hill Road
Waltham, MA 02154

Bob Schwall
Intermagnetics General Corp.
P. O. Box 566
Guilderland, NY 12084

Jim Ho
Physics Department
Wichita State University
Wichita, KS 67208

Steve St. Lorant
Stanford Linear Accelerator Center
P. O. Box 4349
Stanford, CA 94305

Bill McDonald
Wah Chang Corporation
Albany, OR 97321

Dave Sutter
High Energy Physics
Department of Energy
Washington, DC 20545

Eric Gregory
Airco Superconductors
600 Milik Street
Carteret, NJ 07008

Meyer Garber
Brookhaven National Laboratory
Upton, NY 11973

Dave Larbalestier
University of Wisconsin
1500 Johnson Drive
Madison, WI 53706

K. Hemachalam
Magnetic Corporation of America
179 Bear Hill Road
Waltham, MA 02154

F. Fickett
Electromagnetic Technology Div.
National Bureau of Standards
Boulder, CO 80303

R. Boom
University of Wisconsin
1500 Johnson Drive
Madison, WI 53706

14 Users
11 Producers
8 Researchers

NBS-114A (REV. 2-8C)

U.S. DEPT. OF COMM. BIBLIOGRAPHIC DATA SHEET (See instructions)	1. PUBLICATION OR REPORT NO. NBSIR 80-1642	2. Performing Organ. Report No.	3. Publication Date December 1980

4. TITLE AND SUBTITLE

Development of Standards for Superconductors

5. AUTHOR(S)

F. R. Fickett, L. F. Goodrich, and A. F. Clark

6. PERFORMING ORGANIZATION (If joint or other than NBS, see instructions)

NATIONAL BUREAU OF STANDARDS
DEPARTMENT OF COMMERCE
WASHINGTON, D.C. 20234

7. Contract/Grant No.

8. Type of Report & Period Covered

9. SPONSORING ORGANIZATION NAME AND COMPLETE ADDRESS (Street, City, State, ZIP)

10. SUPPLEMENTARY NOTES

☐ Document describes a computer program; SF-185, FIPS Software Summary, is attached.

11. ABSTRACT (A 200-word or less factual summary of most significant information. If document includes a significant bibliography or literature survey, mention it here)

Modern practical superconductors are complex materials and the determination of their critical parameters is a difficult task. Many approaches are possible for determining a given parameter and the results often depend on which one is chosen. The goal of this program, a cooperative venture involving DoE, NBS, and private industry, is to arrive at a set of useful voluntary standards for measurements on modern practical superconductors that will be acceptable to both manufacturers and users. Agreement on a set of standard definitions for the commonly used terms is also necessary. This report describes the status of the program at the end of the second year. The work in FY 80 has concentrated nearly exclusively on the critical current standard. Experimental determinations of the effect of various parameters on the measurement have been made by NBS and by the wire manufacturers. Significant progress has been made in the preparation of the actual critical current measurement standard and the definition standard. Draft copies of both are now ready for comment.

12. KEY WORDS (Six to twelve entries; alphabetical order; capitalize only proper names; and separate key words by semicolons)

Critical current; electrical property; magnetic property; stability; standards; superconductor.

13. AVAILABILITY

☒ Unlimited

☐ For Official Distribution. Do Not Release to NTIS

☐ Order From Superintendent of Documents, U.S. Government Printing Office, Washington, D.C. 20402.

☒ Order From National Technical Information Service (NTIS), Springfield, VA. 22161

14. NO. OF PRINTED PAGES

220

15. Price

$13.00